DESIGN OF PORTABLE LED VISUAL STIMULUS AND SSVEP ANALYSIS FOR VISUAL FATIGUE REDUCTION AND IMPROVED ACCURACY

A THESIS SUBMITTED TO

THE UNIVERSITY OF KENT

IN THE SUBJECT OF COMPUTER SCIENCE

FOR THE DEGREE OF

DOCTOR OF PHILOSOPHY.

By

Surej Mouli

January 2017

Abstract

Brain-computer interface (BCI) applications have emerged as an innovative communication channel between computers and human brain as it circumvents peripheral limbs thereby creating a direct interface between brain thoughts and the external world. This research focuses on non-invasive BCI to improve the design of visual stimuli in eliciting steady-state visual evoked potential (SSVEP) for BCI applications. To evoke SSVEP in the brain, the user needs to focus on a visual stimulus flickering at a constant frequency. Traditionally in research studies, the visual stimulus for SSVEP uses LCD screens where the flicker is generated using black or white patterns, which alternates the colour to produce a flickering effect. However, there are drawbacks for LCD based visual stimuli systems that limit the user acceptance of SSVEP applications. The main limitations are: (i) choice of flicker frequency is limited to the LCDs vertical refresh rate (ii) flicker is mainly limited to black/white patterns (iii) higher visual fatigue for the user due to LCDs background flicker (iv) reduced visual stimulus portability (v) Inaccurate flicker generated and controlled by the software (vi) influence of adjacent flicker causing attention shift when multiple flickers are used for classification and also not being easily adaptable for user requirements.

The impediments in eliciting and utilising SSVEP responses for designing a near real-time platform for controlling external applications are addressed from five main perspectives here: (i) design of standalone LED visual stimulus hardware for precise generation of any frequency for replacing the LCD based visual stimulus (ii) eliciting maximal response by choosing most responsive colour, orientation and shape of visual stimulus (iii) identification of the best luminance level for visual stimulus to improve the comfortability of the user and for improved SSVEP response (iv) control of the duration of ON/OFF period

for the visual stimulus to reduce eyestrain for the user (i.e. visual fatigue), and (v) hybrid BCI paradigm using SSVEP and P300 to improve the classification accuracy for controlling external applications.

The experimental study involved the development of various visual stimulus designs based on LEDs and microcontrollers to minimise the visual fatigue and improve the SSVEP responses. The signal analysis results from the studies with five to ten participants show SSVEP elicitation is influenced by colour, orientation, the shape of stimulus, the luminance level of stimulus and the duration of ON/OFF period for the stimulus. The participants also commented that choosing the correct luminance and ON/OFF periods of the stimulus considerably reduce the eyestrain, improve the attention levels and reduce the visual fatigue. Taken together, these finding leads to more user acceptance in SSVEP based BCI as an assistive mechanism for controlling external applications with improved comfort, portability and reduced visual fatigue.

Acknowledgements

I am deeply grateful to my supervisor Dr Palaniappan for his guidance and support throughout these years of work. I thank him for the support, patience and friendly encouragement throughout the PhD.

I would like to thank all the participants for agreeing and cooperating patiently for the EEG data collection throughout this research even though it was long and sometimes tiring.

I would like to thank my family: my wife, my sister, my brother-in-law and my niece for all their constant support and encouragement throughout these years.

I would like to dedicate this thesis to my mother.

Declaration

I certify that I have read and understood the entry in the Project Handbook on Plagiarism and Duplication of Material and that all material in this Dissertation is my own work, except where I have indicated with appropriate references.

Signed.....

Date.....

Abbreviation List

AIC Akaike Information Criterion

BCI Brain-computer interface

BOLD Blood Oxygen Level Dependent

CCA Canonical Correlation Analysis

COB Chip on Board

CSF Cerebrospinal Fluid

CRT Cathode Ray Tube

DFT Discrete Fourier Transform

DoCs disorders of consciousness

ECoG Electrocorticogram

EDF European Data Format

EEG Electroencephalography

EMI Electromagnetic Interference

ERD/ERS Event-Related Desynchronization/Synchronisation

ERP Event-Related Potential

FFT Fast Fourier Transform

fMRI Functional Magnetic Resonance Imaging

HCI Human-Computer Interaction

HMI Human-Machine Interaction

ITR Information Transfer Rate

LCD Liquid Crystal Display

LED Light Emitting Diode

MEG Magnetoencephalogram

MOSFET Metal–Oxide–Semiconductor Field-Effect Transistor

NIRS Near-Infrared Spectroscopy

PSD Power Spectral Density

RGB Red, Green and Blue

SCP Slow Cortical Potential

SMD Surface Mount Device

SSVEP Steady-State Visual Evoked Potential

sEMG Surface Electromyography

SNR Signal-to-Noise Ratio

TFT Thin Film Transistor

TTD Thought Translation Devices

VEP Visual Evoked Potential

Contents

List of Tables

List of Figures

Chapter 1

Introduction

Interacting and conveying messages within an environment are necessities of humans. In the interactive communication domain, Human-Computer Interaction (HCI) has a prominent place in improving a computer's understanding of user needs with minimal integration time. HCI has evolved in recent years to a more refined form known as Human-Machine Interaction (HMI) which make use of different muscular movements or signals from the human body to communicate with the external world using interfaces. HMI is a cross-disciplinary area, which connects engineering with emotion, action, muscular movement, as well as other intuitive interfaces for developing user interfaces for controlling external applications. The advancement in electronics has catalysed the growth of embedded systems, which forms a bridge between human and machines. These embedded systems could be used to develop low-level interfaces that can be used to acquire data from the human body and process it using intelligent algorithms in real time for meaningful operations.

Human-machine interfaces have become an active research area exploring various possibilities of using brain signals and interpreting the same to control external applications. These operations are complex and need to address various issues related to interactive systems such as knowing the user, understanding the task, maintaining consistency, prevent errors, reversal of action and to improve naturalness (Kim, 2015). In addition to these, situation awareness is also an influential factor that may change the user behaviour

in HMI and that needs to be addressed in the software/hardware that translates the user intent to action.

In HMI, other than physical activity-based control system in which the user utilises the muscular movements to perform the action, the signal from the brain can also be used to control external applications. This neural activity acts a non-muscular communication channel to control external devices using brain signals. Similarly, muscle contraction and relaxation cycles also generate electrical activity that could be measured using Surface Electromyography (sEMG) and also could be used for external application control. Electroencephalography (EEG), which is the electrical activity of human brain discovered by Hans Berger is the stepping stone towards the non-muscular communication between human brain and computers and is termed as a Brain-computer interface (BCI). Over the past 20 years, BCI research has led to many innovations encouraged by the understandings of brain signals. The signals can be taken invasively or non-invasively either from the brain or from the scalp. Non-invasive BCI takes signals that are present at micro-volt levels on the scalp and then amplifies them using the appropriate hardware for analysis. Studies show that patients with access to BCI technology recover more quickly from serious communication disabilities (Pichiorri et al., 2015; Luauté and Laffont, 2015; Van Dokkum, Ward and Laffont, 2015; Hill and Wolpaw, 2016; Daly and Huggins, 2015). Modern HCI research and innovation could contribute to BCI researcher in developing control and feedback mechanisms for interaction. Research also shows promising signs in both preventing and delaying the onset of dementia, Alzheimer's and Parkinson's diseases in elder people (Simon et al., 2017; Lee et al., 2013). BCI could also be considered as an alternative communication medium for disabled people to operate devices such as computers, assistive chairs or to communicate with the external world (Muller-Putz and Pfurtscheller, 2008; Ng, Soh and Goh, 2014; Spuler, 2015; Lopes, Pires and Nunes, 2013). Since BCI is translating a user's voluntary and in some cases involuntary intent to command an external interface, no muscular action is required by the user and this could be used by any paralysed individual (Pires, Nunes and Castelo-Branco, 2012).

BCI can be considered as one of the most exciting emerging technologies that can infer the mental states and intentions of a user by interpreting neural signals. BCI has its advantages in many areas other than just supporting people with disabilities. Normal users can also use BCI which could be employed for hands-free control in gaming, emotion-based control systems, visual stimulus control system or in thought based system control. Basic BCI working methodology is shown in Figure 1.1.

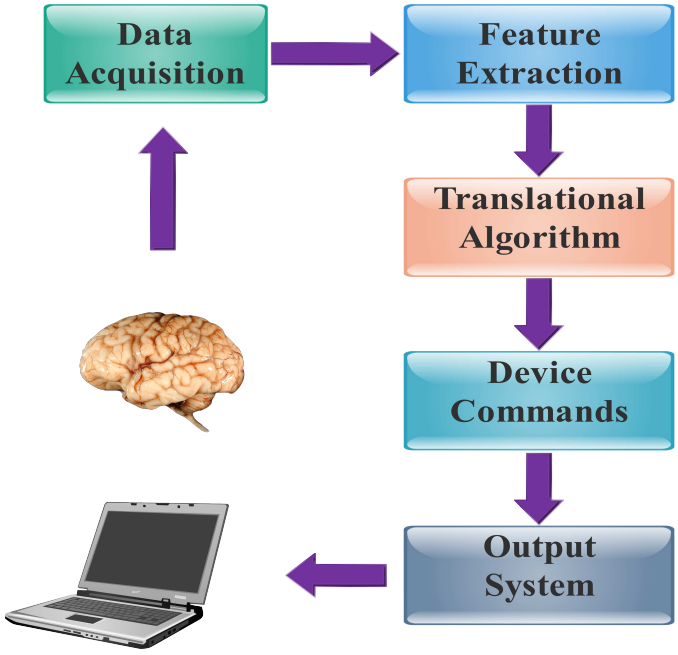

Figure 1.1: Basic data flow in BCI

Brain activity can be measured with several techniques such as Magnetoencephalogram (MEG), Near-Infrared Spectroscopy (NIRS), Electrocorticogram (ECoG), Functional Magnetic Resonance Imaging (fMRI), and by Electroencephalography (EEG). All these techniques have advantages and disadvantages when compared to each other. MEG is a non-invasive technique to measure the brain waves using the magnetic field produced by the brain activity. The process requires expensive equipment and a laboratory environment with a magnetically shielded room to reduce external interference. MEG has its advantages over fMRI and EEG and can provide the timing information of the brain activity

(Nagarajan, Ranasinghe and Vossel, 2016). NIRS based brain activity measurement operates by producing near-infrared radiation with wavelengths from 650 nm to 950 nm which passes through the skull to compare the intensities of the returning and incident light. When there is activity in the brain, an increase in blood flow happens in pre-defined regions and causes the concentration of oxygenated and deoxygenated haemoglobin and this produces the change in the optical properties (Fazel-Rezai, 2013). NIRS based brain activity measurement has the advantage of measuring cortical responses to a depth of two cm from the skull and also can be used to assess hemodynamic responses in the brain. However, the measurement techniques require a well-equipped lab. This is not suited for general BCI due to the delay of a few seconds to attain peak response following a stimulus onset due to the hemodynamic nature.

ECoG is an invasive technique where the electrodes are directly placed on the exposed surface of the brain and the activity is measured. The measured signal would have a higher amplitude, better signal-to-noise-ratio, broader bandwidth up to 200 Hz and be less vulnerable than EEG to artefacts like muscle movements or eye blinks (Leuthardt et al., 2004). The major disadvantage of ECoG is that it is invasive and not suited for general BCI operations. fMRI is based on magnetic resonance imaging MRI that measures the brain activity based on the change in blood flow. This technique of brain activity measurement detects the Blood Oxygen Level Dependent (BOLD) changes in the MRI signal that arises when the neuronal activity occurs when a task is performed or the brain state is changed (Gore, 2003). fMRI is non-invasive and does not involve any radiation making it safer for subjects. fMRI has low temporal and spatial resolution. The downside is the requirement of expensive equipment and the laboratory environment.

The brain activity measurement based on EEG is a widely used technique with many advantages. EEG based systems are non-invasive, cost-effective and do not require any laboratory environment and this makes it popular in the research community. EEG contains detailed information on different states of the brain and is useful in understanding the physiological condition of a person. Electrodes are fitted on specific areas to record

EEG activity in the brain, and this can be monitored in real time. This helps in analysing the EEG for specific disabilities or to evaluate the functional performance of any particular action. The availability of various consumer-grade headsets makes EEG a practical choice for BCI related applications.

In the non-muscular interaction, EEG plays an important role in the development of BCI systems that have led to the innovation of a new pathway for communication for special users. After the initial finding of EEG by Prof Hans Berger in 1924, researchers identified many sub-bands like delta (0 - 3.65 Hz), theta (3.65 - 7.25 Hz), alpha (7.25 - 14.5 Hz) and beta (14.5 - 29 Hz) (Pal, Khobragade and Panda, 2011). Delta rhythms occur when a person is in deep sleep mode, whereas theta waves occur in light sleep or meditation states. Alpha occurs in the awake-state and their oscillations have a smooth pattern.

EEG brain activity can be categorised for the BCI in four different types: event-related Event-Related Desynchronization/Synchronisation (ERD/ERS), Steady-State Visual Evoked Potential (SSVEP), P300 component of the Event-Related Potential (ERP) and Slow Cortical Potential (SCP). Comparing the event-related potentials as shown in Figure 1.2, SSVEP systems have the highest accuracy and higher information transfer rate and are suitable for controlling external applications. To generate SSVEP requires only a few EEG channels and a flickering stimulus at a constant frequency.

SSVEP is a repetitive sinusoidal-like waveform with its frequency synchronised to the frequency of the visual stimulus, and is generated in the human visual cortex (Herrmann, 2001; Pastor et al., 2003). SSVEP can be modulated by the attention of participating subject towards the stimulus and it is possible to ascertain the focus of a subject's attention when presented with multiple target stimuli having specific flicker rates. SSVEP has attracted enormous attention due to its phase-locked characteristics and better signal-to-noise ratio, reduced training time and has the ability to achieve excellent Information Transfer Rate (ITR) in BCI systems (Resalat et al., 2012). Research studies have shown that the amplitude of the response in the specific stimulus frequency varies with different subjects,

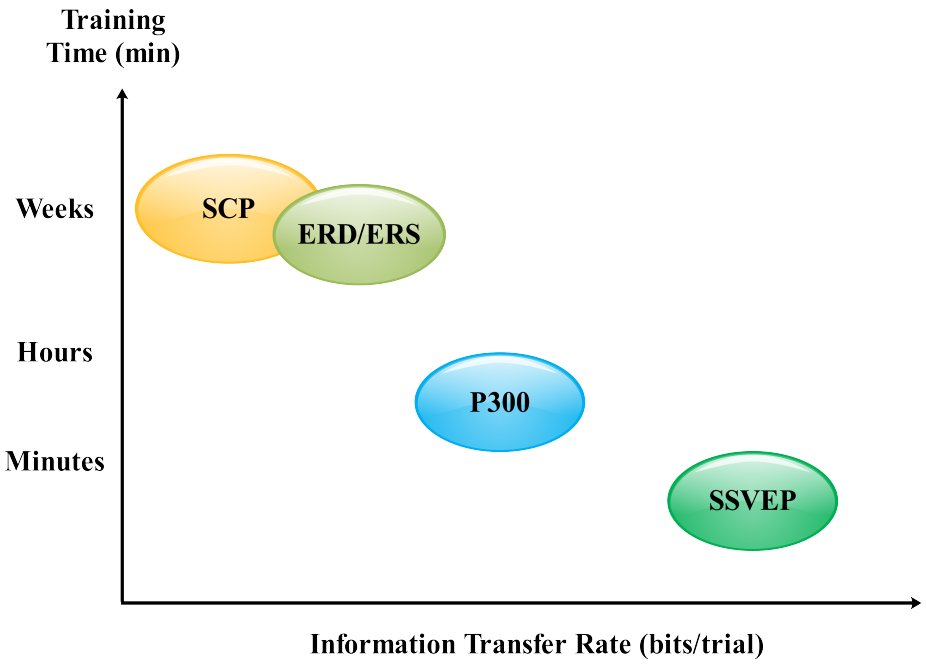

Figure 1.2: EEG Information transfer rate ((Fazel-Rezai, 2013) used with permission from InTech)

colour, intensity and the type of stimulus (Cecotti and Rivet, 2011; Hwang et al., 2013c; Lopez-Gordo et al., 2011; Nishifuji and Kuroda, 2012; Teng et al., 2012). Often SSVEP signals are corrupted with other noise such as background EEG, artefacts and external noise such as power-line interference. Specific signal processing techniques need to be employed to reduce these undesired effects.

Even though SSVEP responses are sufficiently high for practical purposes, it is not always comfortable for subjects for longer periods. Traditionally the flickering stimulus is created on a Liquid Crystal Display (LCD) screen using checker patterns which change state from black to white causing a continuous flicker. Different such flickers are generated which flash at various frequencies that are presented to the user to focus on and that generates the SSVEP in the EEG. The frequencies of visual flicker generated using LCD screens are limited due to the dependency on vertical refresh rate. Users also suffer from visual fatigue in prolonged usage due to the background refresh of the LCD screen, limited viewing angle and have to work closer to the screen (Shieh, 2000; Siegenthaler et al., 2012; Lin and Huang, 2013; Aznar-Casanova et al., 2017).

1.1 Motivation

SSVEP based BCI requires the stimulus frequency to be precise, and ideally to have less visual fatigue than current systems. LCD based stimulus cannot produce a wide range of flashing frequencies since it is dependent on the refresh rate of the screen. Generally, LCD screens have a refresh rate of 60 Hz and the frequencies for the visual stimulus that can be produced would be based on the required frame rates. With a frame rate of 10 frames per second, the visual stimulus can have a frequency of 6 Hz (10 frames / 60 Hz) and with 8 frames per second, the stimulus frequency would be 7.5 Hz. The accuracy of the produced flicker is not very precise as it depends on a secondary parameter, the refresh rate of the screen. It is also not possible to produce frequencies of user choice (example: 7 Hz or 8 Hz) with fixed refresh rates of the LCD. Since all the different flickers are generated on the same screen, the user won't be able to focus on a particular flicker as the adjacent flicker would also influence the EEG. Background flicker that is always present on any LCD screen would also increase visual fatigue and at the same time influence the EEG data.

To reduce visual fatigue, high frequency flicker are also recommended from various studies that require a minimum of 32 electrodes to achieve an acceptable SSVEP response (Won et al., 2014; Dong-Ok et al., 2014). For a portable BCI system, it will not be practical to use large number of electrodes to get the desired output. Since lower frequencies give better SSVEP response, it would be wiser to address the current issues with lower frequencies and develop a portable BCI platform with lower visual fatigue and better SSVEP response.

We thus consider Light Emitting Diode (LED) which can be used to generate flicker with high accuracy and portability. This type of stimulus is not much explored in the research literature especially in terms of colour, orientation and pattern influences for SSVEP EEG. Generating LED based flicker requires hardware that is capable of producing precise frequency flicker consistently. A basic SSVEP LED stimulator (g.STIMbox) is available from g.tech with limited capabilities, the flicker frequencies are pre-programmed for

10,11,12 and 13 Hz (Guger, Edlinger and Krausz, 2011). The hardware is not configurable for experimental requirements such as colour analysis, intensity control, frequency selection, orientation and so on. Since LEDs differ in operating voltages, colours, intensity and shapes, it is required to explore this light source in detail so it could be used as a reliable visual stimulus for SSVEP based EEG. Hardware platforms need to be developed as appropriate that are expandable and versatile to accommodate different types of flicker generation with ease of portability, reliability and also to reduce the visual fatigue.

1.2 Objectives

Therefore, the aim of the research in this thesis is to propose a novel, efficient and portable SSVEP based BCI, with the necessary hardware platform, that is flexible to configure and design experiments. With this aim,

i To investigate if LEDs can be a used to reduce visual fatigue in evoking SSVEP.

ii To identify the influence of basic LED colours in SSVEP response.

iii To identify the influence of frequency selection of LEDs in SSVEP response.

iv To investigate if frosted package LED stimulus can reduce visual fatigue.

v To develop the necessary hardware platform to drive multiple LEDs with high accuracy and expandability.

vi To explore the effect of orientation of LED visual stimulus arrays in SSVEP response.

vii To investigate radial patterns and concentric circles to increase the accuracy and response in SSVEP EEG.

viii To explore the effect of LED visual stimulus luminance in evoking SSVEP.

ix To investigate the influence of duty-cycles in LED visual stimulus in improving the SSVEP response and reducing visual fatigue to improve comfortability for the user.

x To develop a hardware platform for a hybrid visual stimulus to combine P300 and SSVEP to improve the response and detection accuracy using P300 event markers.

xi To control a LEGO robot online to demonstrate all the research findings.

1.3 Thesis Structure

The flowchart in Figure 1.3 shows the overall structure and outcomes of this thesis. The thesis is mainly organised into ten chapters. The background work and the current developments in BCI are discussed in the second chapter. Chapters starting from third till tenth are organised as separate research findings which are organised in an incremental fashion.

Chapter 2 discusses the past and current studies related to various types of BCI implementations. Topics related to BCI paradigms, EEG data acquisition, hardware setup, types of electrodes, BCI applications, limitations of current systems are also discussed in this chapter. The chapter also highlights the necessity of LED based visual stimulus as compared to the traditional LCD/CRT stimulus presentation where the frequency generation is restricted by the LCD/CRT refresh rates.

Chapter 3 focuses on the visual stimulus design stage with different types of LEDs used for generating SSVEP along with the data collection procedures and setup of EEG hardware. Single RGB LED based stimulus was used in the experiment along with clear and frosted package to explore the influence of colour and intensity of the stimulus. User comfortability and visual fatigue reduction with the developed visual stimulus hardware was also explored in this chapter. Some part of chapter 3 is derived from the publications below;

1. **Mouli, S.**; Palaniappan, R.; Sillitoe, I.P.; Gan, J.Q., 2013. Performance analysis of multi-frequency SSVEP-BCI using clear and frosted colour LED stimuli, In 13th IEEE International Conference on Bioinformatics and Bioengineering (BIBE),2013. pp. 1 - 4.

2. **Mouli, S.**; Ramaswamy, P.; & Sillitoe, I.P., 2014. Arduino based configurable LED stimulus design for multi-frequency SSVEP-BCI. In PGBiomed/ISC 2014, the IEEE EMBS UKRI Postgraduate Conference on Biomedical Engineering. Warwick, pp. 1 - 4.

3. **Mouli, S.**; Palaniappan, R.; & Sillitoe, I.P., 2015. A configurable, inexpensive, portable, multi-channel, multi-frequency, multi-chromatic RGB LED system for SSVEP stimulation. In T. A. Cassation, A.E. and Azar, ed. Brain-Computer Interfaces. Switzerland: Springer International Publishing, pp. 241 - 269.

Chapter 4 explores the possibilities of improving the SSVEP response with LED visual stimulus array. An array of LED was used to develop the stimulus hardware using high current MOST drivers. This study investigates the orientation effects of LED visual stimulus for horizontal and vertical orientations to identify the better orientation to obtain the maximum amplitude response, reduced visual fatigue and minimal detection time in SSVEP EEG. Some part of chapter 4 is derived from the publications below;

1. **Mouli, S.** et al., 2015. Quantification of SSVEP responses using multi-chromatic LED stimuli: Analysis on colour, orientation and frequency. In 7th IEEE Computer Science and Electronic Engineering Conference (CEEC), 2015. pp. 93 - 98.

2. **Mouli, S.**; Palaniappan, R.; & Sillitoe, I.P., 2015. Improving Steady State Visual Evoked Potentials Responses from LED Stimuli Through Orientation Analysis. Journal of Medical Imaging and Health Informatics, 5(5), pp. 1070 - 1075.

Chapter 5 moves forward from the traditional LED type; this chapter explores the effect of radial LED visual stimulus in evoking SSVEP. The hardware required was developed based on chip-on-board (COB) LEDs and controlled using a powerful 32-bit microcomputer platform. It compares the radial patterns with horizontal stimulus to identify the best results in SSVEP simulation, detection and user comfortability. Some part of chapter 5 is derived from the publication below;

1. **Mouli, S.** & Palaniappan, R., 2016. Radial Photic Simulation for Maximal EEG Response for BCI Applications. In 9th IEEE International Conference on Human System Interaction (HSI). Portsmouth. UK, pp. 362 - 367.

Chapter 6 concentrates on visual fatigue reduction by controlling the luminance of the visual stimulus. The luminance control hardware was developed for varying the luminance level of the visual stimulus, which was measured with a LUX meter. The SSVEP response was compared for various visual stimulus luminance levels to identify the most responsive and comfortable luminance level for the user. Some part of chapter 6 is derived from the publication below;

1. **Mouli, S.** & Palaniappan, R., 2016. Eliciting Higher SSVEP Response from LED Visual Stimulus with Varying Luminosity Levels. 2016 International Conference for Students on Applied Engineering (ICSAE), pp. 201 - 206.

Chapter 7 discusses further significant improvement of the system for better visual fatigue reduction where the visual stimuli ON/OFF periods were controlled with pulse width modulation that defines the ON and OFF periods of the LED visual stimulus. The hardware and software programs were developed for the visual stimulus with variable duty-cycle so that it reduces the flickering effect seen by the user. Various duty-cycles for the visual stimulus were compared to identify the most responsive ones as well as improving the user comfort for prolonged usage with reduced visual fatigue. Some part of chapter 7 is derived from the publication below;

1. **Mouli, S.** & Palaniappan, R., 2017. Towards a reliable PWM based LED visual stimulus for improved SSVEP response with minimal visual fatigue. The Journal of Engineering (IET).

Chapter 8 treats the combination of SSVEP and P300 to develop a hybrid BCI. This

combination was experimented with to support the SSVEP detection for different frequencies and to increase the efficiency by using additional P300 stimulus. The hardware was developed for receiving the P300 time stamps that were used to improve the detection methods in real time for classification. Some part of chapter 8 is derived from the publication below;

1. **Mouli, S.** & Palaniappan, R., 2017. Hybrid BCI utilising SSVEP and P300 event markers for reliable and improved classification using LED stimuli. In 2017 IEEE Symposium on Computer Applications & Industrial Electronics (ISCAIE), Langkawi, Malaysia, pp. 127 - 131.

Chapter 9 looks at applying the research findings to perform a real-time navigation and control of a wheelchair which is demonstrated using LEGO robot wirelessly, with SSVEP using hybrid visual stimuli for direction control. The hardware developed was used to control individual visual stimulus running at different frequencies simultaneously. The data was successfully classified for the direction control with minimal attention time.

Finally, Chapter 10 concludes the thesis with discussions and suggestions for possible future work.

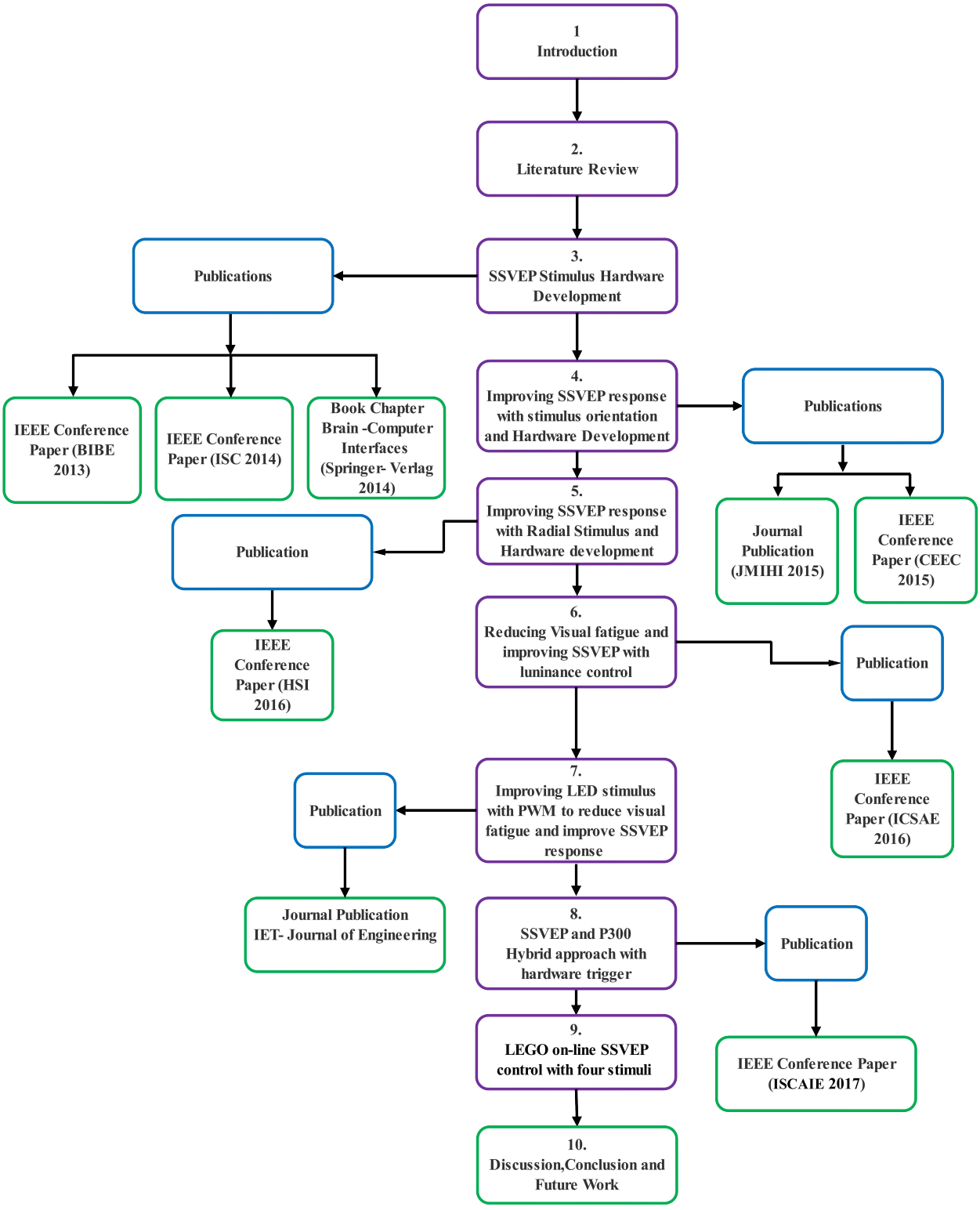

Figure 1.3: Thesis Structure

Chapter 2

Previous Work on EEG Signal Acquisition, Brain-Computer Interface and Steady State Visual Evoked Potential

The Language of the Brain is Not the Language of Mathematics

(Neumann, 1958)

2.1 Introduction to Brain-Computer Interface

Human-machine systems refer to the combination of human and machines to accomplish certain tasks through communication between human and machines. This can be considered as an interaction of two intelligent systems to fulfil some tasks through movement, dialogues or by means of non-muscular action. HCI is a cross-disciplinary area which deals with design and implementation and evaluation of ways that humans can interact with a computing system for fulfilling the desired task. It is an abstract model of inputting the information in a computing device and getting the desired output through external

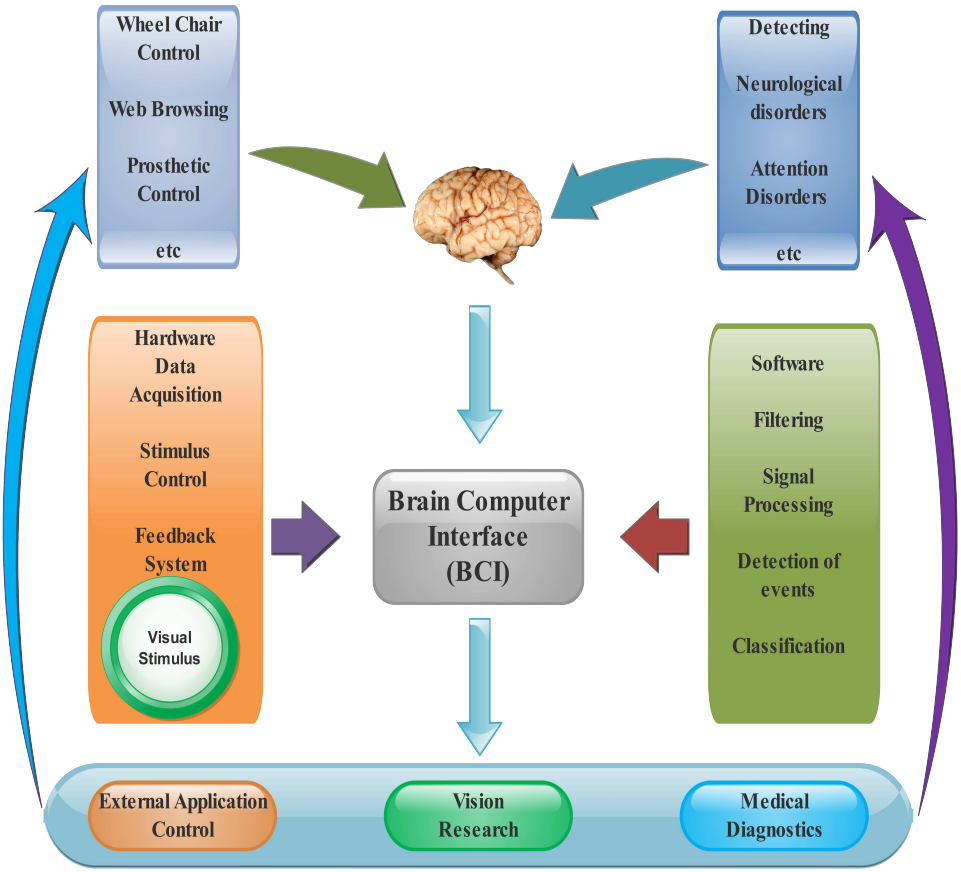

Figure 2.1: Basic BCI data flow

devices or other applications. Many types of HCI exist, some use direct interaction without any detailed processing of data whereas other systems use complex algorithms to get the desired output for performing the tasks. Other than data interaction, figures, images, colours, lights and sound are also used in HCI for performing tasks. The modern HCI systems also use more intelligent interactive systems such as 'learn and process' where the computer analyses the data and interprets it intelligently and consistently to avoid mistakes and improve accuracy (Kim, 2015; Gong, 2009).

Analysis of data in HCI is based on the task and purpose of the system and the task is usually divided into human and computer tasks. Computer tasks usually process data received by the cause of an action performed by an human. Intelligent designs can improve the performance and accuracy of a task with predictive algorithms and minimal user input. With the rapid development of innovative user interaction, HCI is making use of

multiple platforms for interaction for physically challenged people. One such innovative and the widely researched area is BCI. Like any organ in the body, the brain is composed of cells. These are termed neurons and they use electrical signals for communication. Neural communication system can be considered as an exciting technology in cross-disciplinary research, combining neuroscience and engineering. With the developments in embedded platforms and signal processing techniques, BCI researchers are getting a new edge to develop stand-alone systems to process the brain signals to control external applications. BCI research is likely to have substantial growth in the coming years as the technology and science is advancing and also the increasing demand for solutions in areas such as rehabilitation of nervous systems (Berger et al., 2008). Other factors that warrant the requirement for advance BCI are the increasing ageing population with neurodegenerative disorders and the commercial demands for non-medical BCIs.

BCI which is also known as brain-machine interface (BMI) is a non-muscular communication system that enables humans to communicate with their surroundings using the control signals from electroencephalography (EEG) activity (Cincotti et al., 2008; Nicolas-Alonso and Gomez-Gil, 2012; Fazel-Rezai, 2013; Sanchez and Principe, 2007; Prueckl and Guger, 2010; Hassanien and Azar, 2015; Wolpaw et al., 2002). Almost four decades ago, the possibility of using EEG brain signals to control external applications was researched in the University of California, leading to the development of a basic framework for BCI (Vidal, 1973).

In short, BCI is a non-muscular platform that creates a communication channel, which can recognise certain waveforms and patterns in the brain signal for relaying a person's intention to external devices or control systems. Generally, a BCI platform comprises five major components; signal acquisition, signal amplification and pre-processing, feature extraction, classification and external control blocks (Khalid et al., 2009). Even though BCI research has progressed considerably, the basic issues like interpreting the noisy brain signals and co-adaption between brain and interface to accomplish a common goal is yet to be resolved completely (Matthew et al., 2013). The future of BCIs depends on the progress

of comfortability, convenience and stable signal acquisition hardware to be reliable for many different user populations (Shih, Krusienski and Wolpaw, 2012).

EEG signals are directly acquired from the scalp non-invasively by the signal acquisition system using electrodes placed at specific locations. The acquired signal is amplified using low-noise amplifiers and the signal is pre-processed for further analysis. The pre-processed signals are then filtered and features are extracted for identifying the discriminative information in the brain on which the classification will be performed. The classified output can be used for controlling the externally connected devices or other assistive devices like wheelchairs or prosthetic arms. Figure 2.1 shows the basic BCI interface for data acquisition, application interface, and signal processing and feedback system. In a non-invasive BCI system, the signal acquired from the scalp has extremely low voltage potential in the range of microvolts and need to be amplified before conversion to a digital signal. The converted digital signals are filtered and processed at various levels to get useful information for external interaction. For an online BCI, the bio-signal processing is comparatively a complex task due to the low signal quality and fewer electrodes available in order to make the system compact and portable.

One of the most important discoveries in the exploration of the central nervous system is that the nerve impulse is identifiable with it's electric charge (Brazier, 1964). The electrical activity of the brain, which is generally less than $300\,\mu\mathrm{V}$, was initially identified by Berger in 1924 who recorded the first EEG from the human brain using electrodes made of metal strips pasted on the scalp (Berger, 1929). Berger successfully measured very small electrical potentials in the range of $50-100\,\mu\mathrm{V}$ recorded on paper and observed that the patterns in the brainwaves varied with time. The study also noted that the brain waves exhibited periodicities and regularities and were slow with high amplitude and low frequency during sleep (<3 Hz) and low amplitude and high frequency (15 to 25 Hz) during waking behaviours (Bronzino, 2006). The first EEG pattern identified by Berger was named alpha waves, lying in the range of 8 to 12 Hz and is a commonly noted rhythm in clinical EEG (Stern and Jerome Engel, 2015; Buzsáki, 2006). Following the discovery

of Berger, subsequent frequency bands were labelled delta @ 0 - 4 Hz; theta @ 4 - 8 Hz; beta @ 12 - 30 Hz and gamma for frequencies above 30 Hz (Cheryl L. Dickter and Kieffaber, 2014). Delta waves have the lowest frequency with the highest amplitude and are normally seen in infants and young children. These waves are associated with deep levels of relaxation, while abnormal levels of delta activity is a sign of brain injury, learning problems or an inability to think. Theta waves are generally linked to inefficiency and daydreaming. The lowest waves of theta represent the fine line of awake and sleep and abnormal theta activity shows signs of depression or hyperactivity. Alpha which is usually considered to be the first identified brainwave, relates conscious thinking and the subconscious mind. Alpha waves on the higher side show a person is too relaxed or has an inability to focus. Beta waves normally have a symmetrical distribution and are more evident in the frontal region. These waves show the involvement in conscious thinking, logical thinking or solving complex maths. Increased beta activity shows high arousal or stressed condition. Gamma is a high frequency signal which can go up to 100 Hz and denotes the higher processing tasks and cognitive functions. Increase in gamma shows a stressed condition or anxiety (Hassanien and Azar, 2015). The waveforms for different brainwaves discussed are shown in Figure 2.2.

The advent of computers and technologies made it possible to effectively quantify EEG activities. EEG signals have been analysed in greater depth to understand the difference in neuronal pattern of sub-bands. EEG contains detailed information on different states of the brain and is useful in understanding the physiological condition of a person. Each part of the brain processes different types of information as shown in Figure 2.3. Electrodes are fitted on these specific areas to record the brain functions related to a particular task. This helps in analysing the EEG for specific disabilities or to evaluate the functional performance of any particular action and is a complex process.

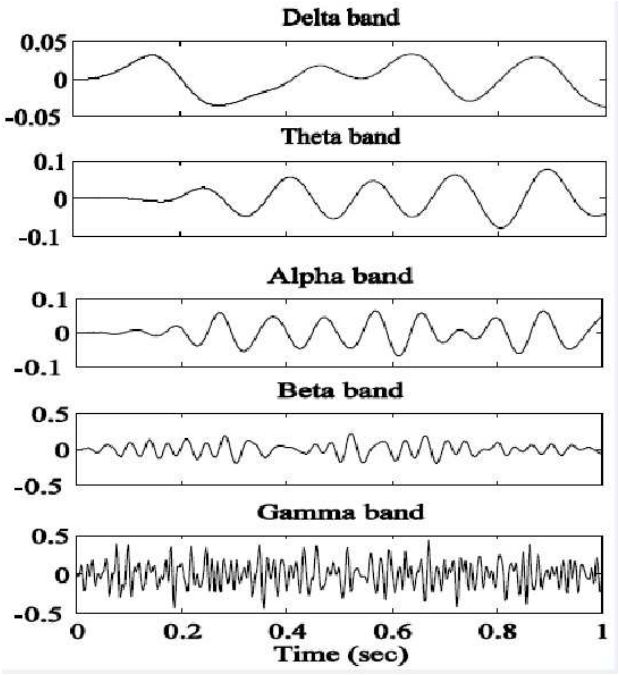

Figure 2.2: Comparison of EEG bands ((Islam, Hirose and Molla, 2013) used with permission from Creative Commons)

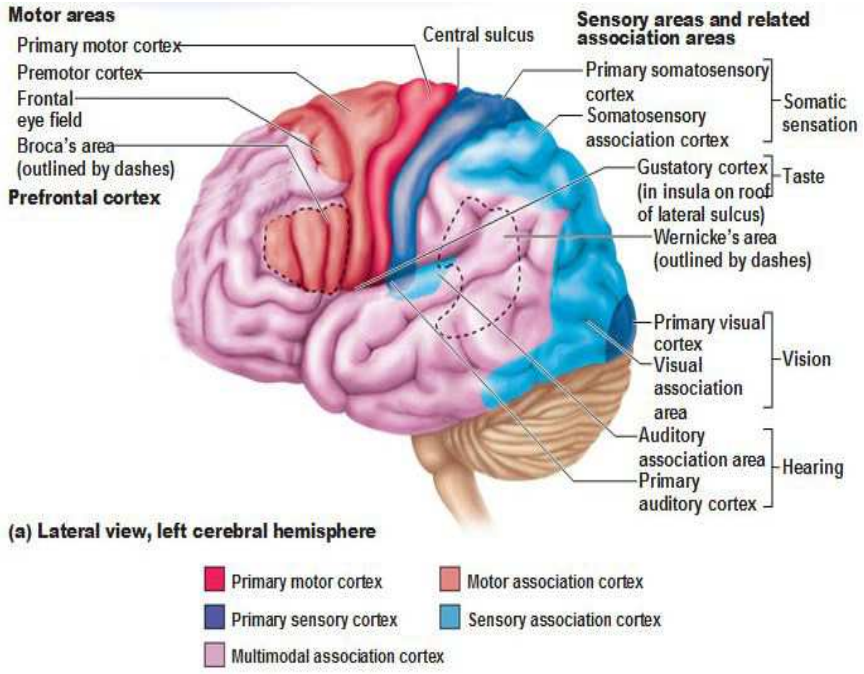

Figure 2.3: Brain cortex locations ((Antranik, 2016) used with permission from Antranik)

Table 2.1: Various BCI modalities

Type	Signal Source	Temporal Resolution	Spatial Resolution	Portability
EEG	Potential associated with cortical activity	High, in milliseconds or better	Coarse, approximately a few cm3	Portable
MEG	Based on magnetic field associated with neuronal activity	High, in milliseconds or better	Coarse, with limited spatial localisation. Better than EEG	Not portable
fMRI	Based on blood oxygenation-level dependent(BOLD) changes in susceptibility weighted MR signal	Low, 1- 2 seconds limited by hemodynamic delays	Good, resolution on the order of 64 mm3	Not portable
NIRS	Based on blood oxygenation-level dependent (BOLD) changes in absorption spectrum of near-infrared light	Medium, hundreds of milliseconds limited by hemodynamic delays	Coarse, in the order of 1 cm3 and limited depth penetration. Maximum sensitivity at the cortical surface	Portable
fTCS	Blood velocity associated with neuronal activity	Medium, tens of milliseconds	Low – limitation, of catheterising perfusion state via large blood vessel	Portable

2.2 Types of Brain-Computer Interfaces

BCI systems can be classified as invasive or non-invasive based on the placement of electrodes used in detecting the brain signals (Berger et al., 2008). Invasive BCI has the electrodes directly inserted into the brain tissue while in non-invasive approaches, the electrodes are placed over the scalp. The non-invasive subsystem usually uses the EEG to detect the neuronal activity and most of the EEG studies are based on non-invasive EEG sensors.

Recent years have witnessed tremendous technological advancements and growing number of applications for neuroimaging based systems. Neuroimaging is a medical

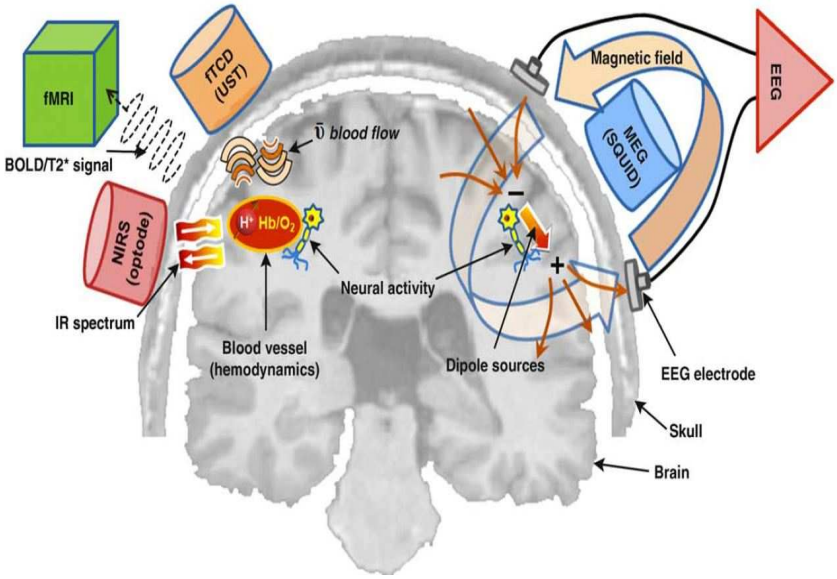

Figure 2.4: Brain signal detection schematic ((Min, Marzelli and Yoo, 2010) used with permission from Elsevier)

paradigm that studies the physiological response of the brain that could be useful in detecting the damage in brain tissue, skull fractures, behavioural disorders, metabolic diseases in a fine order (Fouad et al., 2015). Neuroimaging has two main categories, structural neuroimaging and functional neuroimaging (Caixeta, Ghini and Peres, 2011). Structural neuroimaging deals with the structure including the skull bone, tissues, blood vessel or any other existence of a tumour and functional neuroimaging relate to the detection of electrical impulses, blood flow rate, or change in metabolic activity as a result of a specific task (Bright, 2012). Various BCI approaches based on different neuroimaging modalities exist and they differ in their methodological approaches as listed in Table 2.1 (Min, Marzelli and Yoo, 2010). The brain signal detection mechanisms for different BCI modalities are shown in Figure 2.4.

2.2.1 Modalities in BCI

2.2.1.1. Electroencephalography (EEG)

Inside the brain, neurons communicate with each other by sending impulses and these impulses are measured using EEG. The electrodes are placed on the participant's scalp

at desired locations to capture the electrical signals. EEG is commonly used for medical diagnostics to identify issues such as disorders of consciousness disorders of consciousness (DoCs), emotion assessment or alertness (Luauté, Morlet and Mattout, 2015; Mikołajewska and Mikołajewski, 2014; Subasi, 2005). There are various ways of recording EEG and most commonly used is through the ERP (Luck, 2014). ERP's are time-locked with sensory, motor or cognitive events and consist of a series of oscillations that reflect the time course of neuronal activity with very low resolution (Hillyard and Anllo-Vento, 1998). Other than medical diagnosis, EEGs can also be used to assist people with disabilities to perform certain tasks like controlling a wheelchair or browsing the web (Kobayashi and Nakagawa, 2015; Lopes, Pires and Nunes, 2013; John and Palaniappan, 2011; Spuler, 2015).

To record EEG, dry or wet electrodes need to be placed on exact locations by using an electrode cap or an adjustable headset on the participant's head and should be connected to an EEG amplifier. The electrodes acquire the EEG signals from the scalp and are amplified before being fed to an A/D converter where the signals are digitised for further processing. Minimum configuration for EEG measurement consists of three electrodes, one reference, one ground electrode and one active electrode. Multi-channel EEG configuration can have up to 256 active electrodes with high resolution (Teplan, 2002). Many consumer and research grade EEG acquisition systems *(Gtec, Emotiv, Neurosky)* are available in the market which are easy to install and operate. For event-related EEG acquisition, visual stimulators are required which can be generated on screen or via external dedicated hardware. Due to the large volume of data, EEG analysis is a complex process for feature extraction and also affected by background noise either from the brain or from the scalp. EEG has good temporal resolution, good portability, easier setup and is cheaper to implement than MEG, fMRI or NIRS.

2.2.1.2. Magnetoencephalography (MEG)

Magnetoencephalography is a non-invasive imaging technique used to investigate the human brain activity by means of magnetic induction and measurement of the magnetic fields generated by brain activity (Nicolas-Alonso and Gomez-Gil, 2012; Hassanien and

Azar, 2015). MEG is widely used in clinical practice to identify seizure areas in epilepsy patients and in other medical diagnostics like identifying tumour locations or other brain dysfunctions (Khalid et al., 2015; Duez et al., 2016). MEG requires a highly shielded laboratory environment that completely eliminates any external electromagnetic interference. The advantage of MEG is that it provides signals with higher spatiotemporal resolution than EEG, which minimises the training required and makes a reliable communication that is advantageous for an efficient BCI (Nicolas-Alonso and Gomez-Gil, 2012). Magnetic fields in MEG are less influenced by the electric currents as in the case of EEG, and provide information on neural activity as the signals are directly received from the neuronal electrical activity (Hassanien and Azar, 2015). Even though the MEG can be a reliable BCI, it is not recommended for an assistive system as it is expensive and requires a laboratory environment as well as not being portable.

2.2.1.3. Functional Magnetic Resonance Imaging (fMRI))

This is a non-invasive method based on brain imaging technique across the entire brain with high spatial resolution and moderate temporal resolution. fMRI measures the blood oxygenation level during the neuronal activity using electromagnetic fields (Min, Marzelli and Yoo, 2010). This is usually performed using MRI scanners and can localise the active regions inside the brain. It is not suitable for rapid BCI interaction due to the delays from temporal resolution and hemodynamic response delays (Nicolas-Alonso and Gomez-Gil, 2012). fMRI-BCI can be used in areas which need higher specificity for treatment or other disorders like chronic pain, motor disorders, memory disorders, stroke rehabilitation or other emotional disorders (Sitaram et al., 2007). fMRI can also be used to identify the brain regions involved in motor imagery to explore the influence of kinaesthetic or visual motor (Kilintari et al., 2016). Even though it is used in clinical applications, it is not promoted widely for BCI applications due to its large size and for being highly expensive.

2.2.1.4. Near Infrared Spectroscopy (NIRS)

NIRS is an optical spectroscopy non-invasive method which uses infrared light to penetrate the skull in the frontal cortex or occipital cortex to access the hemodynamic changes

with brain activation (Nicolas-Alonso and Gomez-Gil, 2012). NIRS has been identified as an alternative tool for BCI application where users are unable to use the EEG based BCI (Singh and Daly, 2015; Obrig, 2014; Kirk et al., 2016). Due to shallow penetration of infrared light inside the skull, this neuroimaging technique is limited to outer cortical layer and also the dependency of hemodynamic response requires care be taken in designing studies where higher spatial resolution is required (Cui et al., 2011).

2.2.1.5. Functional Transcranial Doppler Sonography (fTCD)

Functional transcranial doppler sonography is a non-invasive method and uses ultrasonic doppler imaging for analysing the neuronal activity (ŽVAN, 2012). fTCD has high temporal resolution and it helps in the investigation of fast neural activities which are related to the changes in local blood perfusion (Duschek and Schandry, 2003).

2.2.2 EEG – BCI : A practical approach

EEG based BCI has the advantage of being non-invasive and hence the BCI platform could be developed safely by using the brain signals from the scalp. EEG can be considered as one of the prime tools to study brain activity and is being widely used (Hwang et al., 2013b). It has the advantage of low cost, is comparatively easier to use with many modern portable headsets and excellent time resolution. EEG is basically recorded with electrodes on the surface of the scalp using dry or wet electrodes based on the EEG acquisition hardware. If wet electrodes are used, conductive gel placed between the electrode and the scalp is used to minimise the brain signal quality losses. One of the widely used methods in EEG based BCI, is the event related potential (McCane et al. (2015); Trauer et al. (2012); Hillyard and Anllo-Vento (1998); Chang et al. (2016a); Wu (2016); Wang et al. (2015b)).

2.2.2.1. Event Related Potential (ERP)

ERP components are widely researched and form part of tens of thousands of publications, yet there are still explorations to identify the properties of specific ERP components (Kappenman and Luck, 2011). ERP components can be defined as one of the component waves

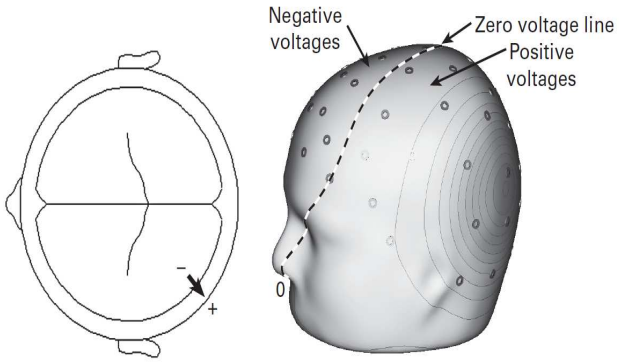

Figure 2.5: Voltage distribution over the scalp ((Luck, 2014) used with permission from The MIT Press)

of a more complex ERP waveform which are sensitive to task manipulations (Woodman, 2010). With ERP, it is possible to measure the brain activity from one millisecond to the next and most of the cognitive aspects appear to operate on a millisecond scale (Sur and Sinha, 2009). An ERP waveform is generated on the scalp and has a series of positive and negative peaks with changes in polarity, amplitude and duration representing neural or psychological processes (Kappenman and Luck, 2011). ERP techniques provide powerful methods for assistive support as well and also assist in medical diagnosis (Hillyard and Anllo-Vento, 1998; McCane et al., 2015; Kaufmann, Herweg and Kubler, 2014; Li et al., 2013). ERP components can be either negative or positive for a chosen electrode location and depend on various factors like whether the postsynaptic potential is excitatory or inhibitory, the location of the reference electrode, the orientation of the generator dipole with respect to the active recording electrode and whether the postsynaptic potential is occurring in the apical dendrite or basal dendrite (Luck, 2014).The scalp surface voltage recorded will be of different polarities on either side of the dipole with a zero separation line between the polarities as shown in Figure 2.5.

ERP components can be classified into main three categories, (a) exogenous, (b) endogenous and (c) motor (Luck, 2014). Exogenous ERPs are triggered by an external stimulus, whereas endogenous ones are based on neural processes and depend entirely on internally induced tasks. Motor based ERPs are based on preparation and execution of

a motor task. The widely used ERP based BCI communication systems are slow cortical potential, motor potentials, event related synchronisation and de-synchronisation potentials, P300 potential and steady-state visual evoked potentials (Berger et al., 2008).

i *Slow Cortical Potential (SCP)* : - These are low frequency potentials approximately less than 2 Hz recorded from the scalp that reflect the changes of activity level of cortical tissues relating to cognitive or sensory-motor events (Berger et al., 2008; Ergenoglu et al., 1998; Birbaumer et al., 1990). These are slow event related, originate from the upper cortical layer and can occur from 300 ms to several seconds. SCP is correlated with cognitive and motor performance. Negative SCP shift exhibits increased cortical excitability and positive SCP shifts reveal the cortical inhibition (Devrim et al., 1999). One of the first Thought Translation Devices (TTD) used SCP to control an on-screen object and were able to support paralysed patients (Birbaumer et al., 2000, 2003). SCP based BCI requires training through several stages by trial and error to perform the task. Even though the communication is slow, experiments have shown that it is feasible to support disabled people through SCP-based BCI (Hai-bin et al., 2009; Birbaumer et al., 1999). SCP requires continuous practice and extensive training to perform the tasks with correct responses (Saha and Lingaraju, 2015). The success of SCP based BCI is determined mainly on the users learning ability to produce a predefined brain response and also depends on the psychological and technical aspects (Hinterberger et al., 2004). An experimental setup of TTD based on SCP driven BCI is shown in Figure 2.6. Several factors influencing the SCP training and reporting experiences include psycho-physiological factors, baseline adaptation, eye movement artifacts, SCP localisations and sequence effects (Hinterberger et al., 2004). A recent study also identifies a decline in SCP based BCIs as compared to other ERP basedBCIs (Hwang et al., 2013b).

ii *Motor Imagery:* - This technique is a window to cognitive motor processes and motor control, and the imaginative power could be used to perform the required tasks. In motor imagery of cognitive processes, the subject imagines that some action is performed without actually performing the movement and without tensing any muscles (Mulder,

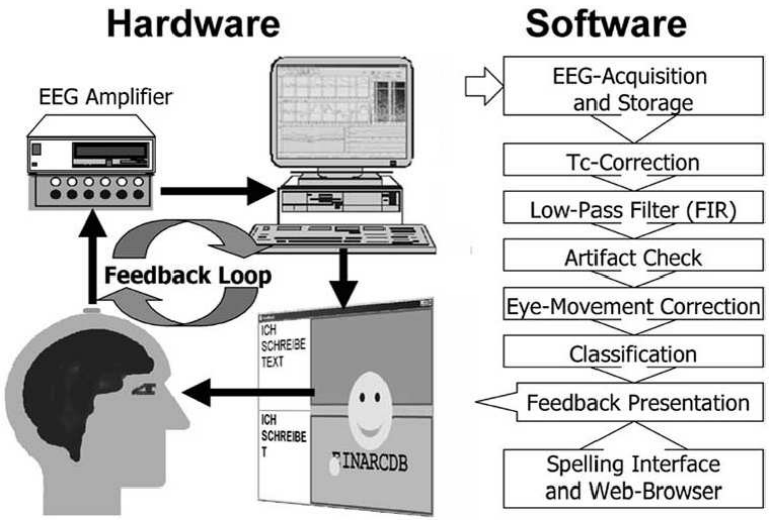

Figure 2.6: Experimental SCP based BCI ((Hinterberger et al., 2004) used with permission from IEEE)

2007). In other words, it is a conscious effort of simulating movements without performing them in an overt fashion and assumed to activate the same representation as the corresponding motor execution. In EEG, motor imagery can be used to generate specific patterns or cortical activations that could be used to control BCI. It is generally assumed that motor imagery tends to activate the same representation as the corresponding motor execution with the same temporal constraints as imagined and executed movements (Halder et al., 2011; Decety, 1996). Motor imagery could be used in the rehabilitation of stroke patients, determination of the strength losses after immobilisation of limbs, sports training or in treatment methods of Parkinson's disease (Munzert and Zentgraf, 2009; Lotze and Halsband, 2006). Recent studies have explored joint and single action motor imagery with good success rates that could be favourable for BCIs (Wriessnegger et al., 2016). Different areas of the brain are activated when a task is performed in single mode and in joint modes. The activation patterns are distinct and clear for both actions as shown in Figure 2.7. Motor imagery based BCI is gaining acceptance with commercially available headsets for controlling external applications, gaming and also in precision multi-task control (Martinez-Leon, Cano-Izquierdo and Ibarrola, 2016; Yu and Sim, 2016; Asensio-Cubero, Gan and Palaniappan, 2016).

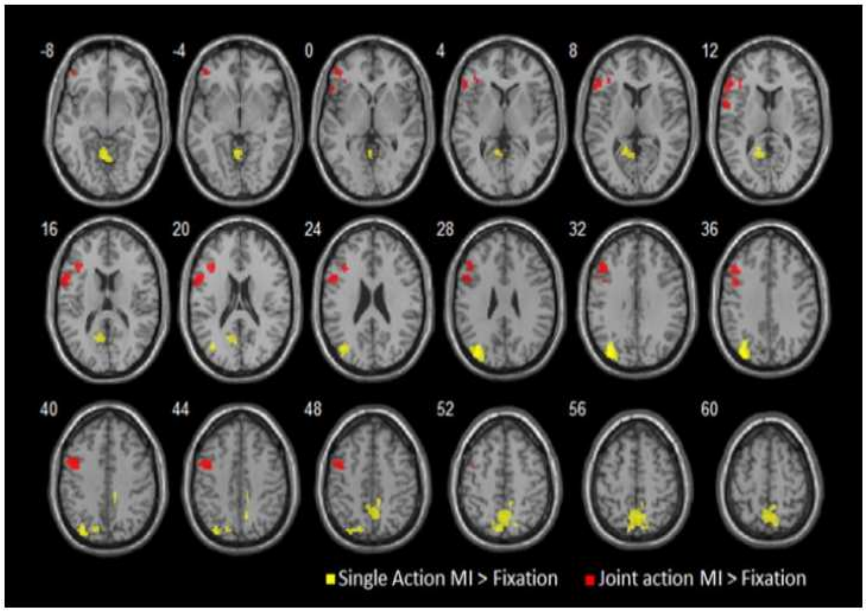

Figure 2.7: Activation areas for single action and joint action motor imagery ((Wriessnegger et al., 2016) used with permission from Elsevier)

iii *Event-Related Synchronisation and De-synchronisation:-* The physical movements and motor imagery induced changes in oscillatory activity can be recorded from the scalp with electrodes. If an increase in synchronous activity in response to an event is detected then it is referred as event-related synchronisation and when the decrease in response to an event is detected, it is termed as event-related de-synchronisation (Berger et al., 2008).

iv *P300 Evoked Potentials:* - P300 evoked potential is a large positive peak in the EEG over the midline areas and elicited due to infrequent auditory, visual or somatosensory stimuli. P300 depends on endogenous cognitive process and one of the most used control signals for EEG-based BCI (Aloise et al., 2011; Alcaide-Aguirre and Huggins, 2014; Wang et al., 2015c; Yin et al., 2015). The P300 large positive deflection also known as P3 occurs in the EEG roughly around 300 ms post stimulus. Usually, P300 based BCI does not require any training, but the habitual usage of the infrequent stimulus can reduce the amplitude of the P300 potential (Ravden & Polich 1999). P300 is well known for use in the P3 speller (Krusienski et al., 2008). Typical P300 based BCI comprises of letters, symbols or commands as shown in Figure 2.8. The system has a 6 X 6 matrix

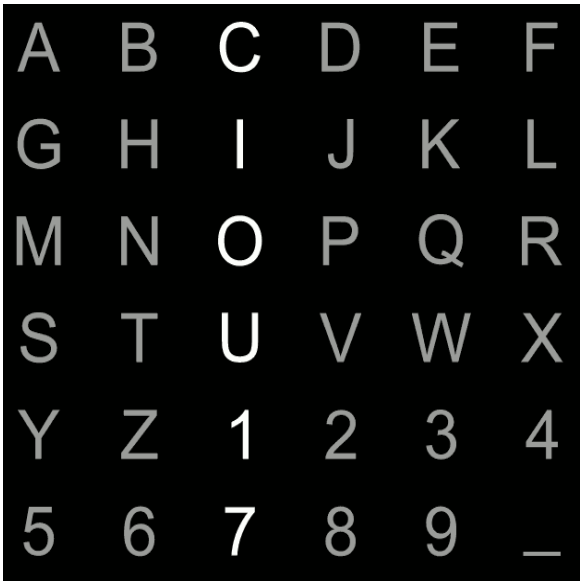

Figure 2.8: Basic P300 speller stimulus

with letters and numbers displayed on a computer screen. The stimulus events are intensified for a row or a column and the subject focuses on one cell in the matrix (Farwell and Donchin, 1988).

v *Steady–State Visual Evoked Potential (SSVEP):* - SSVEP is an exogenous BCI approach and requires minimal training, easy setup, higher bitrate and can work with single EEG channel. SSVEP based BCI produces natural responses to a visual stimulus flickering at frequencies above 6 Hz and produces brain signals with the same frequency as that of the stimulus. When the participant attends a visual stimulus flashing at 11 Hz, rhythms appear over the posterior visual areas with a fundamental frequency of 11 Hz and harmonics of this fundamental at 22, 33, 44 Hz and so on as shown in Figure 2.9 (Berger et al., 2008).

2.2.2.2. SSVEP based BCI development

SSVEP can be recorded from the surface of the scalp over the visual cortex with a minimal number of electrodes and has served as the basis of several BCI designs. The signal transport along the visual pathways is illustrated in Figure 2.10. SSVEP can be recorded from the surface of the scalp over the visual cortex with a minimum number of electrodes while

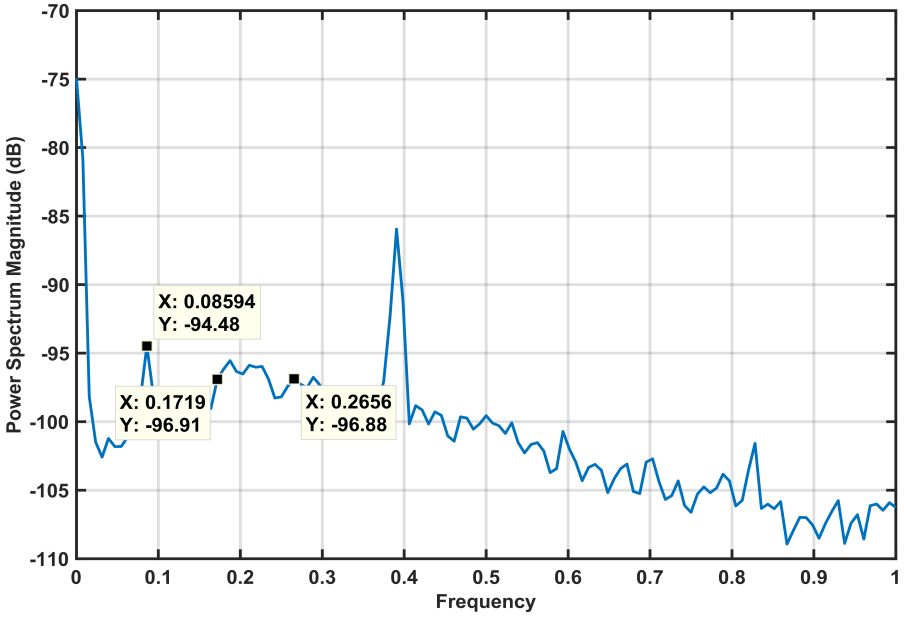

Figure 2.9: SSVEP response at 11 Hz along with harmonics

the subjects concentrate on a visual stimulus flashing at a constant frequency (Kalunga et al., 2016; Berger et al., 2008). In an SSVEP based BCI the primary factors that need to be addressed are the lead position, stimulation frequency and the frequency for feature extraction (Wang et al., 2009). Other than these primary factors, other issues that arise are the visual stimulus accuracy, stimulus portability, increasing the number of simultaneous visual stimuli, user comfort and reducing the visual fatigue.

SSVEP was first investigated for BCI by Middendorf et al (Middendorf et al., 2000) and in their experiment, the participants were presented with a visual stimulus flashing at a specific frequency. The participant's attention towards a specific visual stimulus was determined using spectral measures of the recorded EEG. The maximal amplitude of the frequency domain was at the frequency component identical to the flicker rate of the target that had the subject's attention. This method has become the paradigm of choice by many subsequent BCI researchers using SSVEP. The SSVEP properties allow target stimuli to be independently tagged by flicker rate and make it an ideal paradigm for BCI. Furthermore, SSVEP based BCI has the most important advantage of not requiring prior

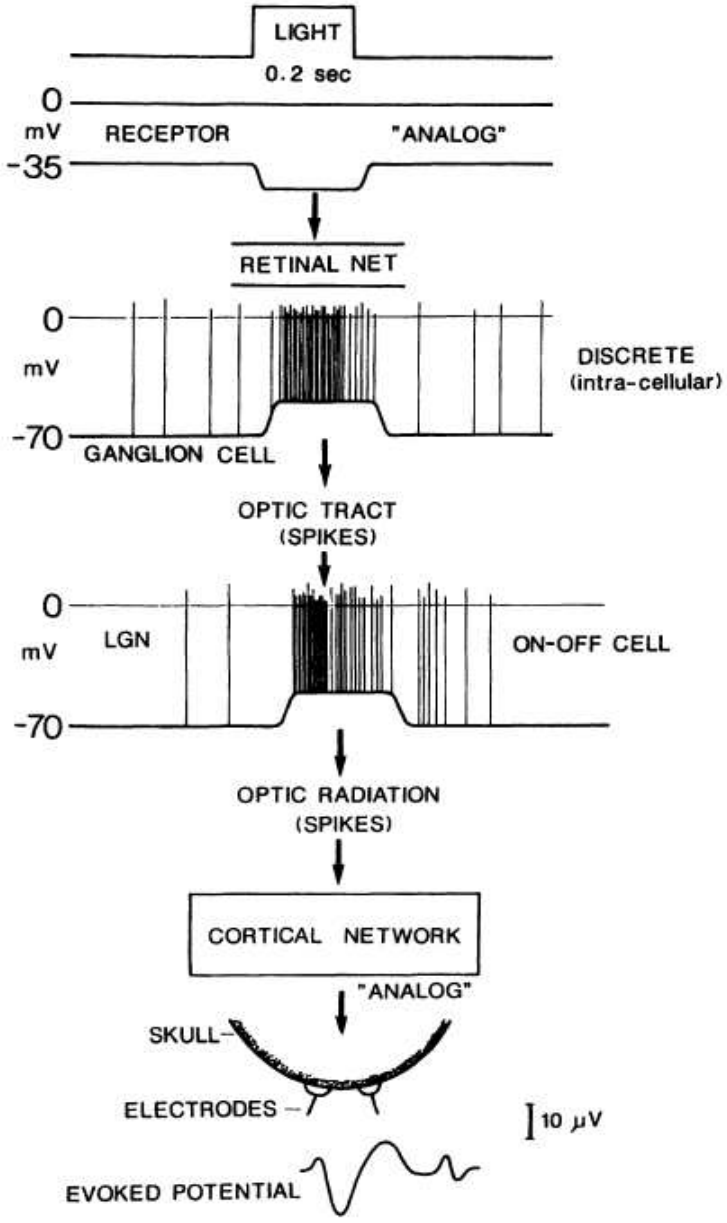

Figure 2.10: Signal transmission for evoked potential ((Henk-Van Der Twell, 1990) used with permission from Elsevier)

training, whilst offering high information transfer rate, and has been found to be suitable for numerous BCI applications such as keypad entry (Yijun et al., 2006; Hwang et al., 2012; Geng et al., 2011), device control (Martinez, Bakardjian and Cichocki, 2007) and assistive control (Muller-Putz and Pfurtscheller, 2008; Diez et al., 2013). The selection of frequencies in SSVEP allows artifact reduction such as blinks and background EEG and therefore SSVEP based BCI systems are more robust than other systems such as transient Visual Evoked Potential (VEP) (that uses P300 potentials below 8 Hz) and imaginary movement based BCI systems (that use mu and beta rhythms) (Volosyak, Cecotti and Gräser, 2009).

Recent research in signal processing techniques has opened more doors towards developing intelligent real-time algorithms for extraction and processing of EEG data that is suitable for SSVEP (Delorme et al., 2011; Iacoviello et al., 2015; Zhang et al., 2013; Wu et al., 2011; Erwei et al., 2015; Wang et al., 2015c). SSVEP studies have also shown that the amplitude of the response for flicker frequencies varies with the subject's focus, the colour of the flickering stimulus and also the visual stimulus shape (Nishifuji and Kuroda, 2012; Singla, Khosla and Jha, 2014; Cheng et al., 2001; Wang et al., 2015a). For practical applications the SSVEP signal needs to be filtered to separate it from the induced noise such as background EEG, artifacts or other external noises from the power-line to improve the classification processes.

Even though SSVEP responses are sufficiently high for practical purposes, it is not always comfortable for subjects for longer periods of time especially when the visual stimulus is presented using LCDs. Amplitude-frequency characteristics of SSVEP in humans have larger amplitudes from alpha to low beta ranges and with frequencies higher than 31 Hz produces poor SSVEP response and weaker signal to noise ratio Signal-to-Noise Ratio (SNR) (Po-Lei et al., 2011). Studies show low frequencies give higher responses as compared to high frequency stimuli, though the latter is more comfortable with subjects with reduced visual fatigue (Dong-Ok et al., 2016, 2014; Kuś et al., 2013). SSVEP elicitation is also influenced by overt and covert attention, where overt mode amplitudes are higher than the covert attention mode (Walter et al., 2012).

In SSVEP one of the major issues is visual fatigue that is caused by the prolonged usage of visualising the visual stimuli by the users. Visual fatigue is a form of eyestrain concerned with different aspects of vision with symptoms such as watery eyes, red eyes, headaches or dry eyes and may occur after prolonged usage of reading, bright lights or staring at a digital screen (Collins, 1959). A study by Weston, (Weston, 1953) explored visual fatigue based on the effect of different systems of lighting defines visual fatigue as a combination of oculo-muscular exertion and mental exertion. Many researchers have conducted studies on the effect of visual stimuli on a subject's comfort and to reduce the visual strain (Punsawad and Wongsawat, 2012; Volosyak et al., 2011; Mun et al., 2012; Makri, Farmaki and Sakkalis, 2015). These studies identify that higher frequencies are more comfortable for subjects and reduce visual fatigue though giving weaker responses.

SSVEP requires precise visual stimulus to evoke the response and traditionally stimulus designs are based on LCD displays. The LCD based stimulus presentation has a direct impact on the user and also on the efficiency of SSVEP generation (Volosyak, Cecotti and Gräser, 2009; Wu et al., 2008). Most available LCD screens are based on 60 Hz refresh rates and can display only a limited number of different flickering objects. Considering an LCD with a vertical refresh rate of 60 Hz, the frequencies that can be generated are 6.66 Hz (i.e. 9 frames per second, 60/9), 7.5, 8.57, 10, 12 and 15 Hz. It is not possible to generate any other required frequency like 7, 8 or 9 Hz or choose high duty-cycles of the visual flicker due to the fixed refresh rate of the screen. Gazing the visual stimulus on an LCD screen for longer periods of time can make the user tired due to visual fatigue not only from the flashing objects on screen but also from the flicker generated by the screen itself which can reduce the SSVEP responses. Since the software controls the flicker generated on the LCD, the accuracy of the generated flicker would not be easier to verify with an oscilloscope as it is also depended on the refresh rate of the LCD. Visual stimulus presentation based on an LCD screen is shown in Figure 2.11. Each block flicker at different frequencies and are displayed at the same time. This can problematic when BCIs rely on covert attention shifts as target stimuli is spatially separated and SSVEP response significantly

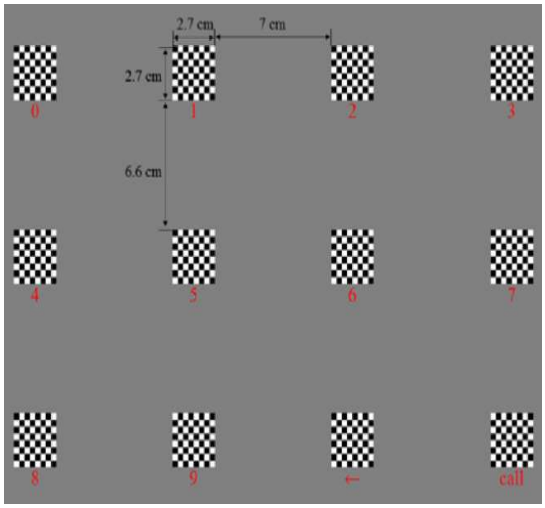

Figure 2.11: LCD based visual stimulus ((Chang-Hee, Han-Jeong and Chang-Hwan, 2013) used with permission from Elsevier)

reduces when the stimulus is out of the centre of the visual field (Dan et al., 2009).

Visual stimulus based on LEDs is getting more attention recently due to its better accuracy in generating the required frequencies as the flickering frequencies can be more precisely controlled (Wu et al., 2008; Po-Lei et al., 2011; Chang et al., 2014; Wang, Wang and Jung, 2010). It is also possible to increase the number of flickering stimuli and can be controlled by dedicated hardware. Figure 2.12 shows a basic LED based stimulus to evoke SSVEP.

LED stimulus has the advantage of generating the required colour using RGB LEDs in the same source thus avoiding the issues in attention shifts. The response in SSVEP amplitude for different colour stimulus could also be studied for different subjects for optimum performance. The locations of the stimulus can be easily customised in comparison with the larger LCD based stimulus. The portability and lower power consumption of the hardware would be an added advantage in making the BCI more portable. Most of the parameters in LED based stimulus like frequency, colour, orientation or intensity can be programmatically controlled and this can reduce the visual fatigue or improve the personal preferences of the user.

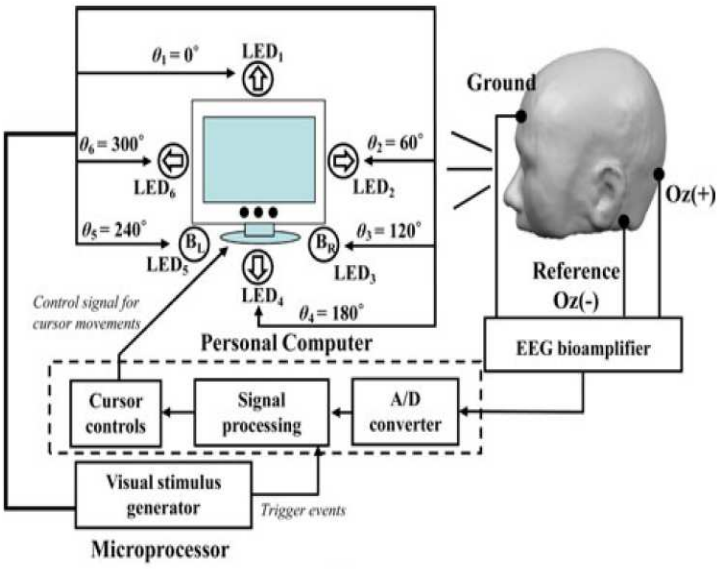

Figure 2.12: Basic LED based visual stimulus ((Po-Lei et al., 2011) used with permission from IEEE)

BCI data analysis requires complex signal processing methods and algorithms. The most common analysis package used is MATLAB (Chua et al., 2004; Elbuni et al., 2009; Hai-bin et al., 2009; Christian Andreas and Scott, 2013; Makri, Farmaki and Sakkalis, 2015; Friganović, Medved and Cifrek, 2016; Chang et al., 2016b; Files and Marathe, 2016). Various toolboxes like EEGLAB and ERPLAB are available as plugins for MATLAB for signal analysis. Most EEG hardware is supplied with data acquisition libraries for data recording in MATLAB or with their own recording platform like Test Bench for EMOTIV. Fast Fourier transforms (FFT) are commonly used for processing of data. A combination of filters is used to shape the EEG signal for the required frequencies in either offline data processing or in the real-time mode. Real-time mode algorithms are more complex as the capture and processing times are reduced to the lowest possible interval. Figure 2.13 and Figure 2.14 shows the FFT amplitude of SSVEP at different stimulus frequencies.

Various studies in SSVEP based BCI shows the flexibility in flicker stimulus usage and the ease of customisation in flickering frequencies either using LCD or high power LEDs. Po-Lie (Po-Lei et al., 2011) performed an investigation on SSVEP using high duty-cycle visual flicker, finding that a higher duty-cycle gave visual comfort to participating subjects.

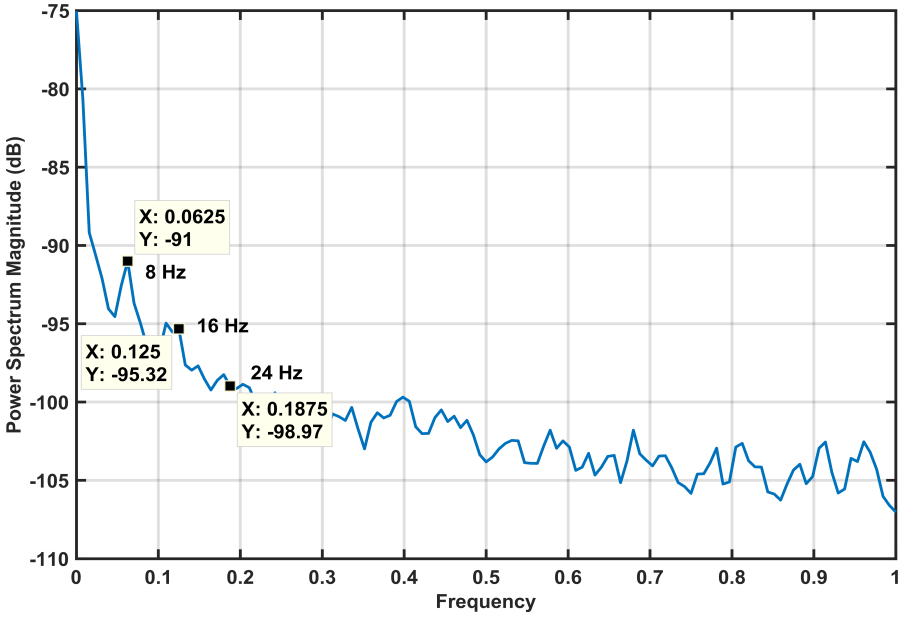

Figure 2.13: FFT amplitudes of SSVEP at 8 Hz

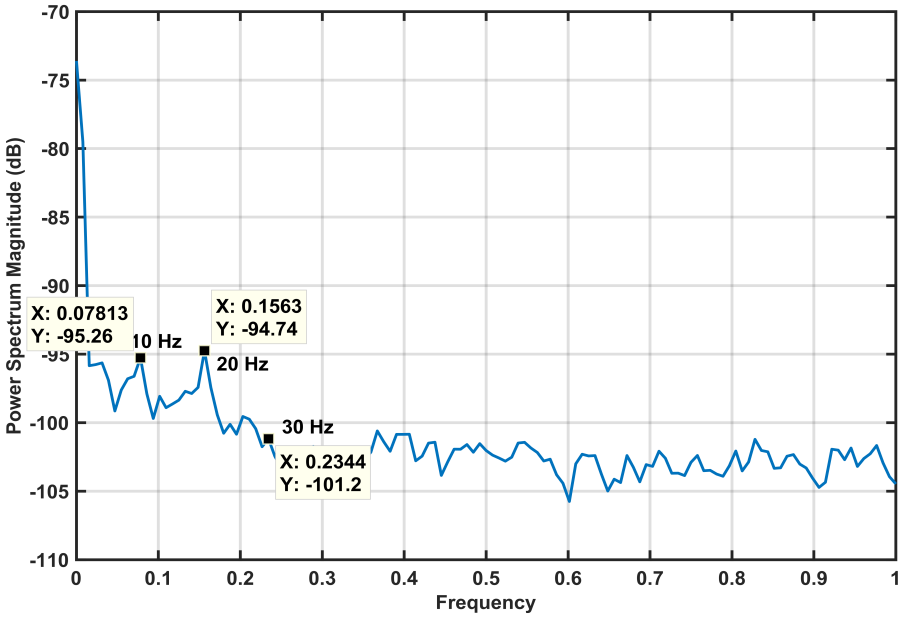

Figure 2.14: FFT amplitudes of SSVEP at 10 Hz

This research also identified that amplitude-frequency characteristics of SSVEP in humans have larger amplitudes from alpha to low beta ranges and reaches a maximum amplitude at approximately 13 Hz. Flicker with frequencies higher than 31 Hz produce poor SSVEP response and weaker SNR. Flicker frequencies lower than 20 Hz achieve higher SNR for SSVEP based BCI but cause the flicker to feel jerky, leading to discomfort.

A study on the effects of overt and covert attention by Walter (Walter et al., 2012) compared the modulations of SSVEP when subjects gazed at a flickering array of static dots and when they covertly shifted attention to the dots while their eyes were centrally fixed. This identified that navigating BCI's with SSVEP is more reliable with overt attention. Horizontal eye movements were avoided in covert attention and only used in overt and were monitored. An amplitude enhancement was greater in trials with overt attention and it was ten times lesser in covert attention. The results, when compared with ERP based BCI, which was 40-50% accurate compared to the accuracy of SSVEP at 55% was remarkable. Overall overt and covert attention differs in their effect on SSVEP amplitudes and behaviour. Lower amplitude modulation by covert attention must be considered for both development and application of classification procedures in covert SSVEP based BCIs. The classification procedures required improvement. The study also examined the impact on SSVEP amplitudes when the subject looked at a flickering stimulus or covertly attended to such a stimulus without moving their eyes from central fixation.

EEG changes associated with mental changes with SSVEP were investigated by Nishifuji et al. (Nishifuji and Kuroda, 2012) in eyes closed conditions and revealed SSVEP amplitude changes with mental focus for flickering stimulus. This study investigated the dependency of the SSVEP amplitude on the mental focus to flicker stimuli in order to apply to the BCI based on SSVEP with eyes closed, for the disabled subjects who are not able to control their eye movement to use conventional SSVEP based BCI. SSVEP based BCI under eyes closed conditions is required to be developed for severely disabled who are not able to control their eye movements. This study investigated the effect of the mental focusing to the flicker stimuli with a single stimulus frequency that was applied

to healthy subjects with eyes closed. Digitised EEG data was analysed using Discrete Fourier Transform (DFT) to estimate the amplitude of fundamental SSVEP at the stimulus frequency. The mental focusing on or paying attention to the flicker stimuli was seen to elicit a significant change of the SSVEP amplitude by an average of 20% with reference to the non-focusing state.

SSVEP-BCI performance without gazing was explored by Lopez-Gordo et al. (Lopez-Gordo, Pelayo and Prieto, 2010) showed efficient communication and improvement in information transfer rate is possible when steadily looking at the visual stimulus. The performance improvement was achieved using both amplitude and phase of the SSVEP in the classification as well as the use or absence of gaze as a way for helping to ignore the stimulus. The test was conducted on six healthy subjects in an insulated room using a single channel active electrode placed on the scalp over the occipital cortex at Oz and the reference electrode at Fz with ground connected on the right earlobe. The data was sampled at 250 Hz and digitised with a resolution of 16 bits. The stimulus was presented using a Cathode Ray Tube (CRT) type monitor with 140 Hz refresh and resolution of 800 X 600. The data collected was transformed by DFT and the coefficients at the fundamental and first harmonics of the SSVEP extracted. Both amplitude and phase of each coefficients were used in classification. The results obtained were quite promising compared with other binary class BCI and were not far from multi-class BCI, but without the need of gazing.

Visual spatial attention tracking using SSVEP, investigated by Kelly et al.(Kelly et al., 2005), suggested that SSVEP can be used as an electrophysiological correlate of visual spatial attention that could be used standalone or with other correlates to control an independent BCI. This research focused on a BCI system, which was independent of eye movements. Sixty four channels of EEG data were recorded from subjects who covertly attended to one of two bilateral flicker stimuli with superimposed letter sequences. Using offline classification, left/right spatial attention was attempted by extracting SSVEP at optimal channels selected for each subject on the basis of scalp distribution of SSVEP

magnitudes and the results yielded an accuracy of approximately 71%. Research focused on SSVEP behaving as an index of visual-spatial selective attention by which the brain identifies and focuses on discrete locations in visual space for preferential processing. This attention selection can be performed independent of gaze direction. The components in peripheral vision (covert) may be selected for processing just as those in foveal vision (overt). The aim was to use high density EEG data to characterise the topography of SSVEP modulations so that features during covert attention to the left and right visual field could be optimised. The study also aimed to compare frequencies within and outside the alpha band. These were performed by offline left/right classification of SSVEP data.

A dry electrode based SSVEP study was performed by Edlinger et al. (Edlinger, Krausz and Guger, 2012) on both endogenous BCIs and exogenous BCIs. This study mainly focused on the usage of dry electrodes in BCI. Different data capture techniques were explored using g.SAHARA dry electrode sensors. The setups were based on P300, SMR (sensorimotor rhythmic), and SSVEP BCI. The major focus was on P300 evoked potentials but also demonstrated the electrode concept works well for SMR and SSVEP based BCI in both endogenous BCI and exogenous BCI. In endogenous BCI, subjects learn and train to perform specific mental tasks to change brain activity. This includes slow SCP, sensorimotor rhythmic (SMR), ERD and ERD based BCI. In exogenous BCIs, an external stimulus evokes a specific change in the brain activity. This depends on focused or selective attention to an external stimulus. This includes P300 response and SSVEP. The study identified one of the limiting factors in BCI is the usage of abrasive gel or conductive paste to mount the EEG electrodes. Subjects reported discomfort participating in EEG experiments or even rejected participation as hair washing was required after the experiments. The study revealed dry electrodes can yield performance comparable to gel electrodes with a P300 BCI. These electrodes can be used for SMR and SSVEP based BCI as well and dry electrode systems can function in relatively unconstrained environments. The biggest advantage of not using abrasive or conductive gel is convenience and the fact that there is no cleaning required. This also increases the acceptance of the technology for a wider range of users.

The position of electrodes and EEG magnitude were explored by Rice et al. (Rice et al., 2013), revealing that the EEG power is strongly affected by electrode position for different subjects. The study identified this is due to the gravity induced changes in Cerebrospinal Fluid (CSF) layer thickness. The thicker CSF layer could greatly decrease EEG signal amplitude. This could also be used to identify certain neuro-degenerative diseases caused by thickening of the CSF layer. The study also explored a number of stimulation protocols and investigated the optimum positions of the electrode for recording EEG and thus maximising SNR.

Research based on customisation of stimulation for enhancing performance in SSVEP based BCIs by Lopez et al. (Lopez-Gordo et al., 2011) showed SNR was significantly dependant on the combination of frequencies in visual stimulus. The study recommended the selection of appropriate stimulus configuration, or else it may cause degradation in information transfer rate. The correct frequency selection of the spacial and temporal frequencies would have a considerable effect on information transfer rate and this must be taken in to account. This study also highlighted that it is also possible to use this technique with subjects who are unable to control their gaze sufficiently.

Investigation on high speed SSVEP based BCI for various frequency pairs and inter-source distances were performed by Resalat et al. (Resalat et al., 2012) where the study showed the volume of stimulus could be small and that the inter-source distance of 14 cm could be practical. The research used a high speed max one classifier for seven different frequency pairs and five different inter source distances. The study identified the best frequency pair as 10 Hz and 15 Hz and gave the highest accuracy, and also that the sweep length of 0.5 seconds has the highest information transfer rate that would be practical in the real-time application of BCI.

SSVEP BCI sensor comparison for dry and non-contact modes were studied by Chi et

al. (Chi et al., 2012) that showed the information transfer rate of dry sensors were comparable to wet sensors. Dry and non-contact sensors could be considered as an enabler towards the practical BCI platforms. Basically non-contact sensors have poor coupling interface through hair and this degrades the signal quality, the trade-off being ease of use, no preparation or conductive gel required. With further improvements to signal amplifier designs, dry and non-contact sensors may become a viable tool for mobile EEG application with real-time requirements.

Research on the effect of the duty-cycle in different frequency domains on SSVEP BCI by Huang et al. (Huang et al., 2012) showed that there was a significant improvement in the performance for the adjustment of duty-cycle and that this is different for different frequencies. The study also found Canonical Correlation Analysis (CCA) was more reliable than Power Spectral Density (PSD) due to its higher noise robustness. The study identified that the stimulus frequencies should not be selected very close to each other as the domain resolution for PSD and CCA depends on the length of the time interval. In a practical real-time scenario the stimulus frequencies should not be near to each other as they can overlap and make false triggers for external control.

A study by Punsawad et al. (Punsawad and Wongsawat, 2012) identified a novel method for visual stimulus in SSVEP BCI using motion visual stimulus to reduce visual fatigue in subjects. The investigation used attention detection and SSVEP detection with a combined classification accuracy of 80%. A motion visual stimulus was achieved with an LCD monitor with vertical strips moving left or right and this evoked the SSVEP. The limitation of this study was the limited availability of visual stimulus when it's implemented for a real-time application.

An investigation on the effect of flashing colours on the performance of SSVEP was undertaken by Teng et al (Teng et al., 2012) who found that white stimuli gave higher performance followed by grey, red, green and blue. The stimulus was presented on an LCD monitor with a refresh rate of 120 Hz. The experiments were based on five flicker stimuli

for offline and sixteen flicker stimuli for online. EEG used a six electrode system and filtered by 0.5 Hz and 60 Hz band-pass filters with 600 Hz sampling rate. The influence of colours affects the SSVEP and could be used to reduce the visual fatigue by choosing the preferred colours for subjects. Since the colour stimulus was presented on an LCD, the colour depth varied according to the LCD manufacture's colour profile. The study also did not mention any colour calibration methods used for presenting the colour stimulus. Even though, the study identified the influence of colour in SSVEP, it needed to be further investigated with visual stimulus based on LEDs which can produce colours with specific wavelengths.

Research on dual frequency stimulation for SSVEP to increase the number of visual stimuli was done by Hwang et al. (Hwang et al., 2013a) and identified the necessity of a greater number of visual stimuli. The experiment was based on combining two different patterns of visual stimuli flickering at different frequencies in one single visual stimulus. This also solved the issues of user attention shift and was confirmed with offline and online experiments.

A study by Chen et al. (Chen et al., 2014) has explored the possibilities of increasing the stimuli through hybrid frequency and phase coding. Using two hybrid frequencies 40 stimuli were presented on an LCD screen with frequencies from 8 – 15 Hz and EEG data were acquired using a nine electrode system. The experiments demonstrated the possibilities of increasing stimuli using an LCD screen with fixed refresh rate. Even though multiple stimuli could be presented on an LCD, it can lead to attention shift since it is closely displayed and would not be suitable for a portable BCI platform due to the size 24" LCD display.

Studies on the effect of higher frequency on SSVEP classification by Dong et al. (Dong-Ok et al., 2016) identified high frequency visual stimuli were beneficial for performance

improvement and were more stable for developing practical SSVEP based BCI applications. The study used three different duty-cycles of 50, 60 and 70% for the visual stimulus which were based on high power LEDs. The experimental setup was based on a 30 character SSVEP BCI speller without calibration and the performance was evaluated for classification accuracy and subjective fatigue. The experiments were repeated for high frequency (>25 Hz) and low frequency (<25 Hz) to compare the classification accuracy and fatigue level. The investigation revealed high frequency classification accuracy was higher when compared with the low frequency system. The visual fatigue was reduced by using high frequency flicker and the participants were comfortable gazing at the stimulus. The higher duty-cycle induced stronger SSVEP response since the LED was on for a longer time. The study used 32 electrodes for this experiment and recommended higher frequency for SSVEP applications. The platform is not suitable for practical BCI due to its higher number of electrodes and is less portable.

Study on the influence of colour on SSVEP based BCI by Aminaka et al (Aminaka, Makino and Rutkowski, 2014) found possible side-effects by monochromatic light can be minimised by utilising green-blue flicker at higher frequencies. The experiment had three participants and the chromatic stimulus exhibited better accuracy than the traditional monochromatic stimulus. The experiment was based on LED based stimulus using an Arduino UNO platform generating square waves for the on/off state for the stimulus. The influence of colour in SSVEP stimulus was also confirmed in this study.

A study by Joel Eaton, (Eaton, 2015) on Brain-computer music interfacing (BCMI) using SSVEP shows a novel approach music making. The study improves the accuracy of meaningful brain signal and s that to control various musical features.The visual stimuli were based on four LED matrix arrays using RGB LEDs and four mini Thin Film Transistor (TFT) screens to display the user choice. The study presents a novel idea for practical SSVEP application and demonstrated the concept with live performance.

2.3 Summary of findings

SSVEP based BCI requires visual stimulus with an accurate frequency based flicker that is hard to generate with traditional LCD screens. Since the LCD screens vary in refresh rates, it would be difficult to generate the same stimulus flicker frequency with another screen from a different manufacturer. The generated flicker accuracy is also depended on the graphics card capabilities and requires a complete computing system to present the stimulus to the user. The screen-based flicker would also influence each other and make it more complicated in classification. The led-based stimulus has higher bit rates as compared to the LCD/CRT based stimulus and also not limited by the refresh rates of the screens (Zhu et al., 2010).

Different LED-based stimulus designs need to be explored as there is only minimal research done in the SSVEP domain. The hardware kit available from g.tech can only generate four flicker with fixed frequency, colour and spacing (Guger, Edlinger and Krausz, 2011). To explore the influence of visual stimulus and make it more adaptable and comfortable for the users is necessary for the development of SSVEP based BCI. For an SSVEP based BCI control platform, the stimulus hardware should be portable, customisable with reduced visual fatigue for the user when used for longer duration.

To study the influences of visual stimulus in SSVEP, parameters such as colours, frequency, orientation, luminance and effect of stimulus duty-cycle needs to be investigated, which could influence the user response as well as reduce the eyestrain for the user and make it more adaptive for real-time usage. The required hardware platform should be developed as a standalone hardware with expandability and portability to generate the required SSVEP stimulus with the possibilities to use the platform for other vision-based studies or medical diagnosis. Various hardware platforms should be developed and tested for different stimuli configuration based on colour, frequency, LED type, stimulus orientation, portability, user comfort and improved user response for a practical SSVEP-BCI control system.

Chapter 3

SSVEP Stimulus Hardware Development

3.1 Introduction

This chapter focused on the stimulus hardware design, based on LEDs to reduce the visual fatigue and improve comfort for the user. The hypothesis is that the choice of LED-based visual stimulus design would improve the SSVEP responses and reduce the visual fatigue for the user as well as improve the portability in presenting the visual stimulus to elicit SSVEP. The new standalone platform would be easier for user customisation for the choice of colours, frequency and mobility. The hardware design is based on a microcontroller platform which can be customised to generate frequency flickers within a range of 5 Hz to 50 Hz precisely. For the visual flicker, a high power RGB LED was used to generate the required colour and frequency combination to evoke SSVEP. The customisable hardware platform and the required firmware was successfully developed to generate the visual flickers and can precisely set the frequencies for prolonged usage. Using the visual stimulus, EEG was recorded from five subjects for different frequencies, colours and LED encapsulation type (conventional clear and frosted) to test the performance of the visual stimulus and qualitative user comfort while attending to visual stimulus. The results were statistically analysed for primary colours Red, Green and Blue with stimulus frequency values 7, 8, 9 and 10 Hz in which 7 Hz Green conventional clear LED gave the

highest response for all the participants when compared with other colours and all other frequencies. Furthermore, all participants indicated that they were more comfortable with the frosted stimulus even though the responses were comparatively lower than the clear LED.

3.2 Visual stimulus design and requirements

Efficient and prolonged usage of SSVEP requires visual flicker with precise frequency, reduced visual fatigue and user comfort. Traditionally, visual flicker is generated using LCD/CRT screens which are based on the primary vertical refresh rate of the screen (Zhu et al., 2010; Erwei et al., 2015; Wang et al., 2015b; Martišius and Damaševičius, 2016; Luzheng et al., 2013). The CRT based visual stimulus also induces unwanted artifacts due to electrical fields from the CRT when the user is closer to the screen (Lyskov et al., 1998). Even though LCD based visual stimulus generation gives better viewing conditions and sharp edged pixels in comparison with the CRT based stimulus, the number of individual visual stimuli that can be generated is still limited to the refresh rate of the screen (Menozzi, Näpflin and Krueger, 1999; Chen and Lin, 2004; Menozzi et al., 2001). Refresh rate defines the number of times the screen is redrawn in one second, 60 Hz implies that the screen is redrawn completely sixty times per second. Even sixty frames per second can cause an imperceptible flicker that may induce visual fatigue when gazed for a longer period and would degrade the quality of the recorded EEG. The frequencies that can be generated for visuals flicker based on a 60 Hz LCD screen is shown in Figure 3.1. The visual stimulus frequencies for the visual stimulus must be chosen as a multiple of the monitor vertical refresh rate. This reduces the possibilities of generating frequency values to 7 Hz, 8 Hz, 9 Hz or similar values with a 60 Hz refresh rate and makes it complex to present more visual stimulus on screen. When multiple visual flickers are displayed on the screen, it makes it difficult for the user to focus on a particular flicker due to attention shift or interference from the adjacent visual flicker displayed on the screen. The frequency accuracy of the generated flicker is dependent on the software based flicker stimulator and would be difficult to verify using an external oscilloscope.

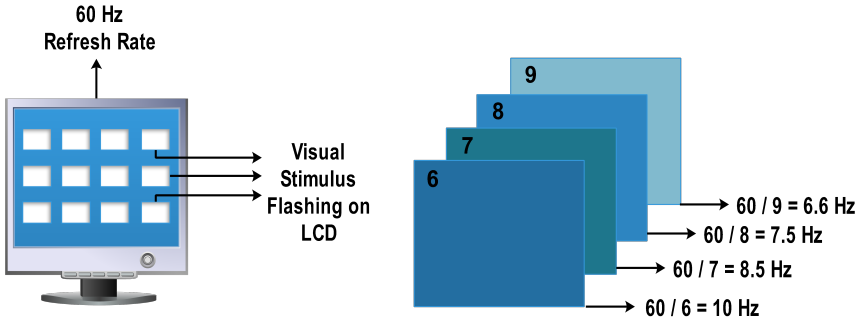

Figure 3.1: Frequencies that could be generated with LCD with 60 Hz refresh

These primary issues could be addressed with visual flicker based on LEDs. LEDs are more common, low cost, easily portable, low power consumption, multi-chromatic and very flexible for customising a visual stimulus (da Silva Pinto et al., 2011; Demontis et al., 2005; Rogers et al., 2012). LED based visual stimulus does not generate Electromagnetic Interference (EMI) in EEG recording while the stimulus is being presented to the user, unlike LCD/CRT based stimulators. LED stimulus has the advantage of generating the required colour using RGB LEDs in the same source thus avoiding the issues in attention shifts and in generating exact colours for repeatability (Dan et al., 2009).

A portable LED based SSVEP visual stimulus design requires a robust customisable standalone platform which can generate a wide range of visual flicker from 5 to 100 Hz, ideally without any restriction in frequency selection accurate for the flicker frequency. Figure 3.2 shows a visual flicker control platform that can generate simultaneous flicker outputs to evoke SSVEP. With LEDs, the generated flicker frequencies can be precisely measured using an oscilloscope. This is an advantage when the signal is pre-processed, filtered and classified. The response in SSVEP amplitude for different colour stimulus could also be studied for different subjects for optimum performance. The locations of the stimuli can be easily customised in comparison with the larger LCD based stimulus where all the visual flicker areas are adjacent. The portability and lower power consumption of the hardware would be an added advantage in the mobilisation of BCI or other visual studies. Most of the parameters in LED based stimulus like frequency, colour or

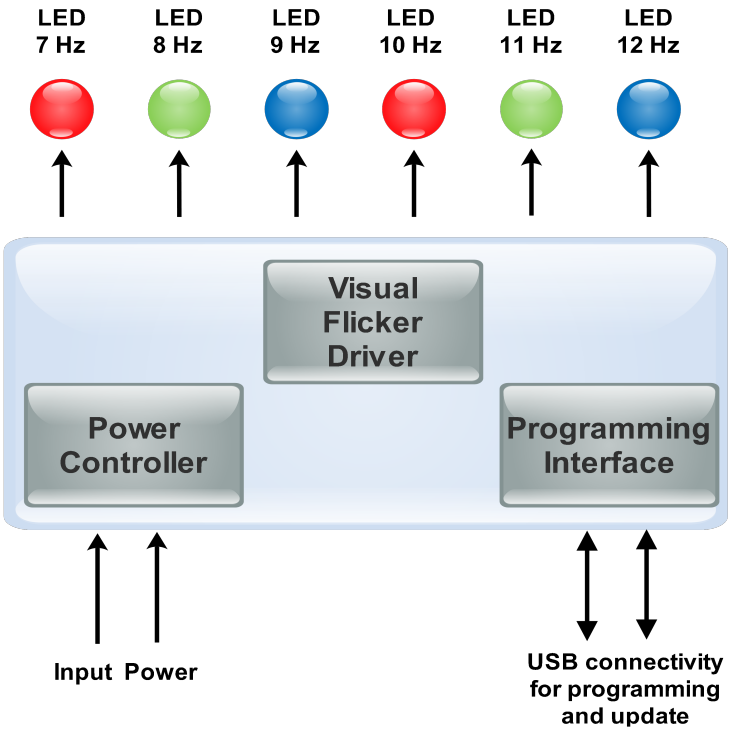

Figure 3.2: Visual flicker control block

intensity can be programmed to the controller and this could reduce the visual fatigue or improve the personal preferences of the user.

Various types of LED were analysed in the design and development of the visual stimulus platform in this thesis. Initially, individual and matrix LEDs as shown in Figure 3.3 were tested. These LEDs come in colours of red, green, blue and white and when all LEDs in the matrix are lit. It produces a bright light. The LED module has a built-in power controller that works with the microcontroller. The microcontroller used to develop the flickering stimulus was based on Microchip 18F25K22 with a built-in clock oscillator and operating speeds up to 16 MHz as shown in Figure 3.4. The firmware developed for this platform was able to generate flicker frequencies from 5 Hz to 30 Hz with a precision of ±0.15 Hz for single frequency flicker. An issue with the system is that when more than one frequency flicker was programmed for simultaneous operation, the system lost its precision by almost 50%, dissipated more heat and finally ceased to work.

Figure 3.3: LED modules tested

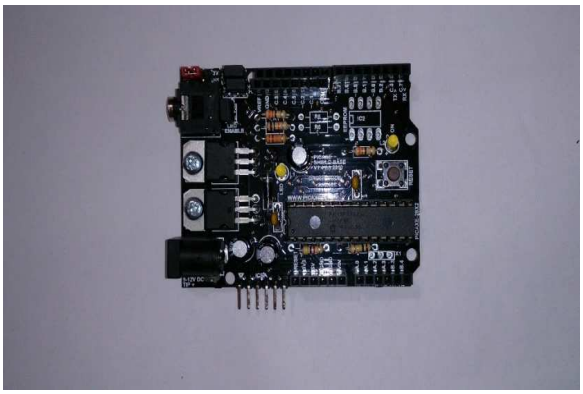

Figure 3.4: Initial hardware platform

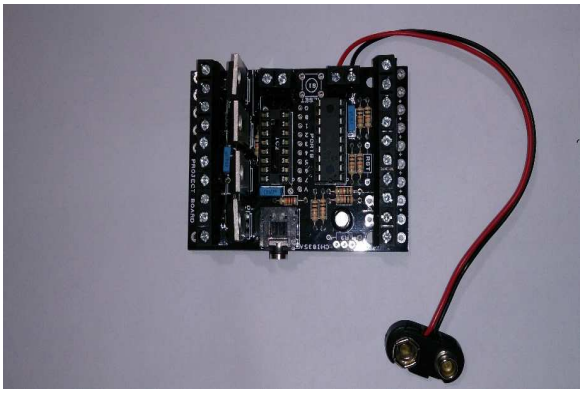

Figure 3.5: Updated version of visual stimulus platform with MOSFET drivers

To address this issue, the basic hardware was upgraded to a Pic-axe platform as shown in Figure 3.5. This platform could simultaneously work with four different frequencies with high precision. It powered the LEDs with a driving MOSFET allowing the system to function for longer periods without any heat issues. The LED matrix system was used as a stimulus and flashed with precise flicker frequency, confirmed with a digital oscilloscope. During the initial tests, the participants did not feel comfortable as the flashes were very bright and each LED in the matrix was seen as an individual light source, causing attention shift issues as well as visual fatigue. With further investigation in light source for visual stimulus, a single high power LED was chosen. Due to the requirement of different colours, an Red, Green and Blue (RGB) 1W power LED was tested, and results were deemed acceptable. The advantages being: the source of light is single, choice of different colours from the same source, no attention shift issues, wide range of operating frequency and availability of different package types (frosted and clear). Figure 3.6 shows the RGB Surface Mount Device (SMD) LED (Part No: YSH-FRGBB-IA) assembly for frosted and clear LEDs used for the experiment. The colour wavelengths were Red – 620 nm, Green – 520 nm, Blue – 460 nm.

With the new LED module, the hardware platform required updating, as the new LED system required voltage sources of 2.9 to 3.2 V DC for different colours. The RGB LED package had six terminals, anode and cathode for each colour. Anode or cathode can be

Figure 3.6: RGB LED stimuli

Figure 3.7: Hybrid voltage regulator

grouped together to form either a common anode configuration or common cathode configuration respectively based on requirement. Due to the power requirements, the 12 V DC working voltage had to be varied and regulated to suit the LED module. Texas instruments PTR08060W switching regulator was used to stabilise the power source according to the requirements for a constant current supply. The regulator could produce the output at a rating of 6 A with an efficiency of 96% with 12 V DC as input and as shown in Figure 3.7. The schematics are shown in Figure 3.8 and the prototype is shown in Figure 3.9.

The multi-turn potentiometer can be used to set the voltage ranges with high precision for any chosen colour. The RGB LEDs were configured as common cathode and mounted on aluminium heatsinks to avoid excessive temperatures that would affect the brightness of LED in prolonged usage (Yueh-Ru, 2010). Each RGB LED required three control pins to generate the required colour. The renewed hardware platform was based on an Arduino

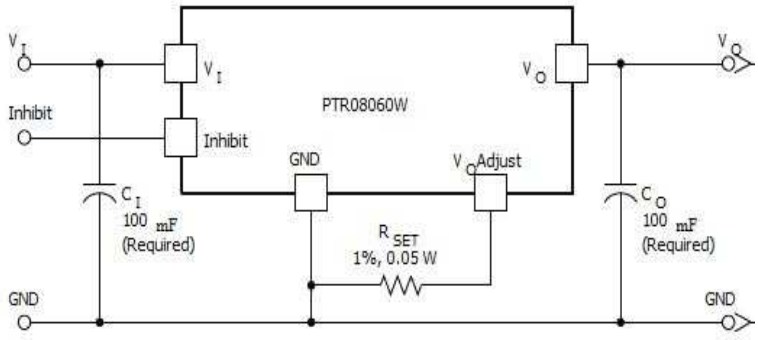

Figure 3.8: Schematic of voltage regulator

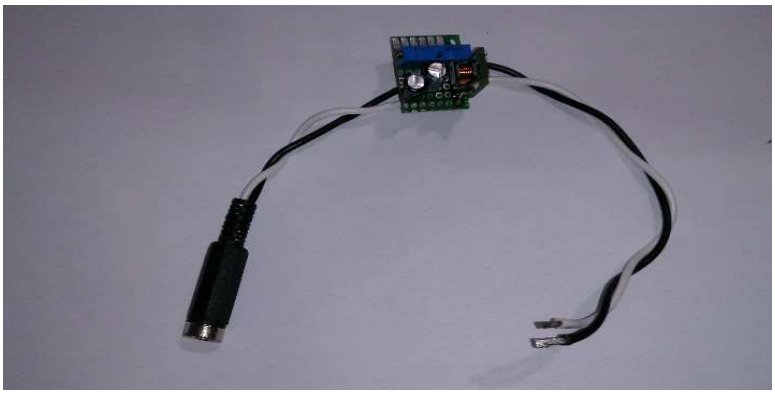

Figure 3.9: Prototype of voltage regulator

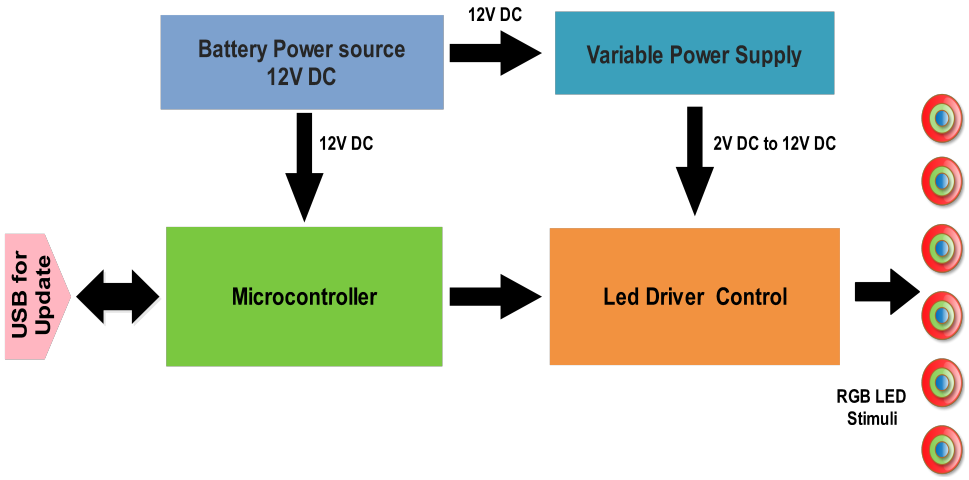

Figure 3.10: Visual stimulus control block

microcontroller which is an open source development platform with several hardware versions.

The upgraded hardware design supports precise frequency generation with an accuracy of ± 0.1 Hz, up to 12 programmable outputs that can generate different frequencies simultaneously. The RGB LEDs were connected through a Metal–Oxide–Semiconductor Field-Effect Transistor (MOSFET) driver to generate the required visual flicker. The new hardware platform is reusable, customisable for different experimental requirements. The firmware was developed to support the hardware based on the experimental requirements to generate various frequency flicker without the need for a new design. Fig 3.10 shows the basic blocks for the visual stimulus.

For a single frequency generation, a microcontroller port has to be assigned as an output to drive the LED through the MOSFET. For 7 Hz flicker generation, the interval time is set as 70 ms. This is calculated with basic time and frequency relation F = 1/T. Here frequency is 7 Hz; time would be 1/7 which is 0.14285 s. For flickering requirements, the LED has to be switched off for every half cycle, hence this requires the time to be divided by two (0.14285 / 2). This theoretical value of 71.4 ms generated a frequency of 6.92 Hz when measured at the LED end. The correction of ±1 Hz was required to get the exact

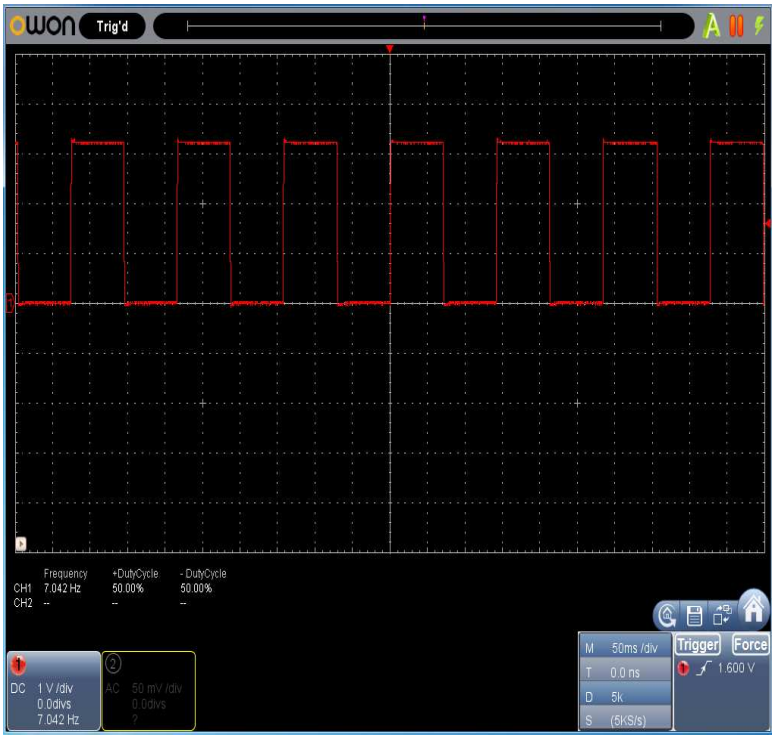

Figure 3.11: 7 Hz waveform generated with Arduino

value of 7 Hz at the LED end and that would be the precise flicker frequency of LED. Error correction values may need change with the lengths of the cables used to connect the RGB LED module and can vary with power sources used for the experiment. For initial setup, the frequency of flicker was confirmed at the LED with an oscilloscope as shown in Figure 3.11 and 3.12 The flicker frequency can be changed by changing the delay value as listed in Table 3.1.

The accuracy of the generated flicker can be observed in the waveforms above at 50% duty-cycle. Assigning each value corresponding to the frequency in the Table 3.1 would generate a square wave with 50% duty-cycle to flash the LED stimulus. This also makes it possible to generate up to 12 different flicker frequencies and all three colours when required. For example, if first RGB LED has green flashing at 7 Hz and red flashing at 10 Hz, the second RGB LED can also flash red at 7 Hz and blue at 15 Hz. Flashing frequency is completely independent of number of times the values are being used to generate the required flicker. The complete range of frequency and time interval values can be calculated

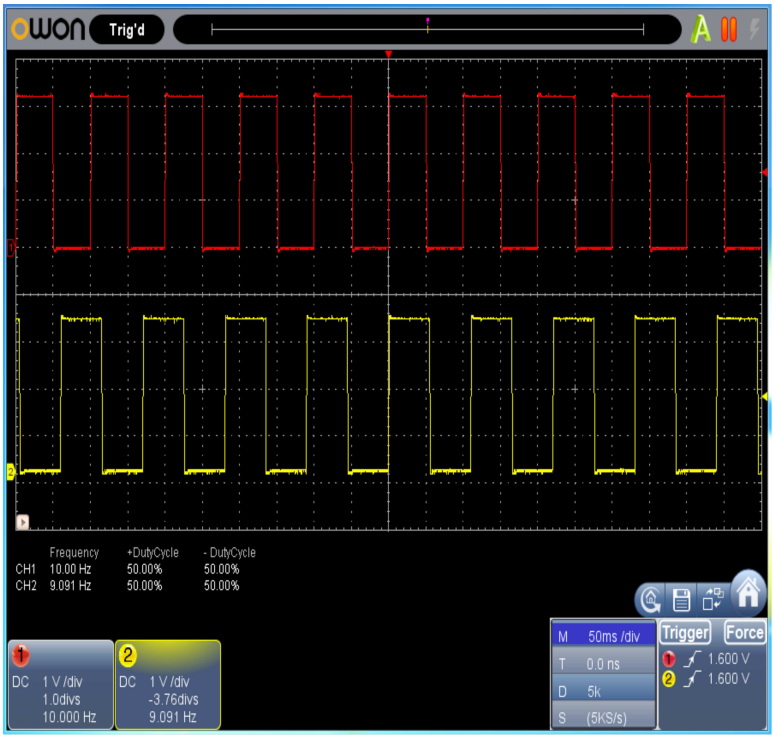

Figure 3.12: 10 and 9 Hz waveform generated with Arduino

with basic frequency and time relation as mentioned before. Appropriate adjustments can be applied to the time interval to get the precise frequency for LED flicker when testing with an oscilloscope.

The LED module needs to be supplied with constant power to maintain the luminance while flickering. Since the module requires more current, a power driver is required to maintain the luminance level for all channels simultaneously. The power driver used is based on MOSFETs built-in, in the form of a shield to drive the LEDs. The hardware FET shield is shown in Figure 3.13 with the LED module connected.

3.3 EEG Recording

The EEG data recording system used for this study uses g.Mobilab+ by gTec. This device is battery powered in order to avoid any external interference from the mains. The connectivity to the computer is via wireless Bluetooth. It assigns a virtual serial port in the

Table 3.1: Frequency lookup table

Frequency (Hz)	Time interval (ms)
7	70
8	61
9	54
10	49
11	44
12	40
13	37
20	24
35	13
25	19

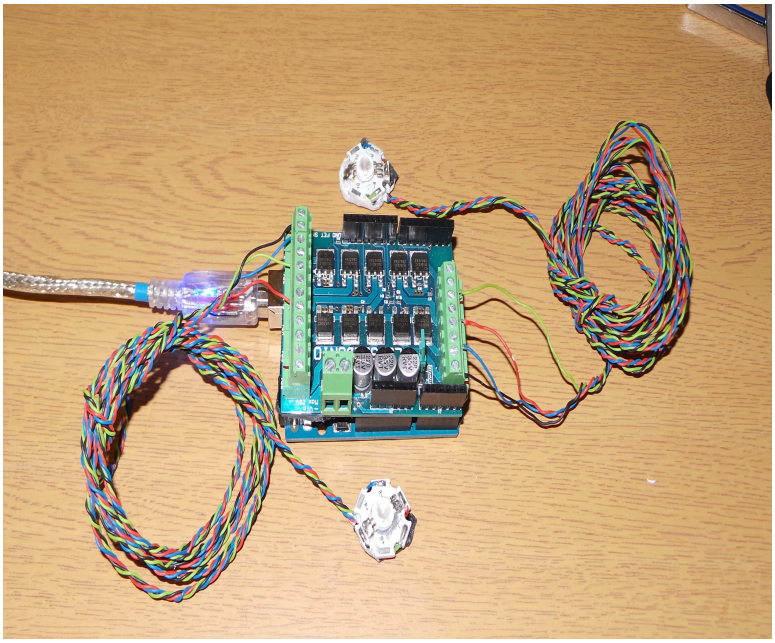

Figure 3.13: FET shield stacked on Arduino

computer and communicates serially. The main unit is interfaced via cable to an external high gain amplifier for recording the EEG data. The sensors are connected to the amplifier unit through GND, CH1 and CH2. Both the main unit and amplifier unit are battery powered and support gel-based electrodes.

The developed visual stimulus hardware was programmed for the frequency range 7 – 15 Hz and RGB LED connected to the output ports of the driver board. In this experimental study, the effects of colour, flicker frequency and the LED package type (conventional clear or frosted) were explored. In terms of colour, primary colours of red, green and blue were used to generate the flicker with the RGB LED at fixed frequencies for both clear and frosted packages.

To explore the effects of different colour, frequency and packages on SSVEP, participants were seated 60 cm from the stimulus, which was fixed at eye level. One EEG bipolar channel using gTec Mobilab+ along with active electrode driver box was used to record the data with electrodes positioned at Oz (midline occipital) and Fpz (midline frontal) with A2 (right mastoid) used as a reference. The visual stimulus flickered at fixed frequency and colour during a complete recording cycle of one second. Figure 3.14 shows a typical trial of EEG recorded for one second. Each colour and frequency had five trials for both conventional clear and proposed frosted packages, which resulted in 150 segments of data for one subject where each segment consisted of one second of SSVEP EEG data. Four healthy people volunteered for this study in the age group 25 – 45 (three females, one male) and none of the subjects had any previous experience with BCI. Table 3.2 shows the tested combinations.

The participants wore an EEG cap fitted with electrodes at the specified locations with conductive gel. This procedure does not require any skin preparation. The electrode position used for this study was based on the international 10/20 standard as shown in Figure 3.15 and located at Oz (midline occipital) as active, Fpz (midline frontal) as ground and A2 (right mastoid) as a reference. All subjects understood a short demonstration/training

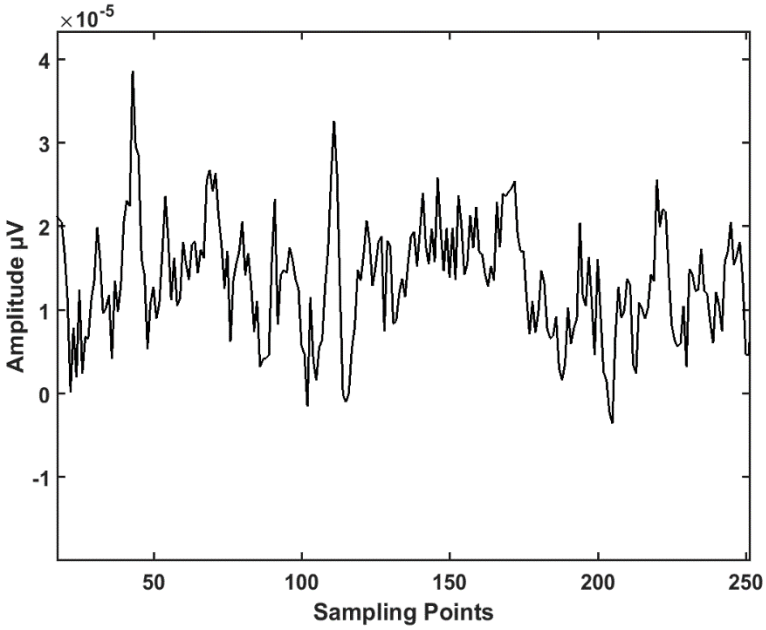

Figure 3.14: One second SSVEP EEG recording

Table 3.2: Frequency, Sample and Time for each LED

Colour	Frequencies (Hz)	No of Samples	Time (s)	Total Time (s)
Red Clear	7, 8, 9,10	4 X 5	30	600
Red Frosted	7, 8, 9,10	4 X 5	30	600
Blue Clear	7, 8, 9,10	4 X 5	30	600
Blue Frosted	7, 8, 9,10	4 X 5	30	600
Green Clear	7, 8, 9,10	4 X 5	30	600
Green Frosted	7, 8, 9,10	4 X 5	30	600

procedure on visualising the stimulus in the experiment. The recording time was set to 30 seconds for each trial with a rest time of one minute between each trial. Each trial began with a five second pause and 30 seconds of data recording. The sequence for data recording was 7 Hz red clear LED followed by 7 Hz green clear LED and 7 Hz blue clear LED. The same step was repeated for frequencies 8, 9, and 10 Hz using the clear LED. The sequence was alternated on different trials to avoid colour habituation effects. Following this, the visual stimulus was replaced with the proposed frosted package LED and all the above steps were repeated. The data recording was done in many session in different days.

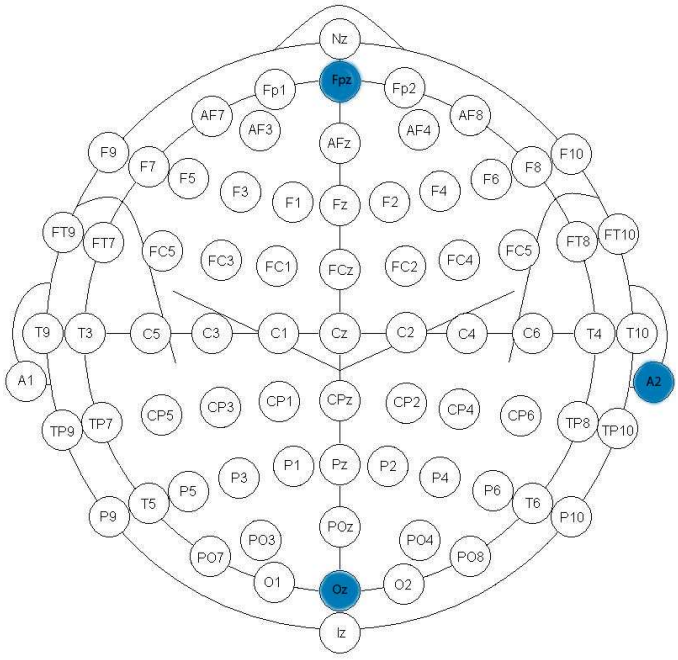

Figure 3.15: Electrode positions used for recording EEG

After starting the visual stimulus, EEG data was recorded with a sampling frequency of 256 Hz. The sampling frequency is fixed by the hardware. Each trial had a duration of 30 seconds thus lasting 1800 seconds for three colours, four different frequencies and five sessions. The rest period between trials was at least one minute. Hence the total time required for completing the EEG recording for each subject was about 90 minutes for 60 trials of conventional type and a similar amount of time for the frosted package LED. The

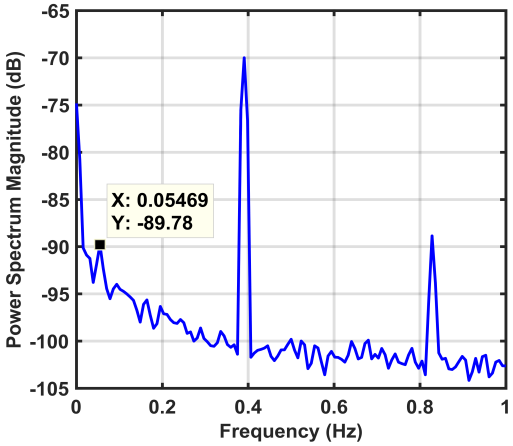

(a) 7 Hz

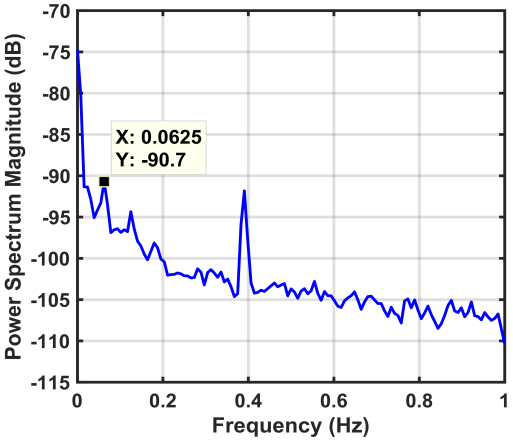

(b) 8 Hz

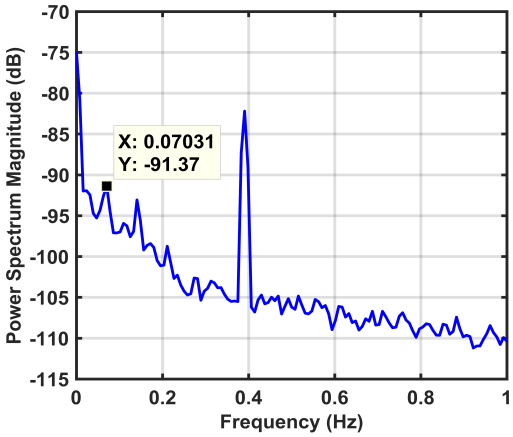

(c) 9 Hz

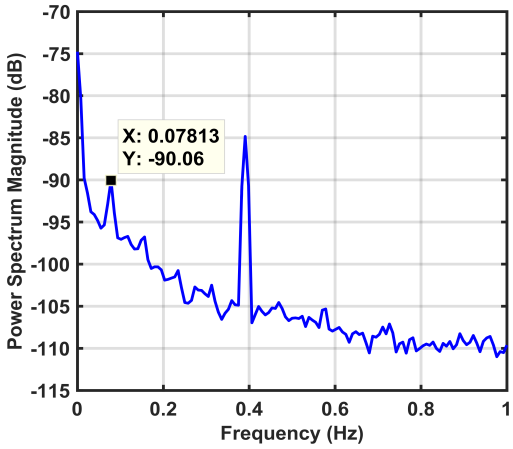

(d) 10 Hz

Figure 3.16: Sample EEG data recorded for 7, 8, 9, and 10 Hz

recorded data were saved as individual 30 second files for each frequency colour and package type. Figure 3.16 (a–d) shows the sample EEG data recorded for different frequencies.

3.4 EEG Data Analysis

The 30 seconds of EEG recording data was filtered with a band-pass filter, and segmented to one second EEG segments and analysed with Fast Fourier Transform (FFT). The filter parameters are shown in Table 3.3. The maximum amplitudes of the FFT using the filtered SSVEP signal for all the 150 segments were computed and stored for further analysis. This process was repeated for all the four frequencies and colours in both conventional clear and proposed frosted visual stimuli.

Table 3.3: Filter parameters

Frequency (Hz)	Order	Pass band edge frquencies (Hz)	Stop band edge frequencies (Hz)	Max pass band ripple (dB)	Min stop band attenuation (dB)
7	4	6,8	5,9	0.1	30
8	4	7,9	6,10	0.1	30
9	4	8,10	7,11	0.1	30
10	4	9,11	8,12	0.1	30

The effect of colour in SSVEP was analysed first in this experiment followed by the frequency analysis and the type of package. Statistical tests were used to compute the p-values to obtain the significance when different parameters were compared. FFT amplitudes for each frequency and colour were compared statistically using t-test statistical test to identify the most significant colour for SSVEP stimulus with the significance value (alpha) set as 0.1. Two colours were compared at a time for each frequency and LED package type. Table 3.4 to Table 3.7 shows the result of the analysis of colours and package type.

From the multiple t-test comparison results in Table 3.4 to Table 3.7, it can be seen that the highest SSVEP performance for all four subjects is from the green LED visual stimulus for all frequencies. The package types were compared for the visual stimulus and the results are shown in Table 3.8. It indicates that the conventional clear responses were better than from the frosted LED. However, all the participants preferred the frosted package as it was comfortable for prolonged usage even though the FFT amplitudes were lower for the conventional clear type.

Table 3.4: Significance comparison for colours and package type for 7 Hz

Subject	Frequency (Hz) & LED Package Type		
	Hypothesis	7 Hz - Clear Significance	7 Hz - Frosted Significance
S1	G >R	0	0.26
	R >B	0.09	0.14
	G >B	0	0.68
S2	G >R	0	0.55
	R >B	0.97	0.21
	G >B	0	0.87
S3	G >R	0	0.55
	R >B	0.95	0.21
	G >B	0	0.87
S4	G >R	0	0
	R >B	0	0
	G >B	0	0

Table 3.5: Significance comparison for colours and package type for 8 Hz

Subject	Frequency (Hz) & LED Package Type		
	Hypothesis	8 Hz - Clear Significance	8 Hz - Frosted Significance
S1	G >R	0	0.84
	R >B	0.78	0.19
	G >B	0	0.98
S2	G >R	0.92	0.62
	R >B	0	0
	G >B	0.95	0
S3	G >R	0.92	.062
	R >B	0	0
	G >B	0.95	0
S4	G >R	0	0.01
	R >B	0	0
	G >B	0.48	0

Table 3.6: Significance comparison for colours and package type for 9 Hz

Subject	Frequency (Hz) & LED Package Type		
	Hypothesis	9 Hz - Clear Significance	9 Hz - Frosted Significance
S1	G >R	0.05	0
	R >B	0	0.05
	G >B	0	0
S2	G >R	0	0
	R >B	0.94	0.25
	G >B	0	0.95
S3	G >R	0	0.92
	R >B	0.93	0.25
	G >B	0	0.94
S4	G >R	0	0.01
	R >B	0	0
	G >B	0.23	0

Table 3.7: Significance comparison for colours and package type for 10 Hz

Subject	Frequency (Hz) & LED Package Type		
	Hypothesis	10 Hz - Clear Significance	10 Hz - Frosted Significance
S1	G >R	0	0.99
	R >B	0.99	0.38
	G >B	0	0
S2	G >R	0	0.27
	R >B	0.68	0
	G >B	0	0
S3	G >R	0	0.27
	R >B	0.68	0
	G >B	0	0.93
S4	G >R	0	0
	R >B	005	0
	G >B	0	0

Table 3.8: Clear versus frosted results

Hypothesis tested	Frequency (Hz)	Participants			
		S1	S2	S3	S4
Clear > Frosted	7	0	0	0.07	0.25
Clear > Frosted	8	0	0.03	0.06	0.01
Clear > Frosted	9	0.41	0.88	0.05	0.92
Clear > Frosted	10	0	0.05	0.08	0

As shown in Table 3.9, participants S1, S2 and S3 gave statistically higher SSVEP response for 7 Hz visual stimulus as compared to other frequencies. For participant S4, both 7 Hz and 8 Hz gave a statistically similar performance. SSVEP performance increased as the visual stimulus frequency decreases and confirms previous research findings (Resalat et al., 2011; Volosyak et al., 2011). All four participants felt the green stimulus was more comfortable followed by blue and the least comfortable was red. The green stimulus also gave the highest SSVEP response of the colours, confirming the results of a previous study on oculomotor systems which found green had more robust effect when compared to white (Chua et al., 2004), and this study extends the result by exploring the other two prominent colours, blue and red.Basically, there are two types of photoreceptors in the human retina, rods and cones. Rods are responsible for low light levels or scotopic vision which do not mediate colour vision whereas cones are for higher light levels or photopic vision and are capable of colour vision. Unlike rods which has single photopigment, cones differ in three types and has photopigment with different sensitivity to light of different wavelengths. These are termed as red, green and blue cones (Purves, George J and David, 2004). Subjects felt the blue stimulus was relaxing and caused them to be sleepy, whereas red was not comfortable for prolonged usage. This also confirms with the previous study by Yoto (Yoto et al., 2007) which explored the effect of colour stimuli on human brain activities. All participants strongly preferred the frosted package for visual stimulus as opposed to clear even though clear LEDs gave higher SSVEP responses. Subjects felt the blue stimulus was relaxing and caused them to be sleepy, whereas red was not comfortable for prolonged usage. All participants strongly preferred the frosted package for visual stimulus as opposed to clear even though clear LEDs gave higher SSVEP responses.

Table 3.9: SSVEP frequency comparison

Hypothesis tested	Participants			
	S1	S2	S3	S4
7 > 8	0	0.024	0	0.12
7 > 9	0	0.37	0	0.19
7 > 10	0.01	0.01	0.06	0.01
8 > 9	0	0.54	0	0.11
8 > 10	0.09	0.99	0.05	0.01
9 > 10	0	0	0	0.17

3.5 Research Findings

The research study investigated the visual stimulus requirements for SSVEP based BCI. SSVEP based BCI systems could get wider acceptance if the issues related to visual stimulus portability, visual fatigue, user comfort and reduced hardware implementation cost is addressed. Visual stimulus presentation is one of the first issues that need to be addressed in SSVEP elicitation, as the traditional stimulus presentation is based on LCD/CRT. This not only reduces the flexibility in building portable BCI hardware platform but also reduces the choice of using required frequency. The background refresh in LCD is always present and that could also increase the visual fatigue when used for longer periods. The choice of colours for SSVEP elicitation and visual fatigue reduction to improve user comfort is not much explored and need to be investigated to build a customisable BCI for application control with precision.

To address the above issues, a customised hardware was developed which is portable, standalone and can generate any frequency from 5 Hz to 100 Hz with high precision. The visual flickers were based on LEDs and could be positioned anywhere with choice of colours for the user to comfortably focus and also reduced the unwanted electromagnetic field and background refresh generated by the CRT/LCD. The developed hardware was powered by a battery and does not induce any power line interferences in the recorded EEG. The distance between multiple visual stimuli can be adjusted to avoid any attention shift or interference from the adjacent stimulus. The platform can be easily programmed for various frequency selection or colour choices using USB connectivity.Experiments

were designed using the developed hardware platform and were successfully tested by investigating the influences of different colours, frequencies, and type of package effect on the performance of SSVEP in BCI.

EEG data collected from four participants were analysed for the SSVEP responses based on colour, frequency and package type with five trials on each paradigm. According to the participants in this study, the green stimulus was the easiest to concentrate and was less of a strain on the eyes when used for longer periods. The results also indicated that green stimulus gave higher responses than the other two colours which also confirms the results of a previous study on flashing lights which found green had more robust effect (Chua et al., 2004). Even though conventional clear package gave higher responses than the frosted LEDs, the participants were more comfortable with frosted LED stimulus for prolonged data recording. Participants also mentioned blue stimulus as relaxing and sleepy, whereas red was not comfortable for longer periods. In the frequency comparison, the lowest studied frequency of 7 Hz gave the highest SSVEP performance when compared to 8, 9 and 10 Hz. To conclude, green coloured 7 Hz frequency conventional clear LED stimulus gave the highest performance even though subjects were more comfortable with the proposed frosted stimulus.

3.6 Publications

Conference proceedings

1. Mouli, S., Palaniappan, R. & Sillitoe, I.P., (2013). Performance analysis of multi-frequency SSVEP-BCI using clear and frosted colour LED stimuli. In IEEE 13th International Conference on Bioinformatics and Bioengineering (BIBE), 2013. pp. 1–4.

2. Mouli, S., Ramaswamy, P. & Sillitoe, I.P., 2014. Arduino based configurable LED stimulus design for multi-frequency SSVEP-BCI. In PGBiomed/ISC 2014, the IEEE EMBS UKRI Postgraduate Conference on Biomedical Engineering. Warwick, pp. 1–4.

Book Chapter

1. Mouli, S., Palaniappan, R. & Sillitoe, I.P., 2015. A configurable, inexpensive, portable, multi-channel, multi-frequency, multi-chromatic RGB LED system for SSVEP stimulation. In T. A. Hassanien, A.E. and Azar, ed. Brain-Computer Interfaces. Switzerland: Springer International Publishing, pp. 241–269.

Chapter 4

Improving SSVEP elicitation using visual stimulus orientation with reduced visual fatigue

4.1 Introduction

This chapter focuses on the LED stimulus orientations influences in SSVEP. The hypothesis is that stimulus orientation influences SSVEP elicitation and with the right stimulus orientation, user comfort can be improved thereby reducing the eyestrain when used for longer periods. A study was constituted to investigate SSVEP amplitude for horizontal and vertical orientation of the visual stimulus. A custom visual stimulus hardware was developed to produce precise flicker frequencies between 7 to 10 Hz for evoking SSVEP. Flickers were produced using three primary colours (red, green and blue) from RGB LEDs, controlled by a stand-alone microcontroller platform and MOSFET based drivers. Individual recording sessions were carried out with horizontal and vertical stimulus orientation with flicker frequencies from 7 to 10 Hz and three colours for analysing the SSVEP responses. The recorded signals were processed with band-pass filtering and were analysed with Fast Fourier Transform (FFT) and autoregressive spectral analysis (AR). The signed - rank statistical results showed horizontal visual stimulus gave the higher response and

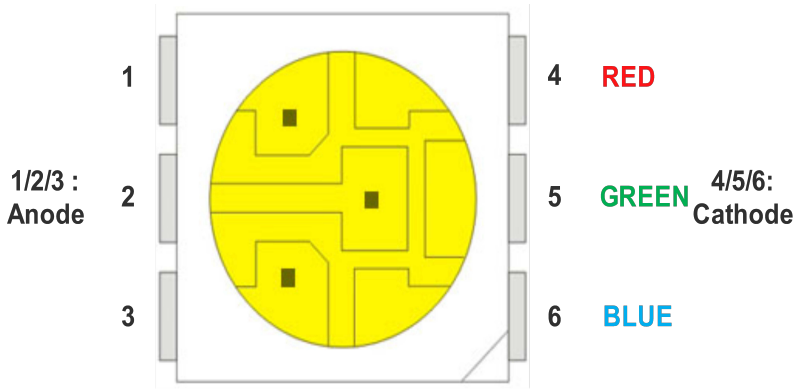

Figure 4.1: RGB LED physical layout

viewing comfort in all subjects when compared to a vertical orientation.

4.2 Stimulus orientation effect

Visual perception has been widely researched in terms of the influences of horizontal and vertical patterns (Taylor, 2001; Howell, Symmons and Doorn, 2013; Blanuša and Zdravković, 2015). To study the influences of visual stimulus orientation when applied to SSVEP elicitation, requires customised hardware to improve the response and comfort for the user.

A visual stimulus was designed with surface mount RGB LEDs with water-clear flat package. The type of LED used was an RGB LED (5050 SMD-RGB) as shown in Figure 4.1 with dimension 5 mm X 5 mm . The LED module consisted of six leads that can be configured as common anode or common cathode based on the requirement. All three colours required different input voltages of 2.0V, 3.2V and 3.2V DC for red, green and blue respectively with a viewing angle of 120 degrees as specified in the manufacturer data (http://www.superbrightleds.com (Accessed online on 15th Jan 2018)). Individual regulated DC power sources were required for each RGB LED and the dominant wavelengths for the LEDs were 625, 520 and 465 nm for red, green and blue respectively.

Individual power sources for the RGB LEDs was designed using MP1584 (monolithic

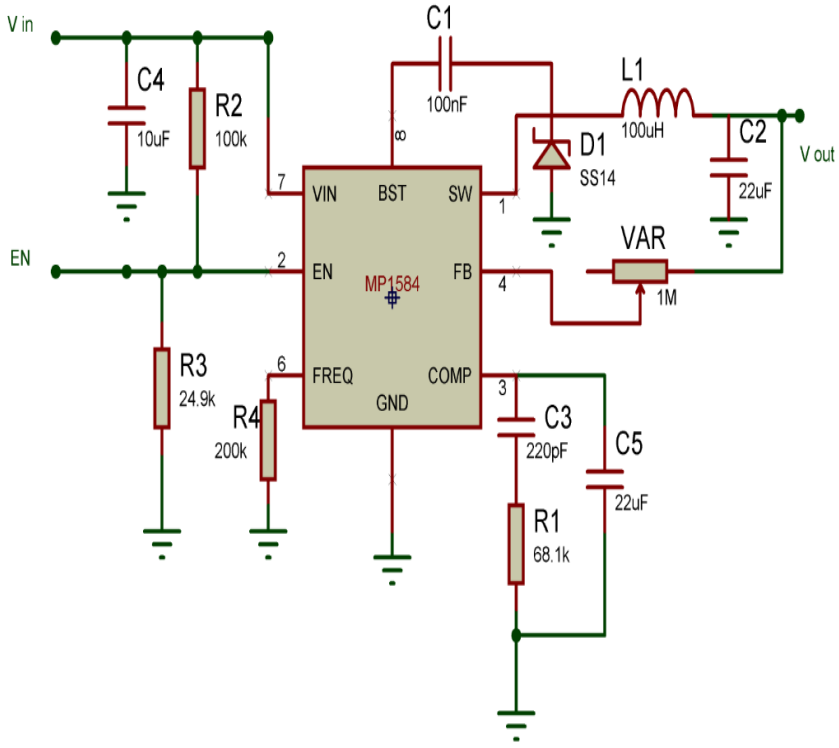

Figure 4.2: High speed switch down regulator for RGB visual stimulus

power systems) high frequency step-down switching regulators. A regulator switching frequency of 1.5 MHz, which would be able to minimise any in-board electromagnetic interference that could be induced in the recorded EEG. The schematic for the voltage regulator using MP1584 designed in Proteus design suite is shown in Figure 4.2. The design can take an input voltage from 4.5 to 28V DC with a continuous output of 0.8 to 25V DC at a constant current of 3A with very low heat dissipation. The output voltage is varied using the potentiometer VAR in the circuit for the desired LED colour.

The visual stimulus for exploring the orientation effect in SSVEP was designed using twelve RGB LEDs which were equally spaced in two parallel rows with six LEDs in a row. The LEDs were wired for each colour individually with all red LEDs connected in parallel followed by an LED bank of blue and green LEDs. The stimulus circuit was developed to control each colour separately as required, with one LED colour active at a time. Each LED colour was provided with a separate power source with the above mentioned power regulator to ensure the correct colour and intensity as specified in the LED data sheet. The

driving circuit for the LEDs used three MOSFETS, one for each colour to provide the required current through out the stimulation for constant brightness for all the twelve LEDs.

The active state of the LEDs was controlled by the MOSFET based on the pulses received from the microcontroller platform, which generated the flicker at the desired frequency. To simplify the microcontroller design, Arduino UNO3 was used for the timing pulses. The microcontroller platform was directly programmed through the USB port and does not require any dedicated hardware for external chip programming. Three port lines from the microcontroller platform were used for each LED colour respectively. To avoid random flicker, the MOSFET gates were clamped to ground level using a $10\,\mathrm{k}\Omega$ resistor which would keep the gate low when the microcontroller port was not active. For the selected frequencies, the microcontroller was programmed to output a square wave pulse with 50% duty-cycle to generate the flicker. Each colour was assigned a port within the program code and was activated when required. The generated frequencies were verified with a digital oscilloscope for their precision and optimised when required with an error correction of ± 0.05 Hz at room temperature. The complete visual stimulus schematic is shown in Figure 4.3. The RGB LEDs are shown in two rows wired to the microcontroller via the MOSFET and the required power for each LED colour is provided by the three voltage regulators shown on the upper part of the schematic. The voltage for each colour can be adjusted individually according to the manufacture specification for the correct intensity and emitted colour. The hardware was connected to a 12 V lead-acid DC battery source with a current capacity of 10000 mA and tested for continuous operation for five hours to verify any drift in the generated frequency or the input voltage provided for the LEDs. The generated frequencies were stable and the frequency drift was within the error correction limit at room temperature. The power consumption was no more than five watts when all the LEDs were flickering continuously, ensuring long time operation and portability of the visual stimulus platform. Figure 4.4 shows the assembled LED array with equal spacing between the LEDs in two rows with a dimension of 170mm X 55mm built on a transparent acrylic board. The board was connected to the microcontroller platform using four cables, three connections for the LEDs and one used as a common ground.

The visual stimulus orientation was changed from horizontal to vertical by rotating the acrylic board. The visual stimulus working in both horizontal and vertical orientations is shown in Figure 4.5.

4.3 Experimental Setup

To explore the influence of visual stimulus orientation on SSVEP, five participants with normal or corrected vision were selected in the age group of 20 – 44 with no prior experience in BCI. The participants were briefed on the objectives and the requirements of the study with a short demonstration of the flashing visual stimulus. The participants were seated 60 cm from the visual stimulus, which was fixed at eye level on an adjustable stand. Even though the visual stimulus could produce red, green and blue colours, the primary investigation was performed using green colour stimulus as it gave the highest performance in the previous single LED analysis. The visual flicker frequency was set for 10 Hz and the hardware was programmed for the set flicker frequency.

The SSVEP EEG data were acquired using Mobilab + from g.tec with three electrodes fitted according to the international 10/20 standard at locations O_z (midline occipital) as active, F_{pz} (midline frontal) as ground and A_2 (right mastoid) as reference. The recording session lasted 30 seconds for each frequency and orientation with a rest period of one minute between each trial. For each selected frequency and orientation, five trials were recorded for the analysis. To avoid any habituation effect of any particular orientation, the recordings were performed with alternated horizontal and vertical recording sessions. In one session, for a desired frequency, recording started with horizontal orientation for 30 seconds followed by one-minute rest and later resumed with vertical orientation for another 30 seconds. This process continued for five sessions in each horizontal and vertical orientation. For each frequency, the recording sessions for each participant took approximately 14 minutes to acquire the SSVEP EEG data for both horizontal and vertical orientation. The recorded data was anonymised and stored in separate files for later

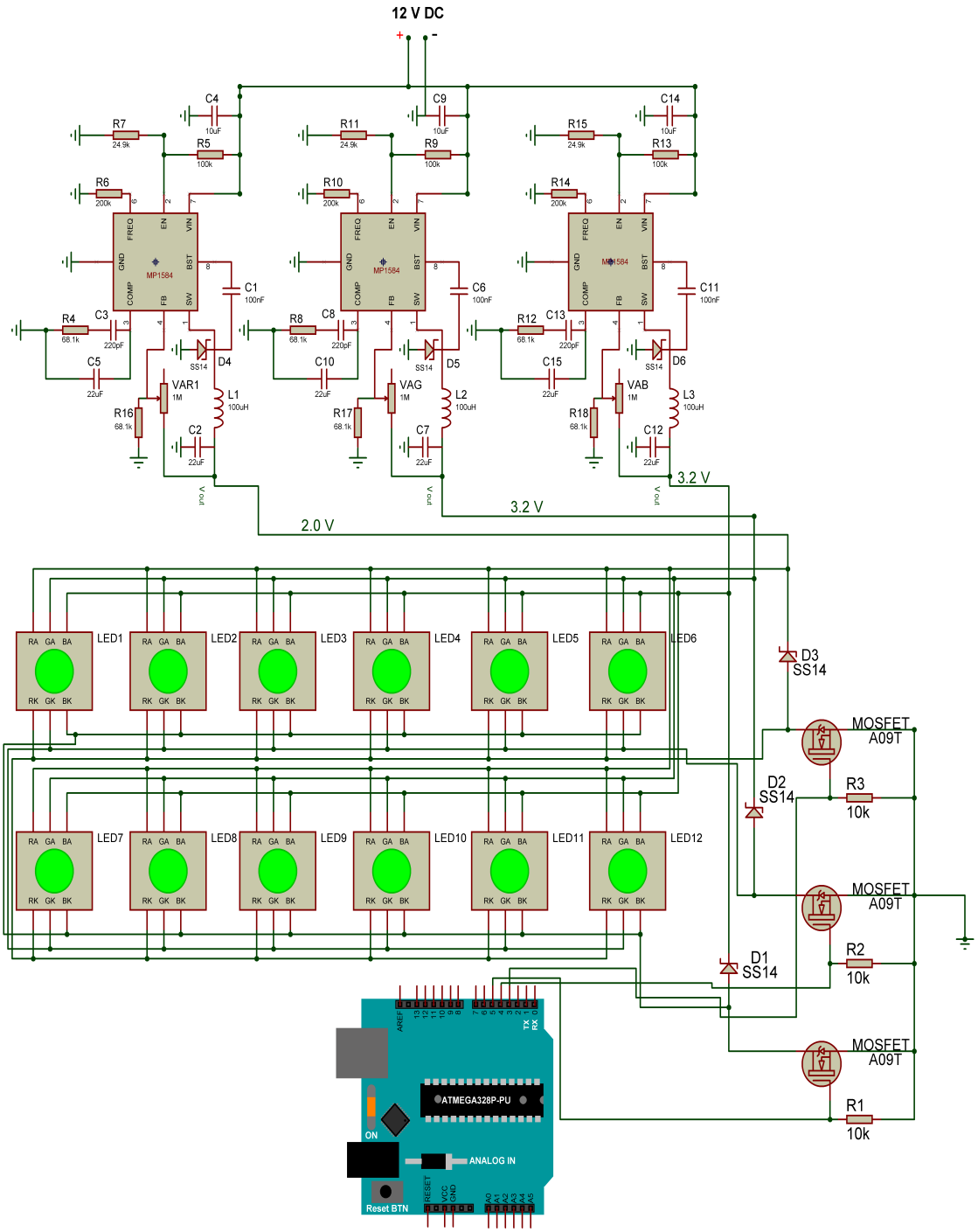

Figure 4.3: Visual stimulus schematic for RGB LEDs

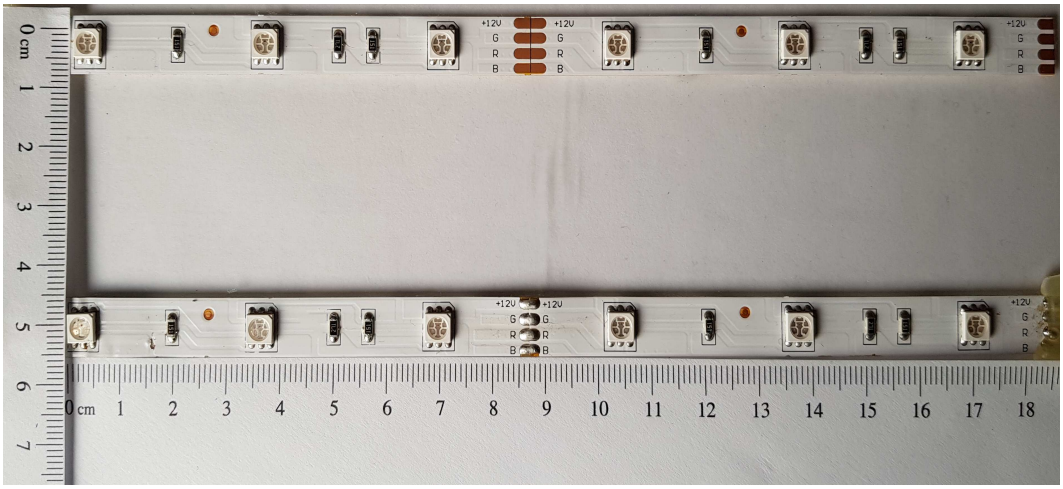

Figure 4.4: RGB LED array

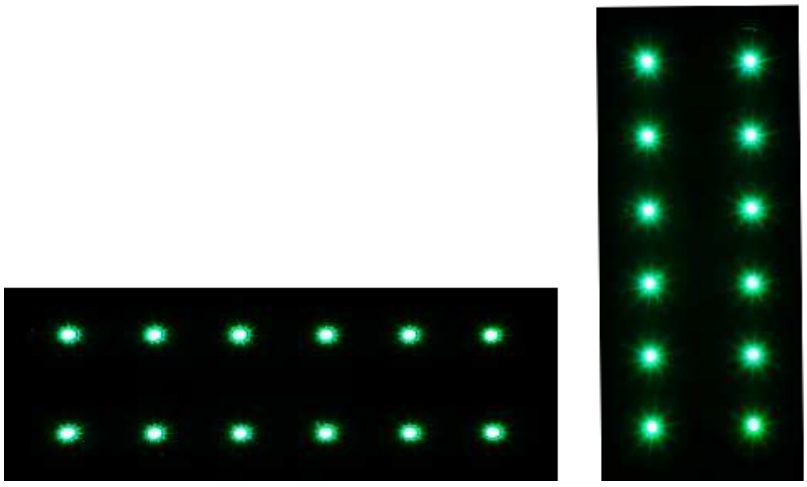

Figure 4.5: Visual stimulus in horizontal and vertical orientation

analysis.

4.4 Signal Processing

The recorded SSVEP EEG 30 seconds data with the 10 Hz visual stimulus in both orientations was filtered with a band-pass elliptical filter with parameters 9 – 11 Hz pass-band, maximum 0.1 dB ripple and with attenuation of 30 dB in stop-band. The order of the filter was chosen as four as sufficient suppression was attained. For analysis, the recorded EEG data was segmented into one-second lengths. One second EEG segments were used in FFT as sufficient number of cycles will be present for FFT analysis. For investigating the orientation influences in SSVEP, the frequency components were analysed using FFT and autoregressive spectral analysis (AR). Both analyses were performed using code developed in MATLAB.

For the first approach using FFT analysis, the frequency resolution was set to be 0.5 Hz since one second of EEG data was padded with one-second length of zeros before the analysis to increase the frequency resolution. From five trials, 150 segments of one second EEG data were computed for maximum spectral amplitude, and then statistically investigated. The procedure was repeated with all participant's data in horizontal and vertical orientations.

The second approach was based on AR spectral analysis which is a popular linear extraction method used when the number of parameters are limited. This type of approach uses the time history of the signal to extract information hidden in the signal, and is considered to be superior to many other biomedical signal-processing methods. (Takalo, Hytti and Ihalainen, 2005). AR is an alternative method to the discrete Fourier transform in determining the power spectrum density function of a time series. AR modelling involves selection of the correct model order and model parameters from the available data. The model evaluation is represented by Equation 1.

$$x(n) = -\sum_{k=1}^{p} a_k x(n-k) + e(n) \tag{1}$$

where $x(n)$ is the current value of the time series, $a1, \ldots.., ap$ are predictor coefficients, p is the model order, ak is the real valued AR coefficients and $e(n)$ represents the white noise error independent of the past samples. AR spectral analysis can provide the number, centre frequency and the associated power of oscillatory components in a time series. The modelling assumes that a data point is closely related to the previous few data points. Techniques like Yule-Walker, Burg's algorithm and Levinson-Durbin algorithm have been used to estimate the AR parameters (Al-Fahoum and Al-Fraihat, 2014; Aydin, 2008). In this analysis, Burg's method was used since it is more accurate for smaller data sets as well as the data points are used directly instead of the autocorrelation function, which is generally erroneous for small data segments. Burg's method also uses more data points simultaneously by minimising not only forward error but also the backwards error. Using the AR parameters, the spectral content is obtained by using Equation 2.

$$S(f) = \frac{\sigma_p^2 T}{\left|1 - \sum_{k=0}^{p} a_k e^{-i2\pi f k T}\right|^2} \tag{2}$$

where S(f) is the magnitude at frequency f, $\boldsymbol{\sigma}$ is the variance of the error term and T is the sampling period. Akaike Information Criterion (AIC) is normally used to select the AR model order (Shiavi, 2007). In this analysis, order two was used, as the SSVEP is pseudo-sinusoidal with one major frequency component, which will be the same as the flickering visual stimulus frequency. Furthermore, the error variances for the AR model were found to be very close to zero when using any order above two.

Similar to the FFT analysis, the maximum spectral amplitude of the filtered SSVEP data for all 150 one-second segments from five trials were computed using the AR method and stored for statistical investigation. This was repeated with all five participant's data in horizontal and vertical orientation of the visual stimulus. Statistical analysis was performed on the data for 150 segments from all five sessions of horizontal and vertical orientation as well as for 30 segments from each session. This procedure was used to analyse all the data from all participants to show the effect of stimulus orientation in SSVEP.

The statistical analysis was performed using sign-rank method, which is a nonparametric test for two paired samples to check the null hypothesis. The test returns a p-value, which determines the acceptance of the hypothesis. The stored data was statistically analysed with sign rank using 150 values from both orientations as well as using sessional data of 30 values from both vertical and horizontal orientations.

The two orientations were tested for the difference in performance in evoking SSVEP. To statistically compare the spectral output from FFT and AR methods, the sign rank was employed with a significance value (alpha) was set to 0.5. The orientations were compared with 150 data segments as well as sessional data of 30 segments. The set of values were compared from the same participants in all five sessions to identify the influence of the orientation on SSVEP response. Table 4.1 and 4.2 shows the mean and standard deviation values for the obtained FFT and AR spectral values. Table 4.3 show the results from the FFT analysis for 150 segments using sign-rank for horizontal and vertical SSVEP EEG data. Table 4.4 shows the sing-rank significance comparing 30 seconds FFT amplitudes in five sessions for vertical and horizontal LED stimuli.

From the data analysed it can be seen in Table 4.3, that for all the participants P1 to P5, the visual stimulus in horizontal orientation gave better results than the visual stimulus in vertical orientation for SSVEP EEG, when 150 segments of one-seconds data were analysed. From Table 4.4, it can be observed that the 30 segments of FFT data analysis for each session using sign-rank reveals horizontal stimulus is better 80% of the time compared to

Table 4.1: Mean and standard deviation values for 30 seconds FFT amplitudes in five sessions for vertical and horizontal stimuli

Participant										
Session	P1		P2		P3		P4		P5	
	Horizontal		Horizontal		Horizontal		Horizontal		Horizontal	
	Mean	SD	Mean	SD	Mean	SD	Mean	SD	Mean	SD
1	1.9e-3	1.5e-4	2.0e-3	1.8e-4	2.8e-3	1.1e-3	5.8e-4	2.1e-4	7.3e-4	2.1e-4
2	2.0e-3	1.8e-4	1.7e-3	1.6e-4	3.0e-3	9.9e-4	4.8e-4	1.4e-4	1.1e-3	1.5e-4
3	1.7e-3	1.6e-4	2.0e-3	2.7e-4	2.5e-3	9.2e-4	5.9e-4	1.5e-4	1.7e-3	3.1e-4
4	1.9e-3	2.1e-4	1.9e-3	2.1e-4	2.6e-3	1.2e-3	6.1e-4	2.0e-4	1.8e-3	1.7e-4
5	2.0e-3	2.7e-4	1.7e-3	2.2e-4	1.2e-3	1.0e-3	6.8e-4	2.0e-4	1.9e-3	1.5e-4
Participant										
Session	P1		P2		P3		P4		P5	
	Vertical		Vertical		Vertical		Vertical		Vertical	
	Mean	SD	Mean	SD	Mean	SD	Mean	SD	Mean	SD
1	1.0e-3	1.4e-4	1.3e-3	2.0e-4	2.7e-3	1.2e-3	2.4e-4	1.0e-4	7.3e-4	3.4e-4
2	1.6e-3	1.4e-4	1.1e-3	2.8e-4	2.2e-3	9.2e-4	3.1e-4	9.5e-5	8.8e-4	2.5e-4
3	9.1e-4	2.1e-4	1.6e-3	2.5e-4	2.2e-3	9.1e-4	2.4e-4	9.3e-5	1.4e-3	2.3e-4
4	1.1e-3	3.1e-4	1.2e-3	1.9e-4	2.1e-3	9.4e-4	2.4e-4	1.1e-4	1.4e-3	3.0e-4
5	1.1e-3	2.5e-4	1.8e-3	2.2e-4	2.2e-3	9.4e-4	2.4e-4	7.8e-5	1.3e-3	2.8e-4

Table 4.2: Mean and standard deviation values for 30 seconds of AR spectral analysis in five sessions for vertical and horizontal stimuli

Participant										
Session	P1		P2		P3		P4		P5	
	Horizontal		Horizontal		Horizontal		Horizontal		Horizontal	
	Mean	SD	Mean	SD	Mean	SD	Mean	SD	Mean	SD
1	2.1e-8	5.2e-8	7.6e-10	5.0e-10	2.4e-8	1.8e-8	4.0e-10	6.4e-10	4.1e-9	1.0e-8
2	7.6e-10	5.0e-10	1.7e-8	3.9e-8	2.8e-8	1.5e-8	1.1e-09	2.9e-9	1.2e-8	3.0e-8
3	1.7e-8	3.9e-8	6.8e-9	1.6e-8	2.0e-8	1.3e-8	1.6e-09	4.5e-9	1.50e-8	2.8e-8
4	6.8e-9	1.6e-8	1.1e-8	2.4e-8	2.1e-8	1.6e-8	1.4e-09	2.8e-9	8.0e-9	3.0e-8
5	1.1e-8	2.4e-8	3.0e-08	6.1e-8	2.5e-8	1.3e-8	9.7e-10	2.8e-9	2.1e-8	5.2e-8
Participant										
Session	P1		P2		P3		P4		P5	
	Vertical		Vertical		Vertical		Vertical		Vertical	
	Mean	SD	Mean	SD	Mean	SD	Mean	SD	Mean	SD
1	1.9e-9	3.0e-9	4.9e-9	1.7e-8	2.3e-8	1.5e-8	5.7e-11	7.4e-11	1.6e-9	3.1e-9
2	2.3e-9	4.0e-9	2.5e-9	4.7e-9	1.6e-8	1.9e-8	3.8e-10	8.8e-10	2.4e-9	6.6e-9
3	1.1e-9	2.9e-9	5.9e-9	9.4e-9	1.4e-8	1.5e-8	1.6e-10	3.6e-10	3.9e-9	8.6e-9
4	1.9e-9	3.3e-9	3.7e-9	7.1e-9	1.5e-8	1.8e-8	1.9e-10	7.2e-10	2.9e-9	5.0e-9
5	1.0e-9	2.3e-9	2.8e-9	6.1e-9	1.4e-8	1.4e-8	1.1e-10	2.8e-10	4.6e-9	1.0e-8

Table 4.3: Signed-rank significance (p-value) results comparing 150 segments of FFT amplitudes for vertical and horizontal LED stimuli

Participant									
P1		P2		P3		P4		P5	
Sig	Hyps	Sig	Hyps	Sig	Hyps	Sig	Hyps	Sig	Hyps
2.9e-26	H >V	3.9e-3	H >V	1.3e-5	H >V	1.1e-24	H >V	1.0e-15	H >V

(Hyps – Hypothesis, Sig - Significance)

Table 4.4: Signed-rank significance (p-value) results comparing 30 seconds FFT amplitudes in five sessions for vertical and horizontal LED stimuli

Session	Participant									
	P1		P2		P3		P4		P5	
	Sig	Hyps	Sig	Hyps	Sig	Hyps	Sig	Hyps	Sig	Hyps
1	1.7e-9	H >V	7.6e-1	NS	7.8e-1	NS	2.8e-6	H >V	8.6e-1	NS
2	6.3e-9	H >V	3.7e-2	H >V	3.0e-3	H >V	2.2e-4	H >V	2.4e-4	H >V
3	1.7e-9	H >V	7.8e-2	H >V	2.3e-1	NS	3.9e-6	H >V	4.2e-4	H >V
4	1.7e-9	H >V	1.8e-1	NS	3.6e-3	H >V	2.9e-6	H >V	1.6e-5	H >V
5	1.7e-6	H >V	8.2e-5	H >V	5.0e-3	H >V	1.7e-6	H >V	1.7e-6	H >V

(Hyps – Hypothesis, Sig - Significance)

vertical orientation. The remaining 20% of cases did not indicate any significance, and are denoted as non-significant (NS).

Table 4.5 shows the AR spectral analysis using Burg's method and statistically comparing the data using signed-rank significance for 150 segments in horizontal and vertical orientations. Again, the results show that horizontal orientation is significantly better than vertical orientation for all the subjects. Table 4.6 shows the results for 30 segments from each session and horizontal orientation is 68% more prominent than vertical orientation.

In general, from both analyses, it can be observed that SSVEP performance is better for visual stimulus in horizontal orientation when compared to vertical stimulus orientation, which confirms previous research findings for other applications (Ahnate and Scott, 2012; Read and Cumming, 2004). In addition, all five participants commented that horizontal orientation was more comfortable than vertical with less eyestrain and easier ability to

Table 4.5: Signed-rank significance (p-value) results comparing 150 segments with AR spectral analysis for vertical and horizontal LED stimuli

Participant									
P1		**P2**		**P3**		**P4**		**P5**	
Sig	**Hyps**	**Sig**	**Hyps**	**Sig**	**Hyps**	**Sig**	**Hyps**	**Sig**	**Hyps**
9.4e-3	H >V	1.6e-4	H >V	1.8e-4	H >V	6.0e-14	H >V	1.7e-2	H >V

(Hyps – Hypothesis, Sig - Significance)

Table 4.6: Signed-rank significance (p-value) results comparing 30 segments with AR spectral analysis for vertical and horizontal LED stimuli

Participant										
Session	**P1**		**P2**		**P3**		**P4**		**P5**	
	Sig	Hyps	Sig	Hyps	Sig	Hyps	Sig	Hyps	Sig	Hyps
1	5.7e-3	H >V	2.1e-1	NS	8.1e-1	NS	2.2e-4	H >V	3.9e-1	NS
2	2.1e-5	H >V	1.4e-2	H >V	8.7e-3	H >V	1.5e-2	H >V	7.6e-1	NS
3	1.0e-4	H >V	9.9e-2	H >V	1.1e-1	NS	3.6e-4	H >V	1.2e-2	H >V
4	3.7e-1	NS	2.2e-2	H >V	9.8e-3	H >V	3.7e-4	H >V	6.4e-1	NS
5	1.0e-3	H >V	1.86e-6	H >V	5.0e-3	H >V	1.2e-4	H >V	6.0e-1	NS

(Hyps – Hypothesis, Sig - Significance)

focus. This reduces the visual fatigue when used for longer periods and produces better results in SSVEP based BCI applications with visual stimulus horizontal orientation.

After identifying the visual stimulus horizontal orientation effect in SSVEP, the study further explored the influences of colours red, blue and green in the flicker frequency range 7, 8 and 9 Hz for horizontal and vertical orientations. The visual stimulus activated with the desired LED colour and EEG was recorded with the same experimental setup as before. Each frequency and colour had five trials for all five participants for each orientation. Each participant completed 120 trials from three colours, four frequencies and two orientations. The total recording time was approximately 120 minutes for each participant which also included the rest time. The 30 second individual recorded files was filtered with a band-pass filter and segmented into one second SSVEP EEG and then analysed using FFT. The filter parameters are shown in Table 4.7

The results were statistically analysed using signed-rank to compute the p-values to

Table 4.7: Filter parameters used in the data processing

Frequency (Hz)	Order	Pass band edge frequency (Hz)	Stop band edge frequency (Hz)	Max pass band ripple (dB)	Max stop band attenuation (dB)
7	4	6,8	5,9	0.1	30
8	4	7,9	6,10	0.1	30
9	4	8,10	7,11	0.1	30
10	4	9,11	8,12	0.1	30

Table 4.8: Signed-rank significance (p-value) results comparing amplitudes for horizontal and vertical orientations of LED stimuli. (R, G and B denote Red, Green and Blue respectively and H and V denote horizontal and vertical)

		Participants				
Freq(Hz)	Hyps	S1 Significance	S2 Significance	S3 Significance	S4 Significance	S5 Significance
7 - H	G >R	Yes	Yes	Yes	Yes	Yes
7 - H	B >R	Yes	Yes	Yes	Yes	Yes
7 - H	G >B	Yes	Yes	Yes	Yes	Yes
7 - V	G >R	Yes	Yes	Yes	Yes	Yes
7 - V	R >B	No	No	Yes	Yes	Yes
7 - V	G >B	Yes	Yes	Yes	Yes	No
8 - H	G >R	Yes	Yes	Yes	Yes	Yes
8 - H	B >R	Yes	Yes	Yes	Yes	Yes
8 - H	G >B	Yes	Yes	Yes	Yes	Yes
8 - V	G >R	Yes	Yes	Yes	Yes	Yes
8 - V	R >B	No	Yes	No	Yes	Yes
8 - V	G >B	Yes	Yes	Yes	Yes	Yes
9 - H	G >R	Yes	Yes	Yes	Yes	Yes
9 - H	R >B	No	No	Yes	Yes	Yes
9 - H	G >B	Yes	Yes	Yes	Yes	Yes
9 - V	G >R	Yes	Yes	Yes	Yes	Yes
9 - V	R >B	No	No	Yes	Yes	Yes
9 - V	G >B	Yes	Yes	Yes	Yes	Yes
10 - H	G >R	Yes	Yes	Yes	Yes	Yes
10 - H	B >R	Yes	Yes	Yes	Yes	Yes
10 - H	G >B	Yes	Yes	Yes	Yes	Yes
10 - V	G >R	Yes	Yes	Yes	Yes	Yes
10 - V	R >B	No	Yes	Yes	No	Yes
10 - V	G >B	Yes	Yes	Yes	Yes	Yes

(Hyps – Hypothesis, Freq – Frequency)

compare the significance of (a) horizontal and vertical orientation, (b) influence of colour in SSVEP, and (c) frequency significance. From the statistical analysis, the significant

Table 4.9: Signed-rank significance (p-value) results comparing amplitudes for horizontal and vertical orientations of LED stimuli (H and V denote horizontal and vertical)

Hypothesis tested Frequency (Hz)	**Participants**				
	S1	**S2**	**S3**	**S4**	**S5**
7 >8	6.0e-09	4.0-09	5.7e-09	7.5e-09	6.6e-09
7 >9	2.1e-24	9.0e-23	4.0e-23	4.2e-22	2.0e-24
7 >10	2.8e-25	3.9e-29	3.3e-24	7.4e-21	4.4e-19
8 >9	4.6e-37	6.0e-26	5.6e-29	5.4e-25	3.6e-34
8 >10	5.1e-34	3.2e-21	3.5e-38	4.6e-28	3.1e-25
9 >10	9.3e-06	8.4e-07	7.4e-08	8.4e-09	7.1e-25

colour in both horizontal and vertical orientation in all frequency ranges was green, which agrees with previous single RGB LED analysis. The complete analysis results are shown in Table 4.8 for all frequency ranges, for both vertical and horizontal orientations. From Table 4.8, it can be observed that in all frequency ranges green LED stimulus gave the maximal FFT amplitude in all trials for all participants.

After identifying green as the prominent colour for SSVEP LED stimulus, the rest of the analysis was based on green LED stimulus for all frequencies in both horizontal and vertical orientations. The results in Table 4.9 show that horizontal green LED stimulus gave the highest SSVEP values for all frequencies for all participants. The frequency comparison was also performed for the horizontal green LED stimulus, which compared all four frequencies 7, 8 9 and 10 Hz. The frequency comparison in Table 4.10 shows the lowest frequency (7 Hz) had the highest SSVEP response among all other frequencies used in this study, which also confirms the previous research findings (Volosyak et al., 2011; Resalat et al., 2012; Mouli et al., 2013).

4.5 Research Findings

The research investigated the influence of horizontal and vertical stimulus orientation in SSVEP for three primary colours and frequencies 7, 8, 9 and 10 Hz. The hardware was

developed was able to control the RGB LED arrays to produce precise frequency flicker throughout the experiments. The hardware was fully customisable to produce all three primary colour flickers without the need for any hardware change.

EEG data were recorded for various experiments from five participants for vertical and horizontal orientations using three colours and four frequencies. There were five trials for each combination. Based on the analysis of the recorded EEG data from five participants, horizontal stimulus orientation is better than vertical orientation. All five participants commented that horizontal stimulus orientation is easy to visualise and more comfortable than the vertical orientation. This also confirms with other research studies which explored horizontal orientation influences in brain (Howell, Symmons and Doorn, 2013; Blanuša and Zdravković, 2015). This would reduce visual fatigue in prolonged usage and would improve the elicitation of SSVEP for BCI applications or other visual studies.

The investigation of stimulus colour shows green stimulus has maximal SSVEP response as compared to other colours like red and blue in all frequency ranges. Participants commented that the green stimulus was easier to focus and was less strain for the eyes. Participant also suggested improving the visual stimulus with uniform lights rather than flickering LEDs, separated at a distance and that could be more efficient in evoking SSVEP with low visual fatigue. To conclude, SSVEP is influenced by visual stimulus orientation, and green horizontal stimulus has the maximal response in evoking SSVEP as well as improving comfort for the user.

4.6 Publications

Journal

1. Mouli, S., Palaniappan, R., & Sillitoe, I. P. (2015). Improving Steady State Visual Evoked Potentials Responses from LED Stimuli Through Orientation Analysis. Journal of Medical Imaging and Health Informatics, 5(5), 1070–1075.

Conference Proceedings

2. Mouli, S., Palaniappan, R., Sillitoe, I. P., & Gan, J. Q. (2015). Quantification of SSVEP responses using multi-chromatic LED stimuli: Analysis on colour, orientation and frequency. In Computer Science and Electronic Engineering Conference (CEEC), 2015 7th (pp. 93–98). Conference Proceedings.

Chapter 5

Improving SSVEP response with reduced visual fatigue using radial stimulus

5.1 Introduction

This chapter investigates the possibility of improving the comfort and reducing the visual fatigue in SSVEP using LED based radial stimulus.The hypothesis is that radial stimulus is easier to focus and reduces eyestrain for the users and improves SSVEP response. To overcome the effect of attention shift with LEDs with fixed spacing, this study used LEDs based on Chip on Board (COB) which produced a uniform light, which was easier for the participants to focus on. The study also compared the influence of different sizes of 70, 90, 110 and 130 mm diameter green COB radial rings in the elicitation of SSVEP. From the previous study, visual stimulus in a horizontal orientation gave the better performance. This study thereby included with a horizontal COB green stimulus of 160 mm length as control. The hardware platform was redesigned and based on a 32-bit microcontroller platform working at 72 MHz to generate precise frequencies of 7, 8, 9 and 10 Hz for prolonged usage. A luminance level controller was also designed to normalise the brightness of the four radial rings and the horizontal COB LED to avoid any influence of brightness

level since the number of LEDs were different in each stimulus. The results from five participants were statistically analysed using a Kruskal-Wallis test to identify the influence of the radial stimulus. Results indicated that the radial ring responses were significantly better than horizontal stimulus for all the five participants. Comparing the ring sizes, the largest gave the maximal response in SSVEP elicitation as well as better viewing comfort according to the participants.

5.2 Radial Stimulus Hardware Design

The stimulus platform was redesigned using a powerful 32-bit ARM Cortex – M4 microcontroller platform based on Teensy 3.1 (www.pjrc.com(Accessed online on 15th Jan 2018)). The Teensy platform works at 72 MHz as compared to the 16 MHz Arduino controllers used previously and the generated frequencies were precise for individual operations as well as for the concentric pattern generation using the radial rings. The LEDs were again driven using MOSFETs.

For this study, four COB LED rings were fixed on a black acrylic board in a concentric fashion as shown in Figure 5.1. The spacing between the radial rings were 5 mm. The surface texture of the board was chosen to be matte to avoid any unwanted reflection that happens normally from glossy surfaces.

The shiny dots on the white surface of the rings in Figure 5.1 represent each individual LED. In COB technology, LEDs are directly connected to the printed circuit board more like a substrate and very closely packed (Cheng et al., 2014; Hu and Wu, 2014; Vakrilov, Andonova and Kafadarova, 2015). This LED design makes it possible to distribute the light more evenly to appear as a single source rather than individual lighting as in the case of normal LED arrays that could introduce attention shift issues for participants when multiple LEDs are flashing. The horizontal COB LED strip used in this study is 160 mm long and 18 mm wide as shown in Figure 5.2.

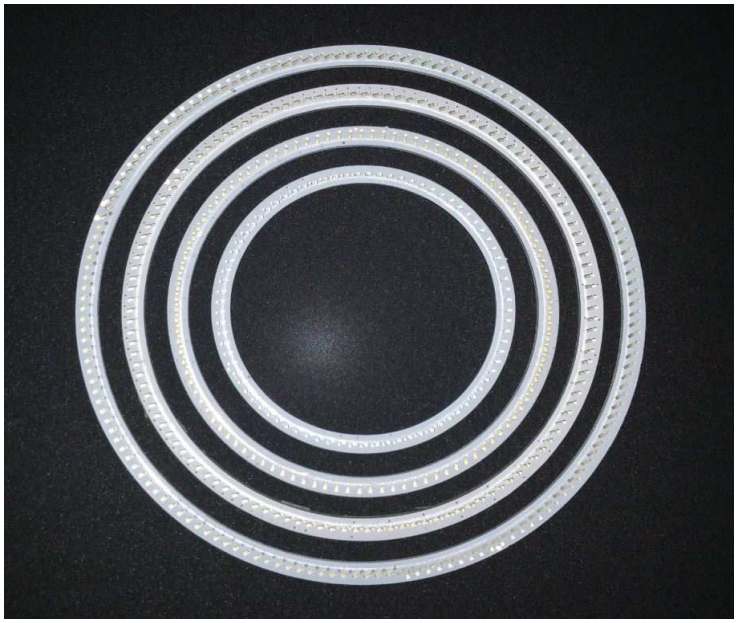

Figure 5.1: COB radial LED rings arranged with incremental size

Figure 5.2: Horizontal COB LED strip

The brightness of the LED rings varied with the sizes, and the number of COB LEDs are different in each ring. The number of LEDs increased with the ring diameter from 81 LEDs for 70 mm to 156 LEDs in 130 mm. This caused the difference in brightness in 70 mm and 130 mm while the stimulus was flickering. The brightness level was normalised with a precision switch down regulator and a flux meter (UT328). The fluxmeter had a range of 20 to 20,000 Lux with an accuracy of ± (3.0%+8). For the normalisation, the 70 mm LED ring was used as a standard as it had the minimum number of LEDs and was set to maximum brightness without any flickering effect. The luminance was measured with an ambient room brightness of 120 – 240 Lux. With full brightness, the 70 mm ring had approximately 820 – 845 Lux in normal room brightness and was taken as a benchmark to normalise the other LED rings. The ring brightness for 90 mm, 110 mm, 130 mm and the horizontal strip were normalised by varying the power fed to the LEDs until the Lux meter displayed a value between 820 – 845 Lux. The distance between the Lux meter and

the stimulus was set to 60 cm.

The hardware schematic is shown in Figure 5.3. It consists of four COB LED radial stimulus and one horizontal COB LED stimulus controlled by the Teensy microcontroller which is programmed via USB port. Each of the radial rings was driven through individual high current MOSFET for brightness stability. Five MP1584 step-down regulators controlled the luminance levels of all the LED stimuli by adjusting the variable control VABx in schematic (Fig 5.3 - variable controls are VAB1,VAB2,VAB3,VAB4,VAB5). The luminance level of all the LED stimuli are normalised via the VABx individually between 820 – 840 Lux. A battery pack with 12 V and 5 V DC outputs with a current capacity of 10,000 mA powered the complete hardware platform to avoid any line interferences.

The firmware was developed for two different types of flicker;

- Basic flickers for horizontal and radial stimulus for frequencies 7, 8, 9, and 10 Hz.
- Concentric circular patterns, which consisted of all the four LED rings lighting in a sequence to produce the desired frequency. The experiment used forward motion to form a concentric circle pattern. The flicker started from the 70 mm ring and moved towards the 130 mm ring and looped back.

For changing the flicker frequency of the visual stimulus, Teensy was reprogrammed with the corresponding code developed for the desired frequency. The precision of the flicker frequency was verified with a digital oscilloscope with probes connected at the stimulus end. Figure 5.4 shows the concentric pattern working at 7 Hz.

5.3 Experimental Setup

To explore the influence of radial stimulus in SSVEP elicitation, three different experiments were carried out. Two were based on radial stimulus and one with horizontal stimulus for comparing radial and horizontal influences in evoking SSVEP. The study collected SSVEP EEG data from five participants in the age group 24 to 45 (two males and

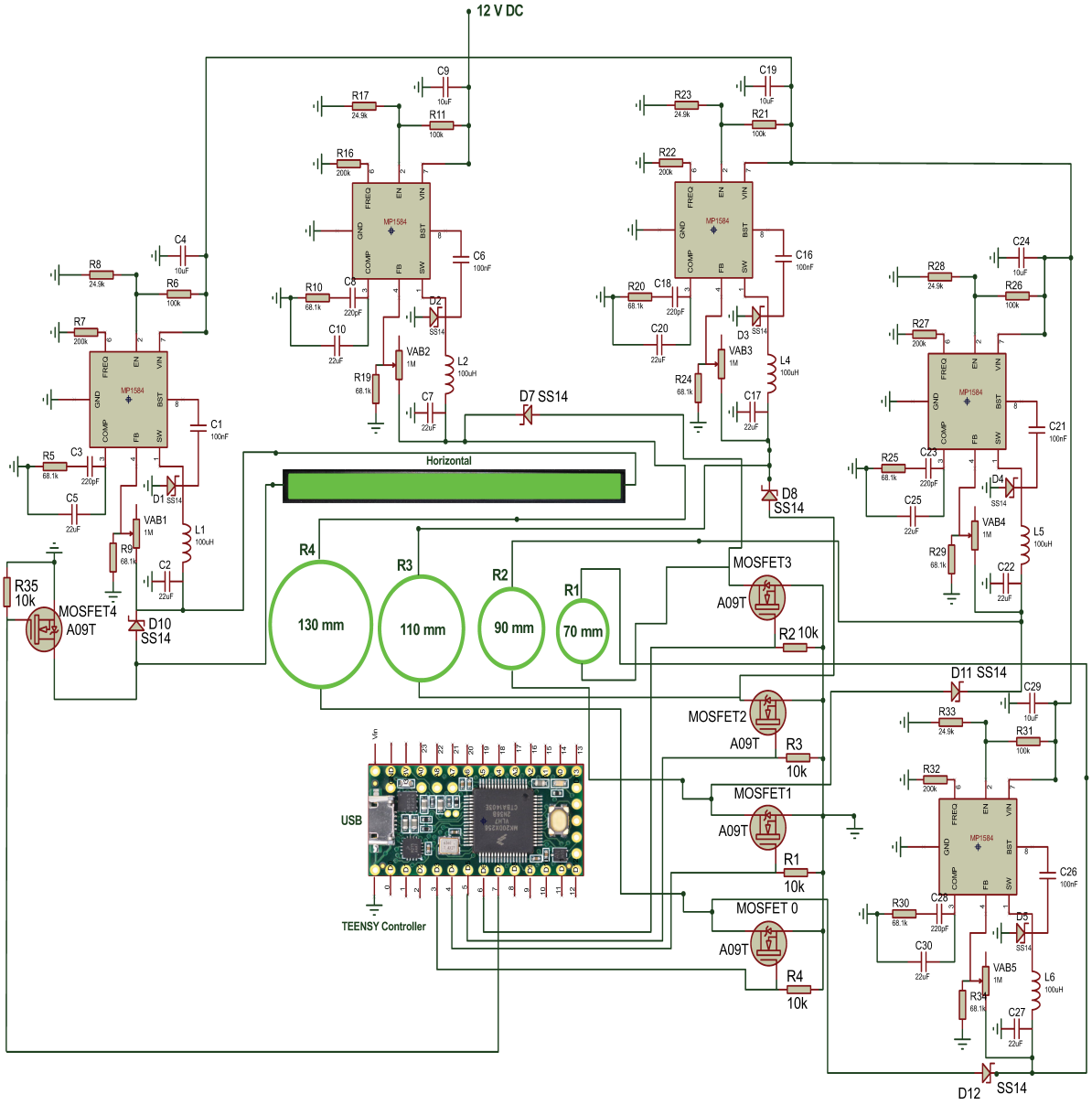

Figure 5.3: Hardware schematic for multiple COB LED stimulus

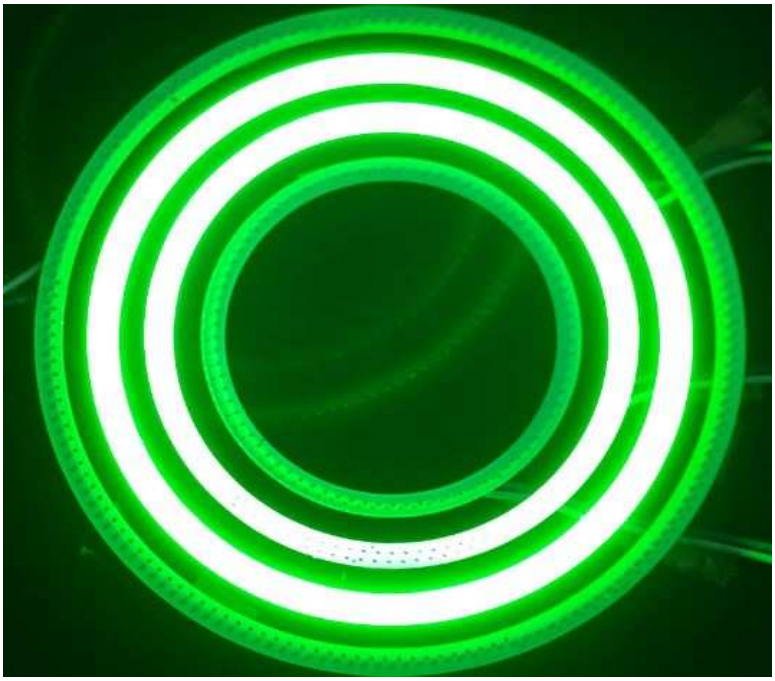

Figure 5.4: Radial stimulus working in a concentric fashion

three females) with perfect or corrected vision. The participants were comfortably seated and the visual stimulus fixed on the acrylic board placed at eye level 60 cm away from the participant. The EEG data was recorded using EMOTIV EPOC research edition as compared to the previous Mobilab + from g.tec. EMOTIV is a research grade wireless headset with 14 active electrodes and two reference electrodes that is widely used in many EEG research areas (Yu and Sim, 2016; Benitez, Toscano and Silva, 2016; Elsawy et al., 2017; Martinez-Leon, Cano-Izquierdo and Ibarrola, 2016; Liu et al., 2012; Duvinage et al., 2013a; Yu and Sim, 2016). The electrode layout is shown in Figure 5.5, and labelled outside the green circle, which is based on the international $10-20$ electrode placement system. The marking inside the green circle represents the corresponding EMOTIV field numbers that are used to store the EEG data in European Data Format (EDF). EMOTIV has the advantage of being fully wireless, hence portable. Cost wise, it is less expensive than Mobilab+. Hence, the decision to move to this electrode set.

For this study, data from electrode O2 was used to analyse the responses from three different stimulus configurations. The EEG data was recorded using EMOTIV test bench

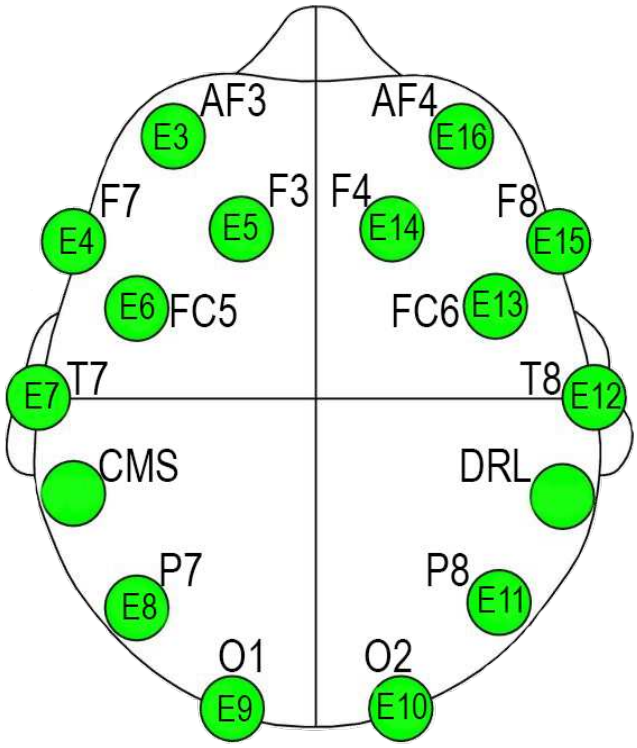

Figure 5.5: EMOTIV electrode location (Emotiv 2016)

software for 30 seconds at 128 Hz sampling frequency. For the data collection, each participant had five trials for each frequency and stimulus type. To begin with, the SSVEP EEG data was recorded for 70 mm radial stimulus flashing at 7 Hz for 30 seconds. This was repeated five times with a break of one minute between the recordings. This was followed by 90, 110 and 130 mm stimulus with flicker frequency 7 Hz and five trials of each. Following this, the frequency was changed to 8, 9 and 10 Hz with the same recording procedure as before and that completed one visual stimulus type. The second visual stimulus used was the horizontal COB LED with five trials for each frequency for 30 seconds from all five participants. The third stimulus was based on concentric circles with the same flicker frequencies as that of the horizontal stimulus with five trials for each frequency from all participants. All the recorded data was stored in separate files for analysis. The total number of trials for each participant is shown in Table 5.1. The total recording time for each participant for three visual stimuli was 60 minutes (120 trials each lasting 30 seconds), but the actual experimental time was slightly longer with breaks and setup.

Table 5.1: Trial count table for five participants

Stimulus Type	Participant Trials				
	S1	**S2**	**S3**	**S4**	**S5**
70mm x 5 x 4	20	20	20	20	20
90mm x5 x 4	20	20	20	20	20
110mm x 5 x 4	20	20	20	20	20
130mm x 5 x 4	20	20	20	20	20
Concentric x5 x4	20	20	20	20	20
Horizontal x5 x 4	20	20	20	20	20
Total trials	120	120	120	120	120

5.4 Signal Processing and Analysis

Since the data was recorded in EDF format, it needed to be converted to MATLAB format for offline analysis using EEGLAB (Delorme and Makeig, 2004). Since the occipital area has the high SSVEP response, the O2 channel was used. The extracted 30 seconds data from this channel was converted to MATLAB and then filtered using a band-pass filter of 2 Hz bandwidth with centre frequency as the stimulus frequency. The filter parameters are listed in Table 5.2.

The filtered data was segmented into one second EEG segments and all five 30 second trials are combined to generate 150 segments of one second EEG data. The data was analysed using FFT and the maximum FFT amplitudes were stored for statistical analysis. Statistical analysis was performed using Kruskal-Wallis tests, as normality was not assumed. Kruskal-Wallis tests were performed on maximal FFT amplitudes of EEG data from all radial sizes, concentric circles and horizontal orientation for all frequencies from five participants. The analysis compared data for identifying the most responsive visual stimulus design from all three stimuli designs. Each participant had six sets of recorded data, that include 70 mm, 90 mm, 110 mm, 130 mm, concentric circles and horizontal stimuli. The box plots from Figure 5.6 to Figure 5.10 shows the obtained maximal FFT amplitudes for 7 Hz from five participants for different radial sizes, concentric circles and horizontal stimuli. The central line shows the median value while the edges of the box are the 25^{th} and the 75^{th} percentiles with the whiskers extending to the extreme values.

Table 5.2: Band-pass filter parameters

Frequency (Hz)	Order	Pass band edge frequencies (Hz)	Stop band edge frequencies (Hz)	Max pass band ripple (dB)	Min stop band attenuation (dB)
7	4	6,8	5,9	0.1	30
8	4	7,9	6,10	0.1	30
9	4	8,10	7,11	0.1	30
10	4	9,11	8,12	0.1	30

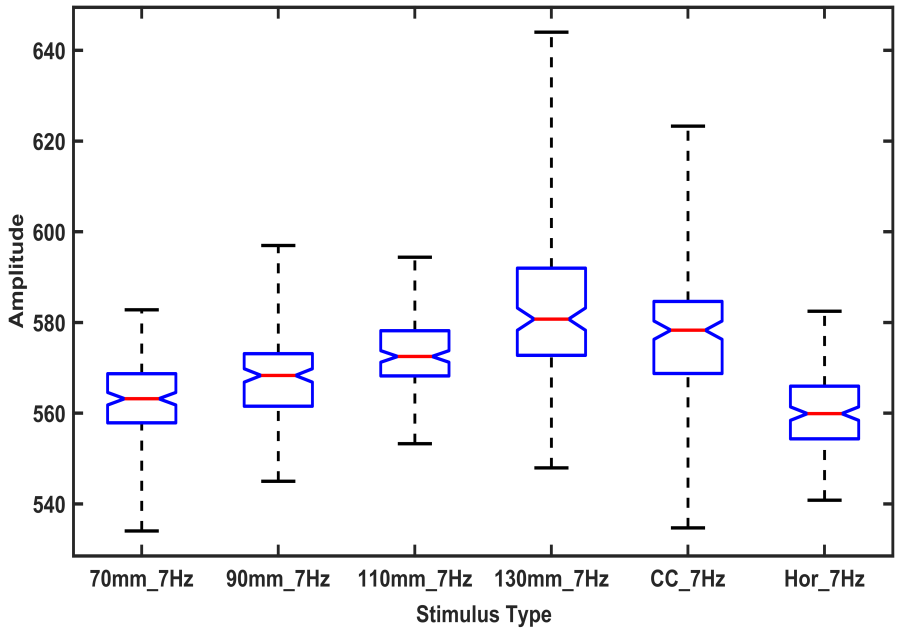

Figure 5.6: Maximal FFT amplitude values from first participant

The above box plots show significant differences between the three visual stimuli designs. The radial stimulus responses are higher than the horizontal stimulus for all five participants when the stimulus was flashing at 7 Hz. In addition, it can be observed that concentric circles stimulus responses are also higher than the horizontal stimulus. Within the radial sizes, 130 mm showed the highest response when compared with the smaller sizes. The Kruskal-Wallis tests results are as below.

$$\text{Kruskal-Wallis tests, } \chi^2(df = 5, N = 150)$$

The results from five participants are:

$$P1 : H = 347.28, p = 6.73e^{-73}$$

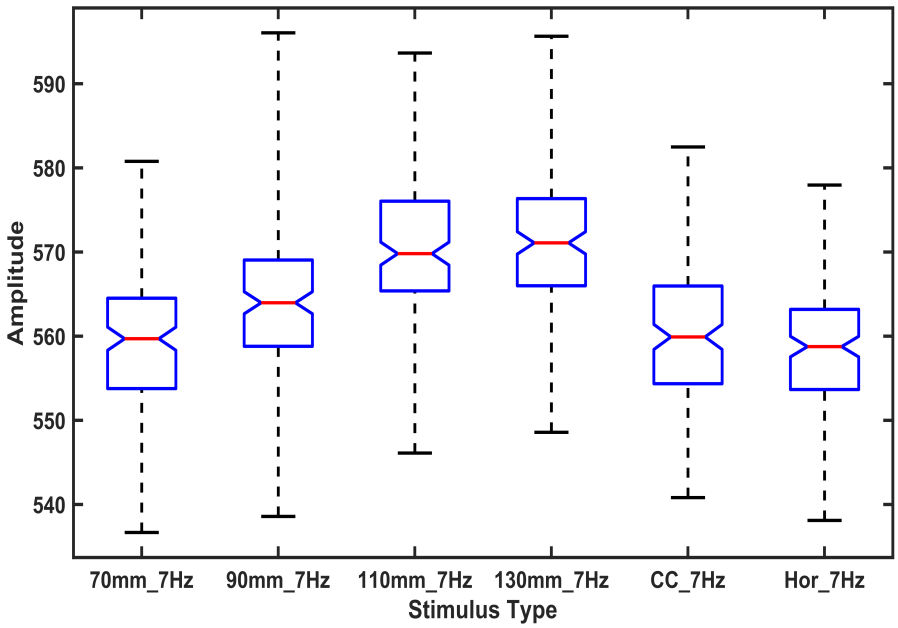

Figure 5.7: Maximal FFT amplitude values from the second participant

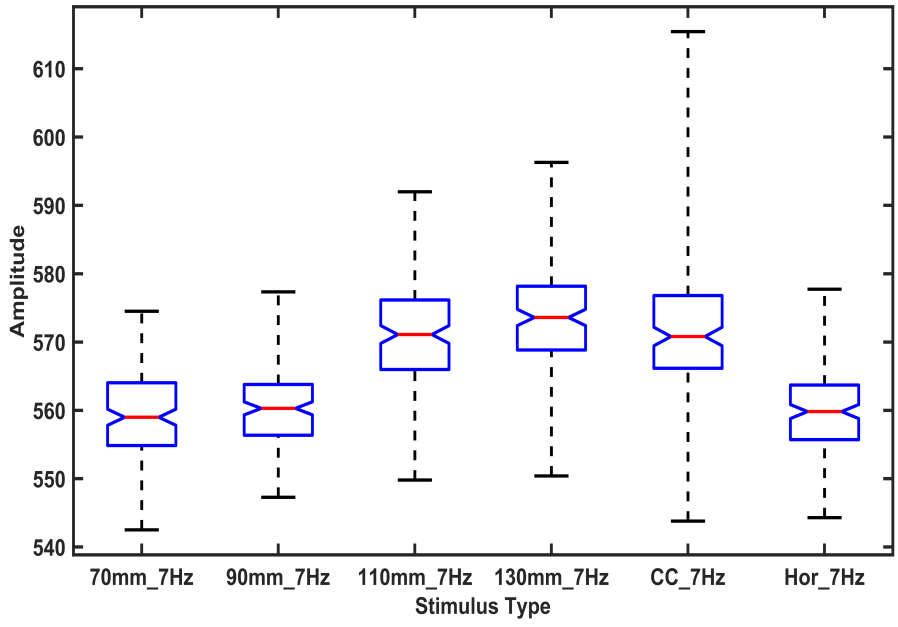

Figure 5.8: Maximal FFT amplitude values from the third participant

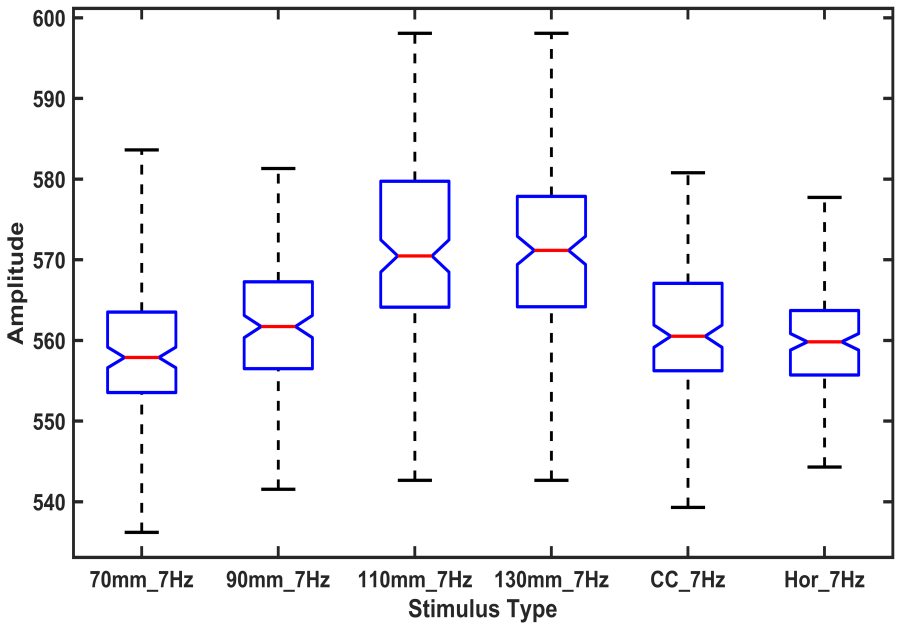

Figure 5.9: Maximal FFT amplitude values from the fourth participant

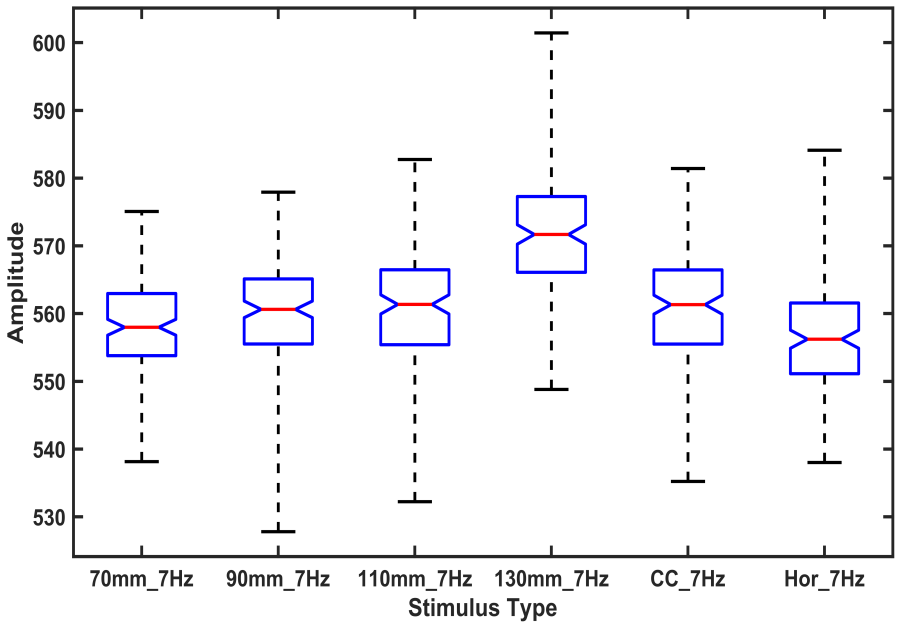

Figure 5.10: Maximal FFT amplitude values from the fifth participant

Table 5.3: Mean rank from Kruskal-Wallis Test for all participants

Stimulus at 7 Hz	**Participants (mean rank)**				
	S1	**S2**	**S3**	**S4**	**S5**
70 mm	291.64	319.98	263.17	309.44	351.91
90 mm	397.38	455.04	288.88	404.93	417.44
110 mm	532.01	640.91	602.48	626.69	450.88
130 mm	668.68	650.52	665.96	634.02	721.62
Concentric	594.11	337.80	599.78	386.43	443.05
Horizontal	219.16	298.74	282.71	341.48	318.08

$$P2 : H = 286.46, p = 8.11e^{-60}$$
$$P3 : H = 402.16, p = 1.01e^{-84}$$
$$P4 : H = 227.94, p = 2.95e^{-47}$$
$$P5 : H = 226.22, p = 6.90e^{-47}$$

The mean ranks for all different visual stimuli for five participants is shown in Table 5.3.

From Table 5.3, it can be observed that the 130 mm radial stimulus gave better performance compared with concentric and horizontal stimulus. The least performance was from the horizontal or 70 mm radial stimuli for all participants. Figure 5.11 shows the box plot representation of all radial stimuli from five participants. For further analysis of the SSVEP responses, different sizes of radial stimuli, concentric circles and horizontal stimulus, data from all five participants were combined for each stimulus type. For each stimulus, 750 FFT amplitude values were used from five participants in Kruskal-Wallis test (150 values from each participant). The highest SSVEP response was for 130 mm radial stimulus followed by 110 mm, 90 mm, 70 mm, concentric circles and horizontal stimulus, confirming the values obtained in Table 5.3 and boxplots in Figure 5.6 to Figure 5.10.

The other frequencies 8, 9 and 10 Hz were analysed using the same procedure for all the participants. To reduce the number of individual box plots, 750 values from each stimulus were combined from all participants for performing the Kruskal-Wallis test. Figure 5.12 to Figure 5.14 shows the box plots for frequencies 8, 9 and 10 Hz. The results showed that the 130 mm radial stimulus exhibited better performance than concentric and horizontal stimuli. The Kruskal-Wallis test results are as below.

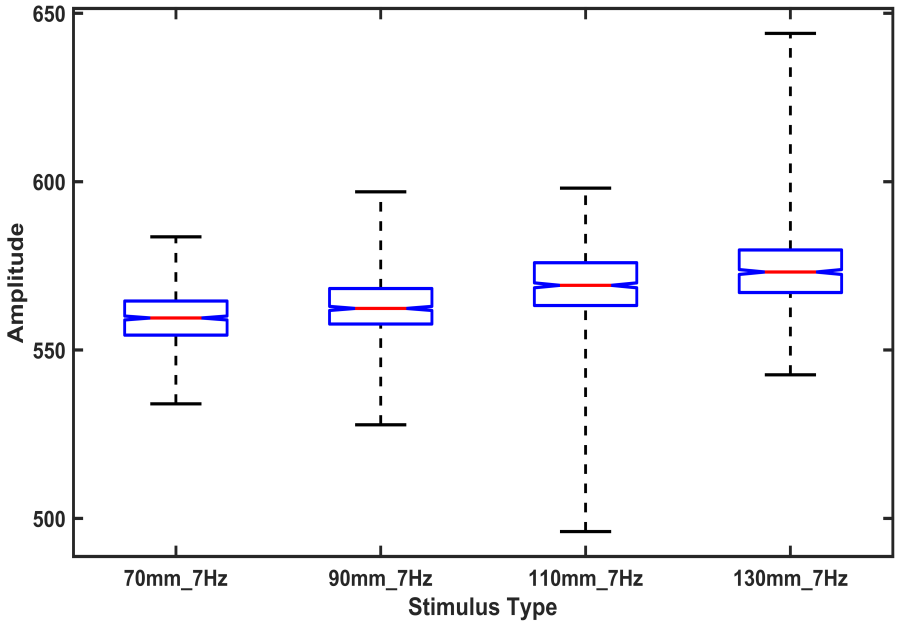

Figure 5.11: Analysis of different sized radial stimuli performance from all five participants

$$\text{Kruskal-Wallis tests, } \chi^2(df = 5, N = 750)$$

The Kruskal-Wallis tests showed significant differences between stimuli for all five participants for 8, 9 and 10 Hz for the three different visual stimulus types.

$$8\ Hz : H = 911.021, p = 6.81e^{-196}$$
$$9\ Hz : H = 1.48e^{+03}, p = 9.29e^{-320}$$
$$10\ Hz : H = 696.99, p = 1.56e^{-149}$$

From the analysis, the lowest response was from the horizontal stimulus when compared with the radial and concentric circles. Comparing the different sizes of radial rings, 130 mm had the highest performance and 70 mm with the lowest in all frequency ranges.

Comparing the SSVEP responses from the four frequencies 7, 8, 9 and 10 Hz, the lowest frequency 7 Hz shows the highest response as compared to other frequencies. Figure 5.15 shows the analysis of frequencies from the most responsive 130 mm radial stimulus. For the analysis, 750 values from all the five participants for each frequency were combined for generating the box plot.

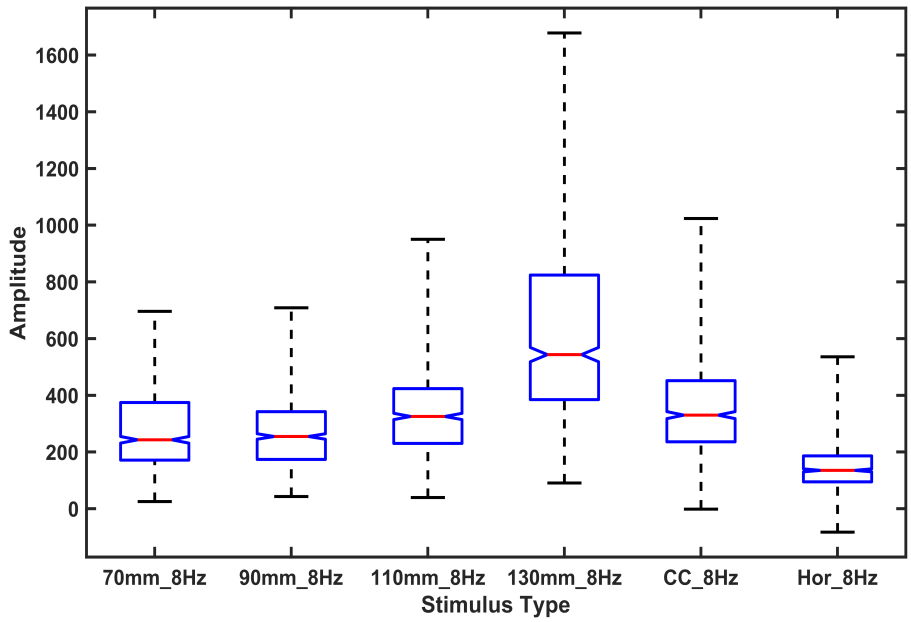

Figure 5.12: Maximal FFT amplitude values from all participant for 8 Hz

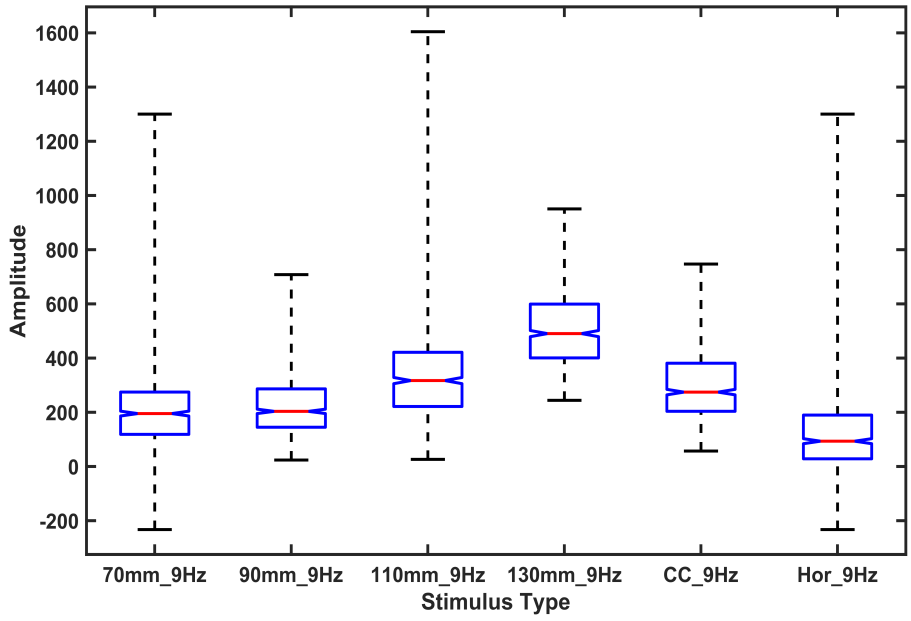

Figure 5.13: Maximal FFT amplitude values from all participant for 9 Hz

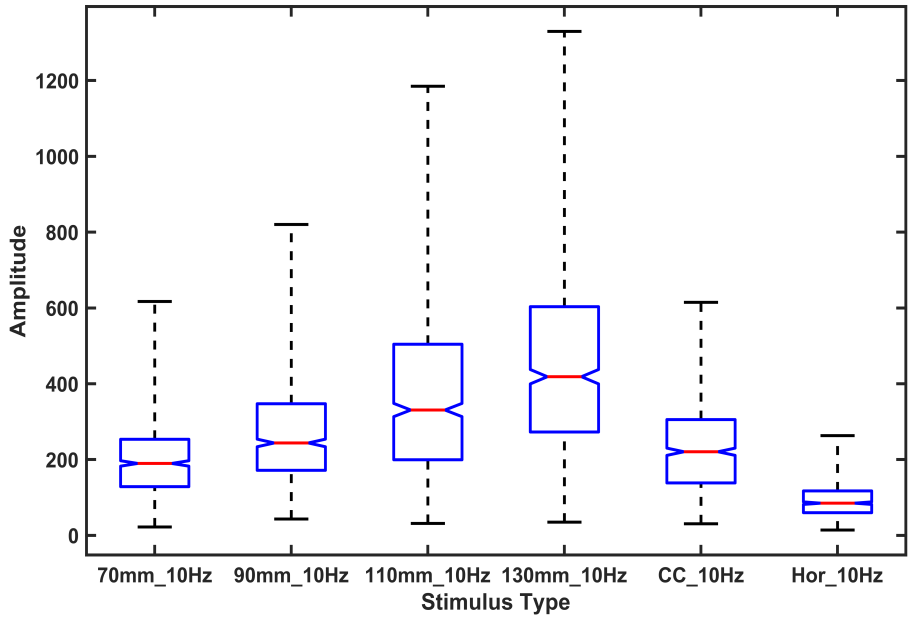

Figure 5.14: Maximal FFT amplitude values from all participant for 10 Hz

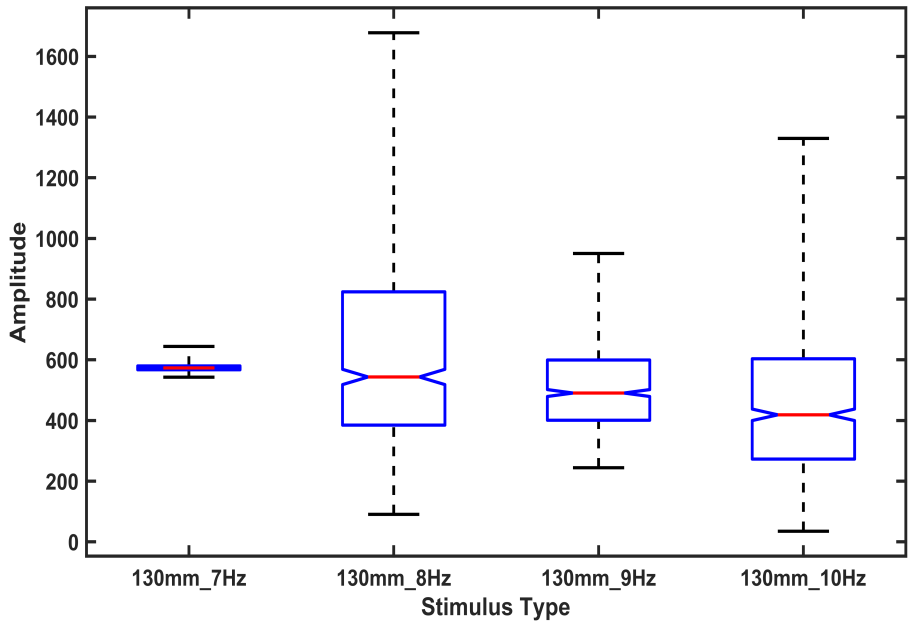

Figure 5.15: Analysis of frequency response from all five participants for 130mm radial stimulus

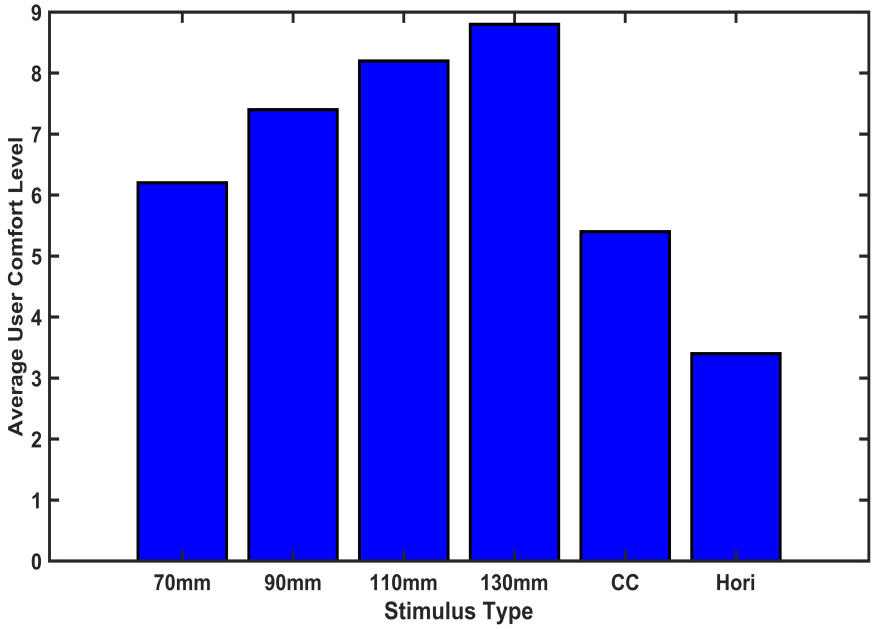

Figure 5.16: Analysis of participant responses for stimulus comfort

From the Kruskal-Wallis tests, $\chi^2(df = 3, N = 750)$ showed significant differences between frequencies 7, 8, 9 and 10Hz for all five participants.

$$PF : H = 256.59, p = 2.45e^{-55}$$

Frequency 7 Hz had the highest response followed by 8, 9 and 10 Hz and this also confirms the previous findings in chapter 3. Viewing comfort was also analysed for the participants for all three visual stimuli. A scale of one to ten (ten being the most comfortable) was used for comparing the stimulus comfort with reduced visual fatigue. The response from participants is shown as a bar chart in Figure 5.16. Even though only five participants completed the questionnaire, all participants responded 130 mm radial stimulus as the most comfortable flicker as compared to other visual stimuli.

5.5 Research Findings

The study investigated the influence of radial stimulus in evoking SSVEP responses in the brain. Comparisons were made between radial, concentric circles and horizontal stimuli that flashed at frequencies 7, 8, 9, and 10 Hz. From the analysis of data from five

participants, radial stimulus exhibited the highest response for SSVEP in all participants followed by the concentric circles and horizontal stimuli. For the radial stimulus, the ring diameter analysis for all the participants revealed that 130 mm had the highest response followed by 110, 90 and 70 mm. The 70 mm radial stimulus gave better performance when compared with the horizontal stimulus.

Furthermore, the participants observed radial stimulus was better for improved viewing comfort as compared to concentric circles and horizontal stimuli. In addition, the 130 mm radial stimulus was more comfortable for viewing than the 70 mm radial stimulus. Therefore, it is suggested that 130 mm radial stimulus can be used to evoke SSVEP for BCI applications due to its maximal SSVEP response among tested configuration, better viewing comfort and reduced visual fatigue.

5.6 Publication

Conference Proceeding

1. **Mouli, S.** & Palaniappan, R., 2016. Radial Photic Simulation for Maximal EEG Response for BCI Applications. In 9th IEEE International Conference on Human System Interaction (HSI),Portsmouth. UK, pp. 362 - 367.

Chapter 6

Reducing visual fatigue and improving SSVEP response with visual stimulus luminance control

6.1 Introduction

This chapter focuses on the influence of the visual stimulus luminance in SSVEP responses in the brain. The hypothesis is that 100% visual stimulus brightness increases the eyestrain and thereby reduce the SSVEP response. Controlling the luminance would reduce the visual fatigue and improve the user comfort when used for longer period. For this study, 130 mm radial green COB LED stimulus was used to generate the visual flicker controlled by the 32-bit microcontroller described in chapter 5. Four different frequencies of 7, 8, 9, and 10 Hz were used in generating the flicker. The luminosity level of the radial stimulus was externally controlled through a fast switching step-down controller at levels of 25, 50, 75 and 100% of the maximum stimulus brightness. All experiment was conducted in the same room with the same ambience and background light measured with the lux meter. Five participants took part in the study and the SSVEP EEG data was recorded for 30 seconds with five trials for four luminosity levels and four frequencies. The data was analysed and the results indicated that luminosity at 75% of the full LED brightness gave a significantly

higher response and reduced visual fatigue for all participants when compared to other luminous levels of the visual stimulus.

6.2 Luminosity control for SSVEP elicitation

To explore the influence of visual stimulus luminosity in SSVEP, a 130 mm green COB LED radial stimulus was used with different brightness levels and with four different frequencies. From the previous experiments that were detailed in the previous chapters, SSVEP responses were influenced by colour, nature of LED lens, orientation of the stimulus and the shape of the stimulus. Radial stimulus evoked the maximum SSVEP response with reduced visual fatigue for all participants in the previous study.

Stimulus brightness analysis studies are very limited and a recent study used LCD based stimulus presentation with the stimulus brightness controlled through the software (Oralhan and Tokmakçi, 2016). Few studies that have used LED based stimulus were based on LEDs at maximum brightness which would make the participants tired with prolonged usage (Yu and Sim, 2016; Friganović, Medved and Cifrek, 2016; da Silva Pinto et al., 2011). With the COB LEDs, the light is much more uniformly distributed and the brightness can be individually controlled if multiple stimuli are present without any interference from the adjacent stimulus. The basic data acquisition model using a microcontroller based flicker and luminosity controlled stimulus is shown in Figure 6.1.

The hardware as in chapter 5 was designed using the same Teensy microcontroller and MP1584 step-down power controller as in chapter 5. Teensy was programmed for single stimulus operation for frequencies 7, 8, 9 and 10 Hz. The complete hardware platform schematic is shown in Figure 6.2.

The hardware platform consists of two modules, one for generating the flicker frequencies and other for adjusting the luminosity levels through a MOSFET driver. For

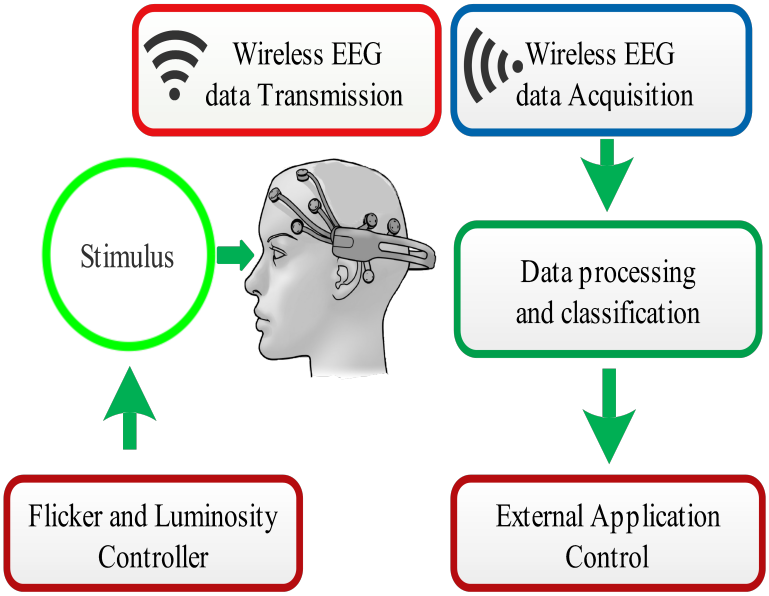

Figure 6.1: Microcontroller based visual stimulus for BCI operation

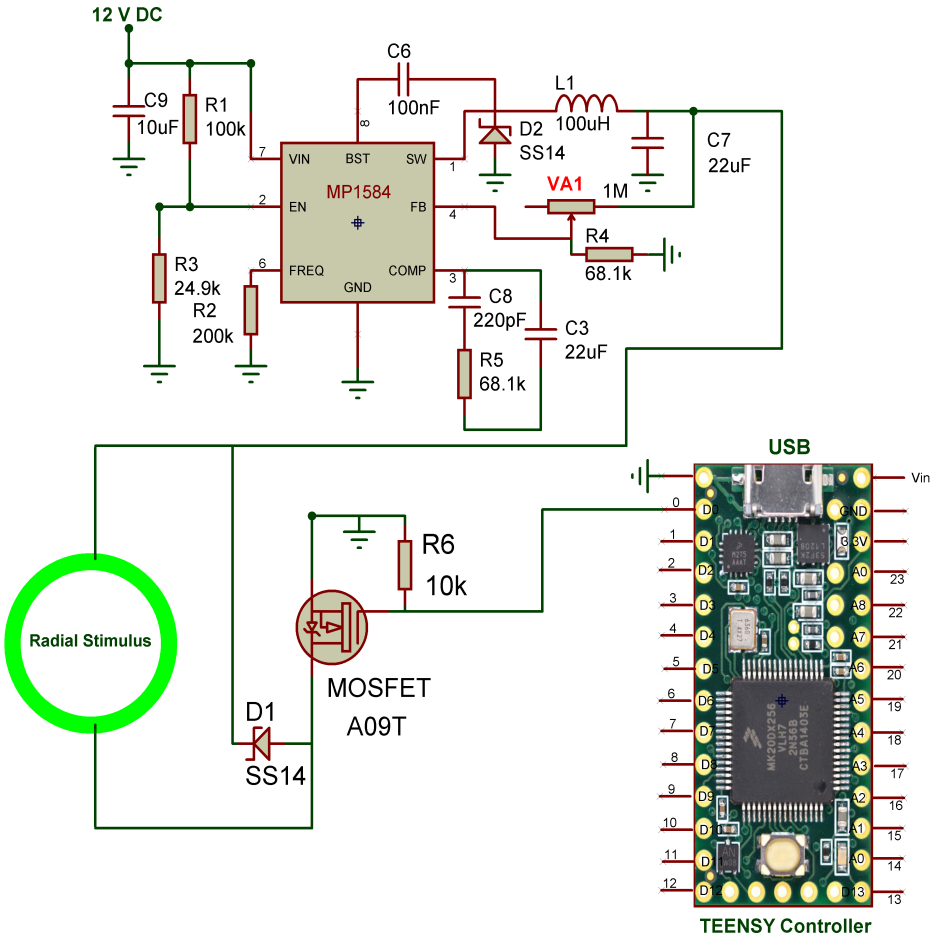

Figure 6.2: Visual stimulus platform with integrated luminosity controller

Table 6.1: Look-up table for luminance levels, terminal voltage and Lux values

Luminance (%)	Input Voltage DC (V)	Lux Value (lx) ±20
100	11.5	1430
75	10.6	1072
50	9.5	715
25	8.9	357

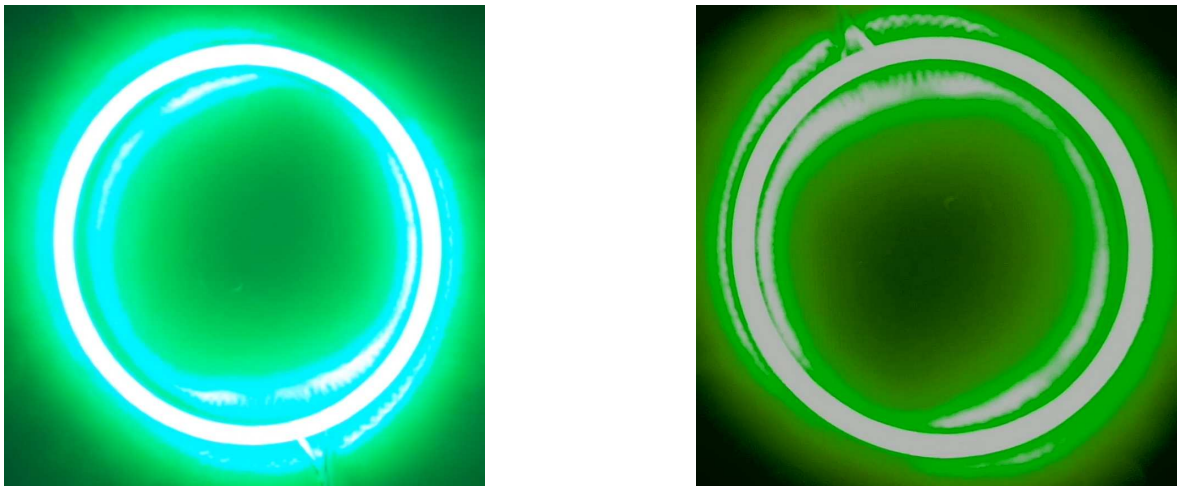

(a) 100% Luminance (b) 75% Luminance

Figure 6.3: LED flashing with 100% and 75% luminosity

adjusting the luminosity of the LED, the variable control VA1 was adjusted for the required settings. The base reference for the luminosity was set as 100% LED brightness. From 100% it was reduced to 75, 50 and 25%. The variation was made by monitoring the brightness level with a Lux meter and monitoring the voltage at the LED terminals. With 100%, brightness the luminance level was approximately 1430 ±20 Lux with a terminal voltage of 11.5 V. Based on the maximum luminance value, 75, 50 and 25% of the maximum luminance values were calculated along with the LED terminal voltages recorded. All the luminance values were measured with an ambient room brightness of 120 – 124 lux. The distance between the Lux meter and the stimulus was 60 cm when the luminance values were recorded. The luminance values along with the terminal voltage and four luminance levels are shown in Table 6.1.

The visual stimulus at 100 % brightness and visual stimulus at 75 % of the full brightness is shown in Figure 6.3.

6.3 Experimental Setup

To investigate the influence of visual stimulus luminance in SSVEP responses, five participants with perfect or corrected vision were chosen in the age group of 24 to 46 (three males and two females). The visual stimulus was fixed at eye level at 60 cm distance from the participant on an adjustable stand. For recording the EEG, EMOTIV EPOC+ research edition was used with all 14 electrodes prepared with saline soaked felts. The contact quality was tested with Test-bench software and the electrodes were adjusted accordingly. Only electrode O2 data was used for this study since the SSVEP is higher in the occipital region.

The visual stimulus controller was programmed with the desired frequency to evoke SSVEP for the recording trials. The frequency accuracy of the visual stimulus was verified with a digital oscilloscope at the COB LED terminals whenever new firmware was loaded to alter the flicker rates. The recording process started with a visual stimulus frequency of 7 Hz and the luminance level at 25 %. Each recording was for 30 seconds and five trials each for the same frequency and luminance level for each participant. The recording continued with the 7 Hz frequency, but the luminance value was changed to 50% by using the reference voltage in Table 6.1, by adjusting VR1 for five trials. After each 30 seconds recording, a break of one minute was given to the participant for any previous responses to subside. The same procedure was followed for 75 and 100% at 7 Hz. SSVEP data recording from frequencies 8, 9 and 10 Hz followed the same procedure with five trials each for different frequencies and luminance levels.

In total, each participant had 80 trials from four frequencies, four luminance levels and five trials each with one frequency and one luminance combination with a total recording time of 40 minutes excluding breaks and setup.

6.4 Signal Processing and Analysis

The five trials from each luminance level and frequency combination had 150 segments of one-second EEG data that was filtered using a band-pass filter and then analysed with Fast Fourier Transform. The maximum amplitude was stored for further statistical analysis. For analysing the influence of visual stimulus luminance in evoking SSVEP, statistical analysis was performed using Kruskal-Wallis tests as normality of the data was not assumed. The test performed the analysis of maximal FFT amplitudes from four different luminance levels for all four frequencies and from five participants.

The analysis compared the data statistically to identify the most responsive visual stimulus luminance level from the four different selected luminance intensities. The data set had 150 amplitude values for each frequency and luminosity. Four sets of data from each participant (25, 50, 75 and 100%) were analysed for each selected frequency (7, 8, 9 and 10 Hz). Figures 6.4 to 6.8 show the box plots for the maximum FFT amplitudes obtained for 7 Hz visual stimulus with four luminance levels from five participants. The central line in the boxplots shows the median value and it can be seen that 75% luminance had the highest SSVEP response.

Statistical analysis of Kruskal-Wallis tests $\chi^2(df = 3, N = 150)$ showed significant difference between visual stimulus luminance levels for all five participants:

$$P1 : \chi^2 = 528.57, p = 3.07e^{-114}$$
$$P2 : \chi^2 = 486.76, p = 3.51e^{-105}$$
$$P3 : \chi^2 = 555.48, p = 4.49e^{-120}$$
$$P4 : \chi^2 = 411.98, p = 5.58e^{-89}$$
$$P5 : \chi^2 = 418.49, p = 2.18e^{-90}$$

The mean ranks for all the different luminance levels for visual stimulus for five participants is shown in Table 6.2. From the values in the Table 6.2, it can be observed that 75% luminance gave the highest performance when compared to other luminance levels.

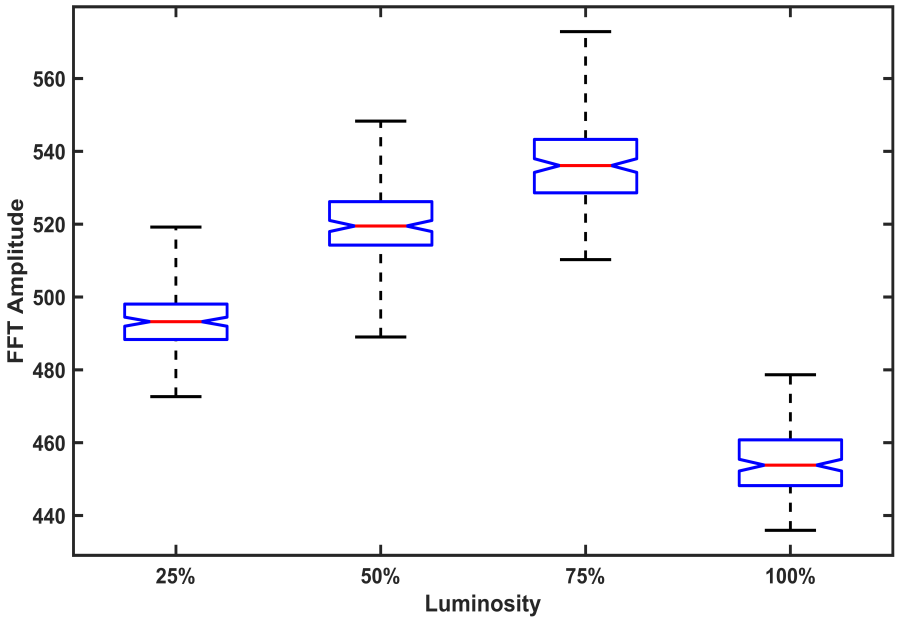

Figure 6.4: Maximal FFT amplitude values from first participant

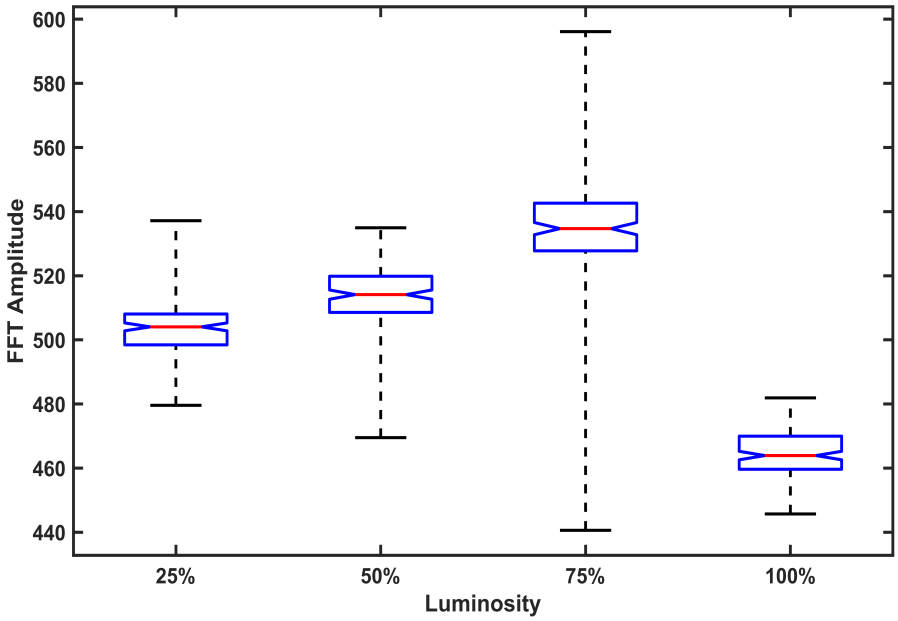

Figure 6.5: Maximal FFT amplitude values from second participant

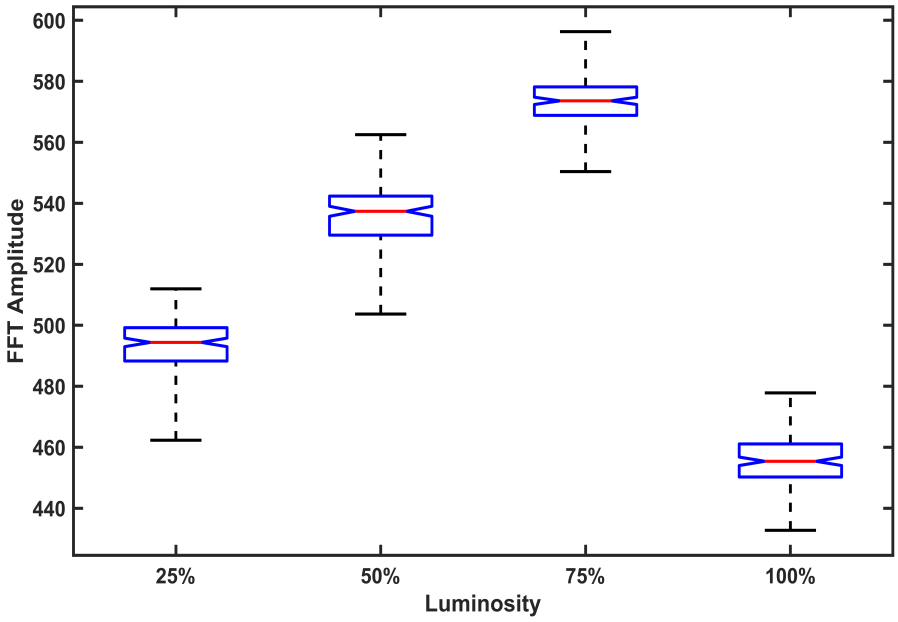

Figure 6.6: Maximal FFT amplitude values from third participant

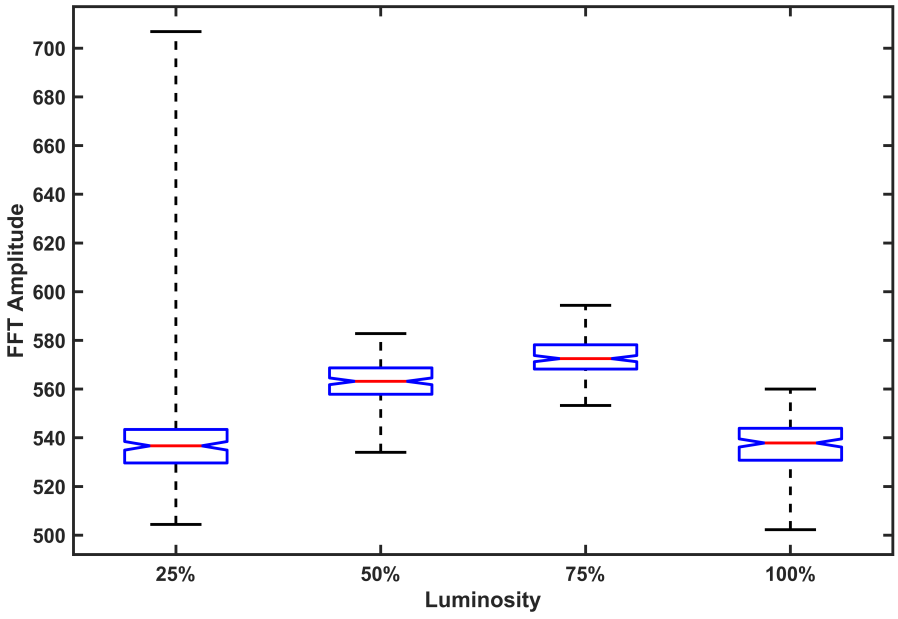

Figure 6.7: Maximal FFT amplitude values from fourth participant

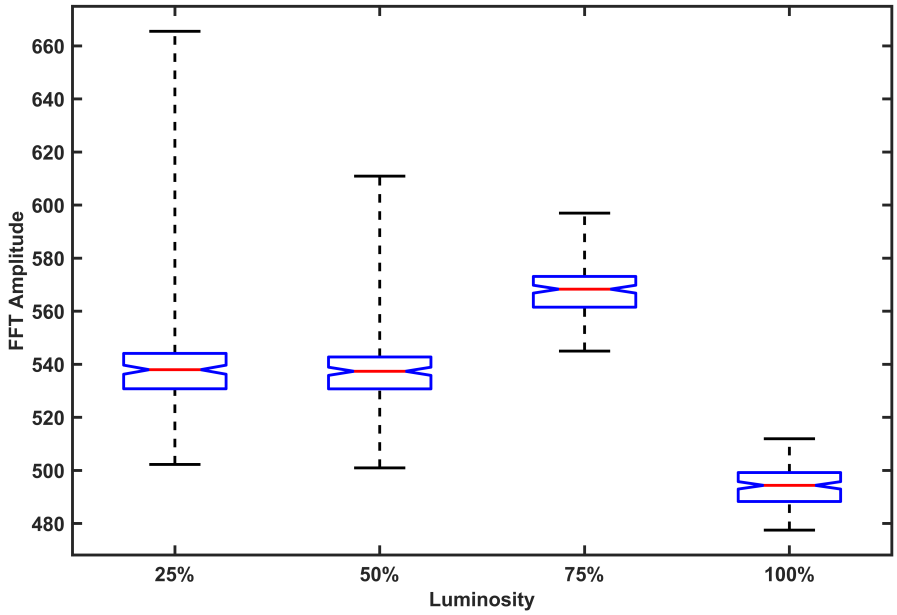

Figure 6.8: Maximal FFT amplitude values from fifth participant

Table 6.2: Mean rank from Kruskal-Wallis test for all participants at 7 Hz

Luminosity (%) at 7 Hz	**Participants (mean rank)**				
	S1	S2	S3	S4	S5
25	230.09	258.84	225.52	172.14	280.98
50	390.16	357.88	379.63	425.70	310.69
75	**506.17**	**507.53**	**521.34**	**460.79**	**509.25**
100	75.57	77.73	75.50	143.36	101.06

The least performance is from the highest luminance value.

For other frequency and luminance levels, analysis was performed using the same procedure for all the participant data. The data was analysed by combining 750 FFT values from five participants (150 values each from five trials) for each luminance level with Kruskal-Wallis test.

Kruskal-Wallis tests $\chi^2(df = 3, N = 750)$ showed significant difference between visual stimulus luminance levels for all five participants for 8, 9 and 10 Hz.

$$8Hz : \chi^2 = 1.88e^{+03}, p = 0$$

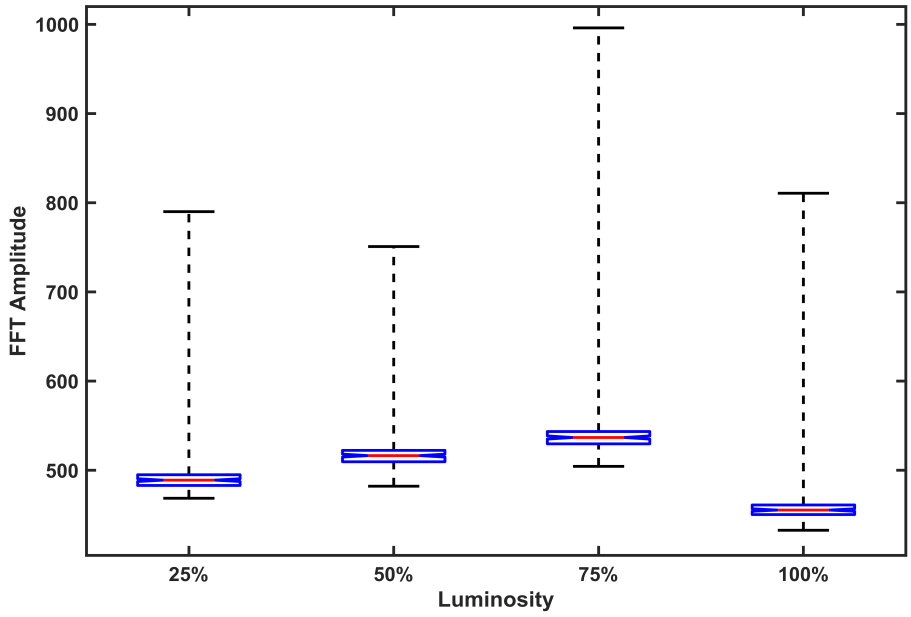

Figure 6.9: Maximal FFT amplitude values from five participants for 8 Hz

Table 6.3: Mean rank from Kruskal-Wallis test for all participants at 8 Hz

Visual Stimulus Frequency - 8 Hz				
Luminance %	25	50	75	100
Mean Rank	1270	1810	2390	529

$$9Hz : \chi^2 = 2.22e^{+03}, p = 0$$

$$10Hz : \chi^2 = 2.11e^{+03}, p = 0$$

The lowest SSVEP response was from the maximum luminance and the highest SSVEP response was from 75% of the maximum luminance for all the five subjects. Figures 6.9 to 6.11 show the box plots for 750 FFT values from all the subjects for the selected frequencies. The mean ranks for all different visual stimulus luminance levels for five participants are shown in Tables 6.3 to 6.5. The results showed that a luminance level of 75% gave the highest SSVEP for all five participants.

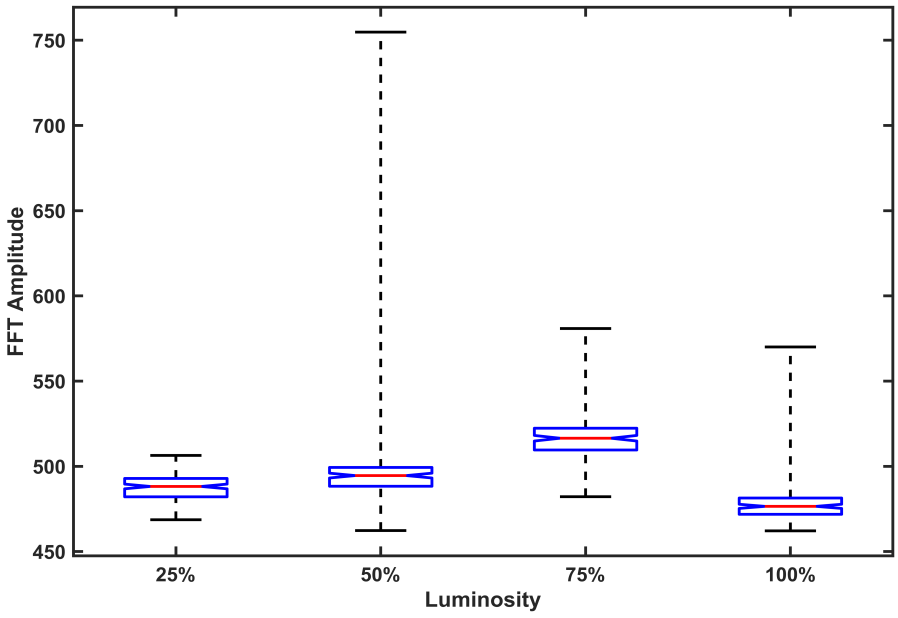

Figure 6.10: Maximal FFT amplitude values from five participants for 9 Hz

Table 6.4: Mean rank from Kruskal-Wallis test for all participants at 9 Hz

Visual Stimulus Frequency - 9 Hz				
Luminance %	25	50	75	100
Mean Rank	979	1810	2560	653

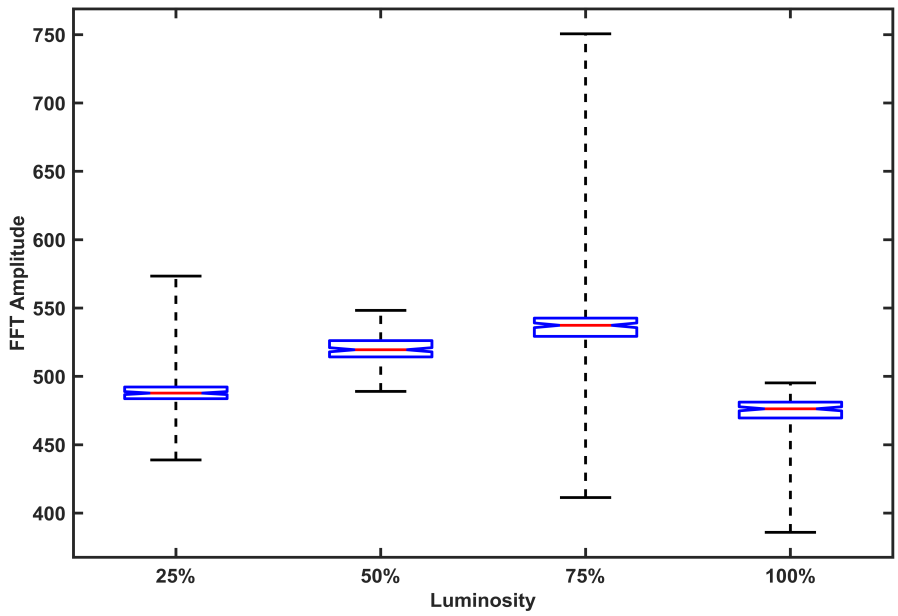

Figure 6.11: Maximal FFT amplitude values from five participants for 10 Hz

Table 6.5: Mean rank from Kruskal-Wallis test for all participants at 10 Hz

Visual Stimulus Frequency - 10 Hz				
Luminance %	25	50	75	100
Mean Rank	1170	1690	2550	573

6.5 Research Findings

The study investigated the influence of luminance in evoking SSVEP. A COB radial 130 mm LED with uniform circular light distribution was used to compare the luminance levels with flicker frequencies of 7, 8, 9 and 10 Hz and the SSVEP responses compared. From the data analysed from five participants, 75% of the maximum visual stimulus luminance gave the highest response as compared to 25, 50 and 100%. Maximum brightness not only reduced the SSVEP response but also increased the visual fatigue for the participants (as confirmed with participants verbally after the experiments).Reduction in EEG responses due to high luminance level was also reported by a study which explore attention level (Min et al., 2013). Participants also observed, 75% luminance level was easy to focus and gave better viewing comfort as compared to lower luminance levels. With much lower luminance levels, participants required higher attention levels that also increased eyestrain.

The study identified the luminance level between 1000 – 1500 Lux using COB LEDs would give the maximal response and better viewing comfort in evoking SSVEP for BCI applications. This would also reduce visual fatigue and attention shifts that might be an issue with multiple LED arrays.

6.6 Publication

Conference Proceeding

1. Mouli, S. & Palaniappan, R., 2016. Eliciting Higher SSVEP Response from LED Visual Stimulus with Varying Luminosity Levels. 2016 International Conference for Students on Applied Engineering (ICSAE), pp.362–367.

Chapter 7

Towards a reliable pulse-width modulation based LED visual stimulus for improved SSVEP response with minimal visual fatigue

7.1 Introduction

This study explores the influence of pulse width modulated signals in controlling the ON/OFF timings of the visual flicker to improve SSVEP response and reduce visual fatigue caused due to the flickering light. The majority of LED based visual stimulus designs are based on equal ON/OFF times, namely a 50% duty-cycle (da Silva Pinto et al., 2011; Teikari et al., 2012; Puanhvuan and Wongsawat, 2011; Dong-Ok et al., 2016; Friganović, Medved and Cifrek, 2016). The hypothesis is that the 50% ON period of the LED could increase eyestrain for users causing visual fatigue and at the same time lower the attention level and reduce SSVEP response. This could be addressed by reducing the OFF periods, making the flicker effect less visible from the visual stimulus and at the same time maintaining the frequency accuracy of the visual stimulus. With Pulse Width Modulation (PWM), it

is possible to control the ON/OFF periods of a LED with the microcontroller through custom firmware. For this study, flicker frequencies 7, 8, 9 and 10 were used with duty-cycles of 50, 80, 85, 90 and 95%. Data recorded from ten participants was analysed statistically to identify the most responsive and comfortable duty-cycle value that gives the highest SSVEP response. The results showed, 85% duty-cycle gave the highest SSVEP response with lower eyestrain and improved comfort for all participants.

7.2 PWM based Stimulus Hardware Design

To investigate the effect of ON/OFF timing (duty-cycle) in visual stimulus design, five different duty-cycle values were selected for frequencies 7, 8, 9 and 10 Hz. For the control platform, Teesny was chosen as the microcontroller as it supports PWM outputs. With this technique, the ON/OFF time can be defined by developing code for the switching timings. The ON/Off time, which is termed the duty-cycle, can be defined as,

$$Duty - cycle = (T_{ON})/(T_{ON} + T_{OFF}) * 100\% \tag{3}$$

Figure 7.1 shows a graphical representation of duty-cycle which is shown by a square wave with ON and OFF periods marked. It shows a full cycle with a longer ON (T_{ON}) period and a shorter OFF (T_{OFF}) period.

Figure 7.2 shows square waves of different duty-cycles that were used in this study, It shows the 50% that is widely used in SSVEP studies with equal ON/OFF times, and also the higher duty-cycle pulses generated for this study.

Even though in theory, duty-cycle is defined as in equation (3), the practicality in generating a higher duty-cycles with precisely maintained frequency requires various trials and code optimisations. Since the selected frequencies have only one count difference in

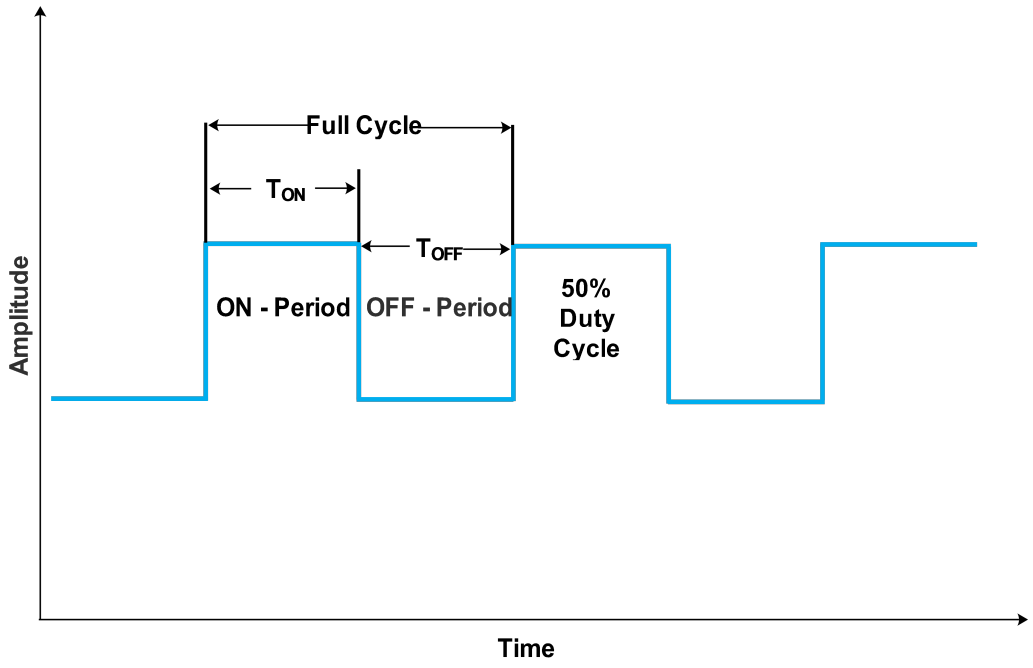

Figure 7.1: Duty-Cycle representation

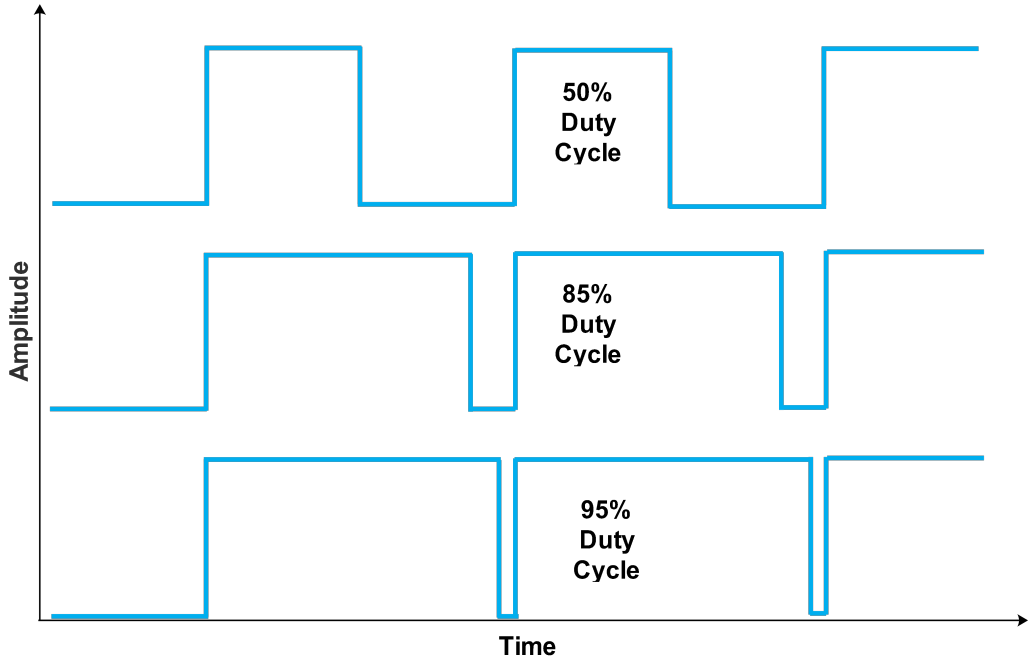

Figure 7.2: Waveforms with various duty-cycles for visual stimulus

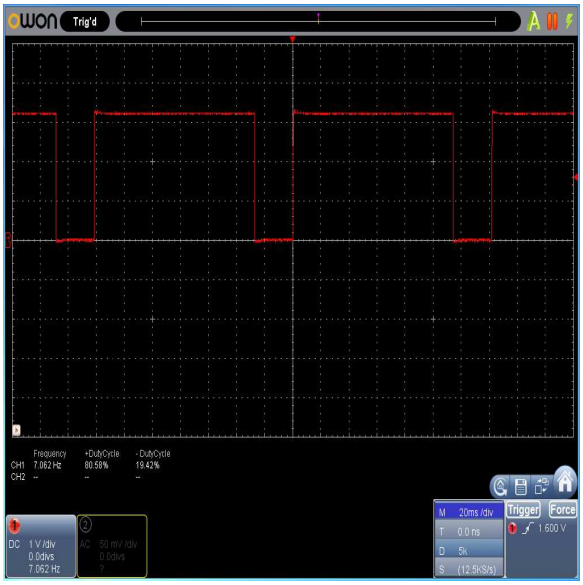

(a) Signal at 80% DC

Period = 141.6 ms	Frequency = 7.062 Hz
RiseTime = <100.0 us	FallTime = <100.0 us
+PulseWidth = 114.1 ms	- PulseWidth = 27.50 ms
+DutyCycle = 80.58%	- DutyCycle = 19.42%
Vpp = 3.360 V	Vmax = 3.320 V
Vmin = -40.00 mV	Vamp = 3.240 V
Vtop = 3.240 V	Vbase = 0.000 mV
Overshoot = 2.47%	Preshoot = 1.23%
Vavg = 2.568 V	Vrms = 2.881 V

(b) Waveform details

Figure 7.3: Information snapshot of duty-cycle at 80% for 7 Hz

between, the generated flicker has to be precisely maintained while changing the duty-cycle. The schematic of the hardware platform is similar to the schematic in Figure 6.2 from chapter 6, except that the Teensy I/O pin used is 3 with PWM support. The Teensy microcontroller drives the COB LED via the MOSFET and the brightness is adjusted to 75 % via the variable controller VA1. The brightness level was verified with the Lux meter and the terminal voltage as specified in Table 6.1 in chapter 6.

The pulse width waveforms generated with custom code are shown from Figures 7.3 to 7.5. The accuracy of the generated pulses were very precise as shown in the waveforms and are measured with a digital oscilloscope. Below each snapshot of the generated square wave, the detailed information of the pulse is shown. The designed portable hardware and the firmware can be customised to generate many frequencies with the required duty-cycle, which is not normally possible with traditional LCDs as widely used for stimulus presentation.

On the flicker side, a 130 mm radial COB LED was used to generate the visual flickers with different duty-cycles. The radial ring had 156 individual LEDs densely packed, which produced a uniform green light. The desired frequency along with the required

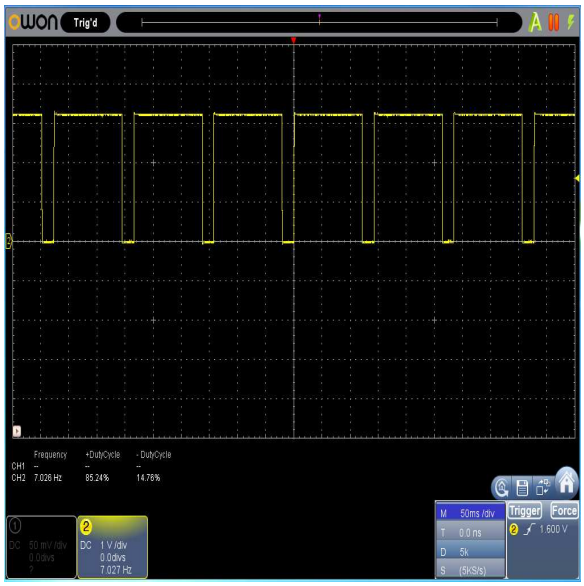

(a) Signal at 85% DC

Period = 142.2 ms	Frequency = 7.034 Hz
RiseTime = <250.0 us	FallTime = <250.0 us
+PulseWidth = 121.3 ms	- PulseWidth = 21.00 ms
+DutyCycle = 85.24%	- DutyCycle = 14.76%
Vpp = 3.400 V	Vmax = 3.320 V
Vmin = -80.00 mV	Vamp = 3.280 V
Vtop = 3.240 V	Vbase = -40.00 mV
Overshoot = 2.44%	Preshoot = 1.22%
Vavg = 2.749 V	Vrms = 2.982 V

(b) Waveform details

Figure 7.4: Information snapshot of duty-cycle at 85% for 7 Hz

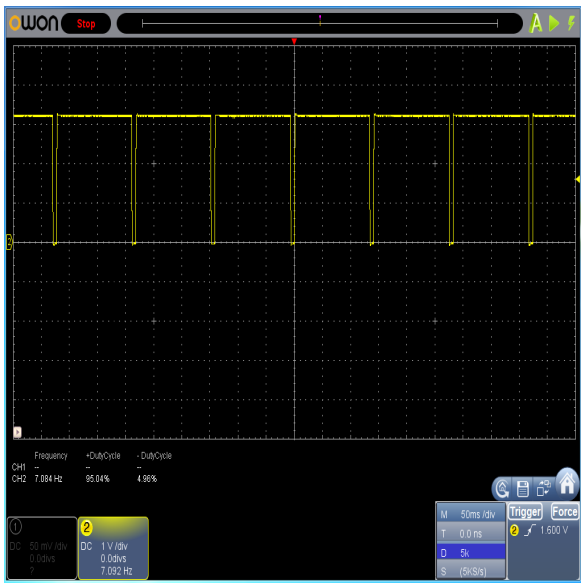

(a) Signal at 95% DC

Period = 141.2 ms	Frequency = 7.084 Hz
RiseTime = <250.0 us	FallTime = <250.0 us
+PulseWidth = 134.0 ms	- PulseWidth = 7.000 ms
+DutyCycle = 95.04%	- DutyCycle = 4.96%
Vpp = 3.360 V	Vmax = 3.280 V
Vmin = -80.00 mV	Vamp = 3.280 V
Vtop = 3.240 V	Vbase = -40.00 mV
Overshoot = 1.22%	Preshoot = 1.22%
Vavg = 3.067 V	Vrms = 3.147 V

(b) Waveform details

Figure 7.5: Information snapshot of duty-cycle at 95% for 7 Hz

duty-cycle was programmed in the Teensy module for the EEG recording sessions.

7.3 Experimental Setup

The EEG data was recorded using the EMOTIV EPOC+ research edition headset with 14 channels and two reference electrodes. In order to identify the best duty-cycle for the visual stimulus, only data from channel O2 was used for all the different frequencies and duty-cycle combinations. For EEG recording, EMOTIV test bench was used and data was recorded for 30 seconds for each trial, with a sampling frequency of 128 Hz, which was fixed in hardware but was sufficient to avoid aliasing as the highest EEG stimulus frequency was 10 Hz. Each participant had trials from four frequency and five duty-cycle combinations with a total recording time of 50 minutes excluding the rest and setup time (100 trials lasting 30 seconds each).The visual stimulus luminance level was set to 75% of the total luminance as it gave the highest SSVEP response in the previous study for all duty-cycle values.

To explore the influence of duty-cycle in visual flicker, ten participants with perfect or corrected vision within an age group of 25 to 46 (four females and six males) were chosen for this study. Ten participants were used to ensure the validity of the final proposed paradigm to improve the SSVEP BCI. Participants did not have any prior experience with BCI or any other visual stimulus based studies. The participants were comfortably seated 60 cm from the visual stimulus, which was placed at eye level. The recording started with 7 Hz flicker and a duty-cycle of 50% and the data was recorded for 30 seconds. Five trials of the same combination was recorded with a break of one minute between trials. For the second set, the stimulus was programmed with 7 Hz with 80% duty-cycle and five trials were recorded. Similarly, all frequency and duty-cycle combinations were recorded from all ten participants.

7.4 Signal Processing and Analysis

The EEG data was filtered using the same band-pass filter of 2 Hz bandwidth with centre frequency as the stimulus frequency and segmented into one second EEG segments as in the previous experiments. The five trials recorded for each session had 150 segments of one second SSVEP EEG data which was analysed using Fast Fourier Transform (FFT) and the maximum FFT amplitudes stored from each segment for further statistical analysis. The Kruskal-Wallis test was used to identify significance of the difference in influence of duty-cycles in SSVEP. The analysis was performed on maximal FFT amplitudes of EEG data for all five duty-cycles to identify the most responsive ON/OFF period.

For each data set, there were 150 amplitude FFT values for each frequency and duty-cycle from one participant. Each participant had 20 sets of data which included four frequencies and five duty-cycle values using the same LED visual stimulus. Figures 7.7 to 7.10 show the box plots for the obtained FFT amplitudes for different duty-cycles and frequencies 7, 8, 9 and 10 Hz. Each box plot data consists of combined 1500 values from ten subjects with same duty-cycle value and with same visual stimulus frequency. The central line in the box shows the median value while the edges of the box are at 25^{th} and 75^{th} percentiles with the whisker values not displayed.

The Kruskal-Wallis tests, $\chi^2(df = 4, N = 1500)$, shows significant differences between different duty-cycle values for all ten participants and significance p-values very close to zero.

$$7Hz : \chi^2 = 4.6e^{+03}$$
$$8Hz : \chi^2 = 4.2e^{+03}$$
$$9Hz : \chi^2 = 5.1e^{+03}$$
$$10Hz : \chi^2 = 5.3e^{+03}$$

Table 7.1 shows the average mean ranks for all the different duty-cycles for ten participants with four different frequencies. The mean ranks were individually computed for each frequency with different duty-cycle to analyse the influence of duty-cycle in SSVEP

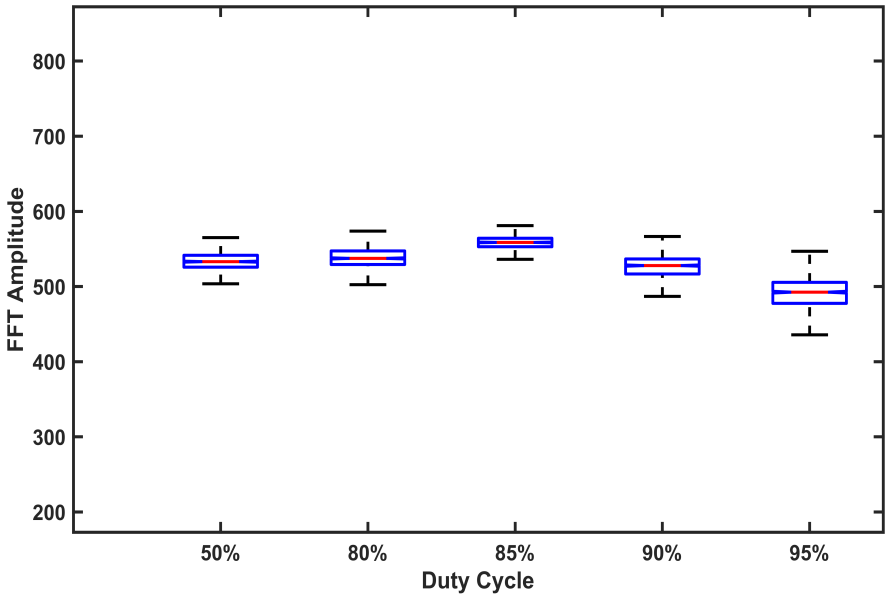

Figure 7.6: Maximal FFT amplitude values from ten participants at 7 Hz

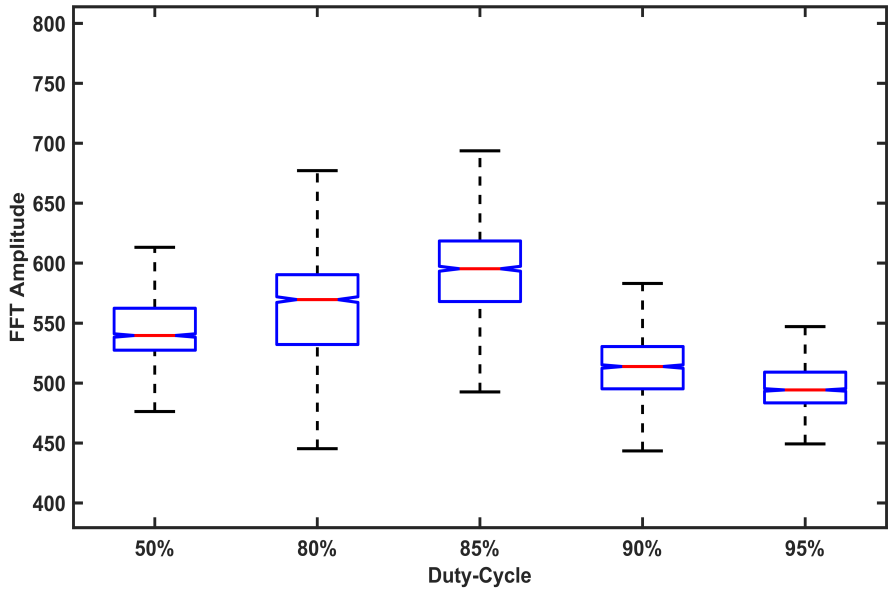

Figure 7.7: Maximal FFT amplitude values from ten participants at 8 Hz

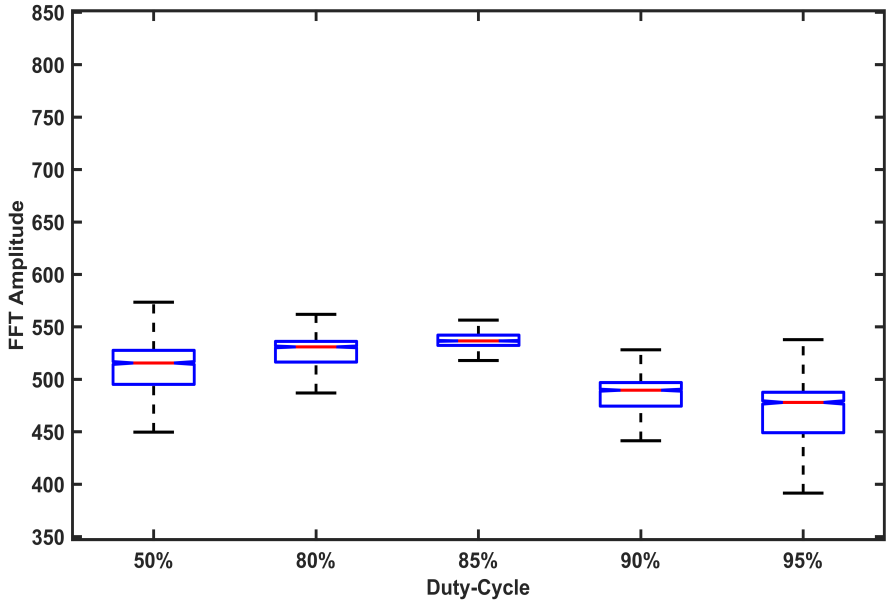

Figure 7.8: Maximal FFT amplitude values from ten participants at 9 Hz

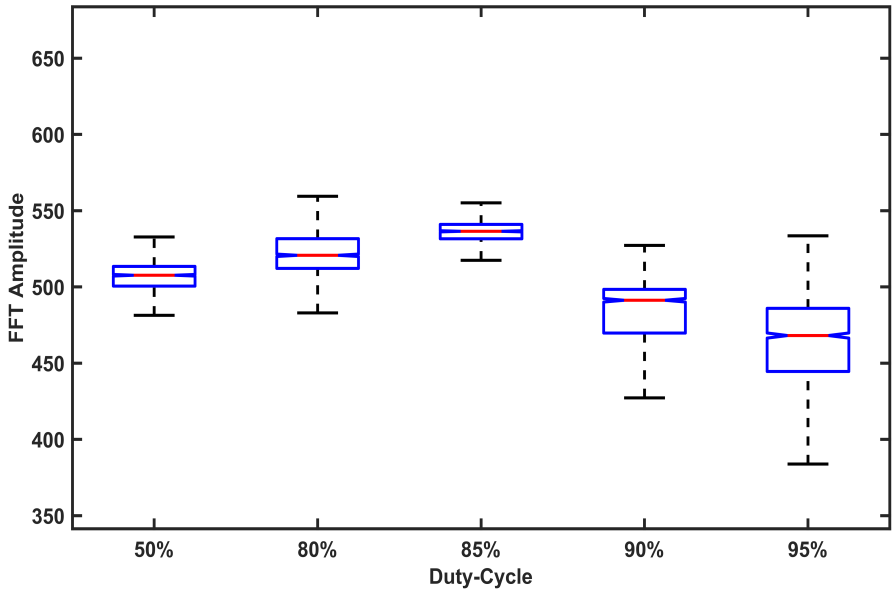

Figure 7.9: Maximal FFT amplitude values from ten participants at 10 Hz

Table 7.1: Kruskal-Wallis mean rank, average of maximal FFT (and standard deviation) 10 participant's average

Freq (Hz)	Duty-Cycle									
	50%		80%		85%		90%		95%	
	Mean rank	Average ± SD	Mean rank	Average ± SD	Mean rank	Average ± SD	Mean rank	Average ± SD	Mean rank	Average ± SD
7 Hz	385.18	533.13 ± 5.0	447.15	537.87 ± 5.7	**645.57**	558.44 ± 7.5	310.46	525.36 ± 8.9	89.03	486.26 ± 6.58
8 Hz	391.10	549.33 ± 7.1	495.94	565.03 ± 6.1	**640.78**	599.49 ± 6.7	285.95	512.19 ± 7.0	116.97	497.76 ± 4.5
9 Hz	398.78	518.03 ± 5.1	534.43	525.69 ± 5.3	**620.11**	538.93 ± 3.8	214.42	478.63 ± 6.6	109.52	465.70 ± 5.9
10 Hz	394.97	507.80 ± 5.1	517.57	519.47 ± 6.2	**636.03**	535.35 ± 5.5	213.52	483.73 ±7.9	114.56	465.42 ± 5.8

response and averaged for ten subjects in Table 7.1. The individual data for each subject is included in the Appendix E. It can be observed that, 85% duty-cycle gave the highest performance as compared to other duty-cycles. The SSVEP responses decreased above 85% duty-cycle even though the participants reported an increase in comfort. The lowest SSVEP response was from 95% duty-cycle in all frequency ranges. With the increase in duty-cycle the flicker was barely visible for higher frequencies and the response was very low.

The study also explored the level of comfort for the users with different duty-cycles in all frequency ranges. A scale of one to ten (ten being the most comfortable) was used for comparing the stimulus comfort with reduced visual fatigue for different duty-cycles. The participant response is shown as a bar graph in Figure 7.11. Even though 90 and 95% duty-cycle shows the highest comfort value, the SSVEP responses were less compared to the responses from the 85% duty-cycle. With 85% duty-cycle, even though the visual fatigue level (measured here with the subject's comfort rating) was higher compared to longer duty-cycle of 90 and 95%, the SSVEP evoked had the maximal response with 85% and hence 85% duty-cycle is recommended for the visual stimulus for BCI applications.

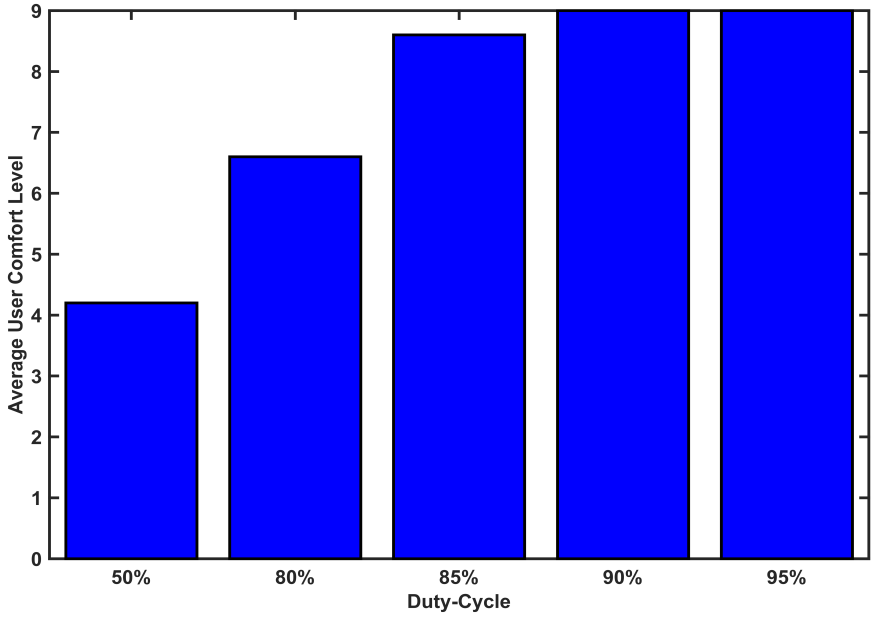

Figure 7.10: Analysis of participant responses for visual stimulus comfort

7.5 Research Findings

This study explored the influence of different duty-cycle values for visual stimulus, in eliciting SSVEP for reducing visual fatigue and improving the comfort of the user while giving improved response. The results were compared for frequencies 7, 8, 9 and 10 Hz with duty-cycle values of 50, 80, 85, 90 and 95%. The results show that there is an influence of duty-cycle in SSVEP responses and also the comfort improved with reduced visual fatigue. The data analysed from ten participants showed that the stimulus with 85% duty-cycle exhibited the highest response with minimal visual fatigue and improved comfort. The participants commented that they were able to gaze attentively for longer periods without discomfort, while producing better SSVEP responses. Duty-cycles above 85% showed a decrease in SSVEP response that could likely be due to the very small T_{OFF} period which might appear to the human eye to be constant light rather than flicker.

All the participants felt there was improvement in comfort when focusing on the visual stimulus when the duty-cycle increased as the stimulus was 'ON' with longer periods as compared to the conventional 50% ON/OFF duty-cycle which produces eye strain with

prolonged usage. Furthermore, the use of various higher duty-cycles would also help in presenting multiple visual stimuli for classification purposes suited to BCI applications. Each stimulus could be customised with different duty-cycle values to override the influence of adjacent stimulus in multi-stimuli configuration using lower frequencies that are more influential for SSVEP.

7.6 Publication

Journal

1. Mouli, S. & Palaniappan, R., (2016). Towards a reliable PWM based LED visual stimulus for improved SSVEP response with minimal visual fatigue. The Journal of Engineering, (IET). DOI: 10.1049/joe.2016.0314.

Chapter 8

Towards a hybrid BCI utilising SSVEP and P300 using event markers for improved classification using four LED stimuli

8.1 Introduction

This chapter explores the possibilities of combining SSVEP and P300 for developing a hybrid portable visual stimulus platform with four radial stimuli for SSVEP and four single LED stimuli for evoking P300. The hypothesis is that combining two BCI paradigms would improve the accuracy in classifying visual targets and reduce the number of false alarms in external application control. The four radial stimuli were used to generate four independent flickers with frequency 7, 8, 9 and 10 Hz that could be used for studying the accuracy of SSVEP classification. For P300 event generation, four red high power LEDs have used that flash randomly inside the green radial rings. Each P300 flasher generated a marker event while flashing and was recorded along with the SSVEP EEG data. The hardware platform used five independent microcontrollers, four of them were used for

evoking SSVEP and one microcontroller was used for the P300 markers. The data analysed from five participants to identify the classification accuracy of the hybrid stimulus showed that SSVEP classification could be improved using P300 events for developing reliable BCI platforms and it could also reduce the number of false alarms that could occur with a single EEG paradigm.

8.2 Design of Hybrid Stimulus Platform

Most BCI platforms are based on a single EEG paradigm, which may not work for all participants or conditions and could generate false alarms when classification is performed. This could be addressed using a hybrid BCI system to reduce the false alarms and improve accuracy. Hybrid BCIs are a combination of more than one EEG paradigm to improve usability and accuracy (Combaz and Hulle, 2015; Panicker, Puthusserypady and Sun, 2011; Müller-Putz et al., 2011). Almost all hybrid stimuli are based on stimulus presentation on the screen, especially for the P300 types. In this study, a standalone stimulus was designed based on LEDs, which could be customised with high precision. The hybrid stimuli have the advantage of presenting both SSVEP and P300 in the same space which reduces the attention shift from one stimulus to another. Figure 8.1 shows a hybrid stimulus BCI configuration using SSVEP and P300 for controlling different applications. It consists of four radial stimulus shown as green rings with flashing frequency of 7, 8, 9 and 10 Hz. Inside each ring, a high power red LED is placed at the centre to generate the P300 events, which are marked along with the flashes and stored with the SSVEP EEG data. The red LEDs flash individually at random timings controlled by a microcontroller. The red flash events are transferred as serial data from the microcontroller.

The hardware design consists of two independent control systems as shown in Figure 8.2. The first module controls the SSVEP stimulus hardware and the other controls the P300 LED drivers as well as and for sending markers to the Test-bench recording software. The first module had four independent microcontrollers to generate four different frequencies with high precision. The microcontrollers generated the frequencies 7, 8, 9

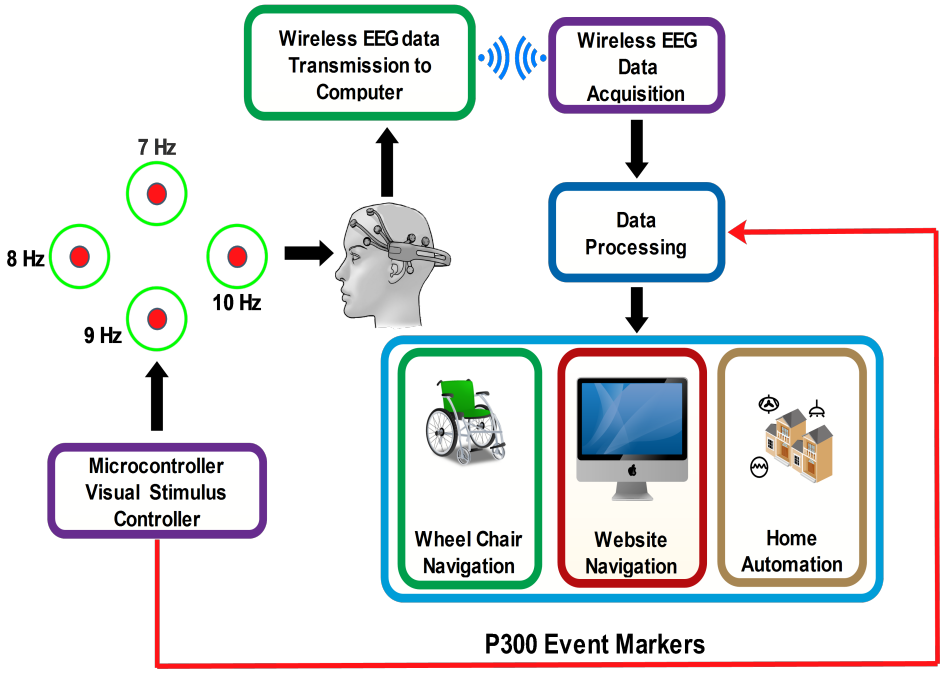

Figure 8.1: Hybrid BCI utilising SSVEP and P300

and 10 Hz individually with a duty-cycle of 85% as that duty-cycle gave the highest performance. The luminance of all the radial rings was set to 75% of the total brightness. The hardware design for all four SSVEP radial stimuli was the same as used in chapter 7.

For generating the P300 events, a separate Teensy module was used that could generate four random flashes and at the same time send the event markers for each flash separately. Sending the event marker data from the microcontroller to the recording software required communication between the microcontroller and computer, in this case we used a serial link, where Teensy serial ports (Rx and Tx) were used to communicate with the computer. Since Teensy Rx and Tx are transistor-transistor logic levels (TTL), it needs to be level shifted to standard RS232 serial communication level before sending the data to the computer. A MAX 3232 level shifter chip was used to convert from TTL to RS232 for this stimulus. The serial data from Teensy, was fed through the MAX3232 to the computer serial port. The schematic for the P300 stimulus is shown in Figure 8.3. Teensy also drives four red LEDs via four MOSFETs for randomly displaying the red flashes.

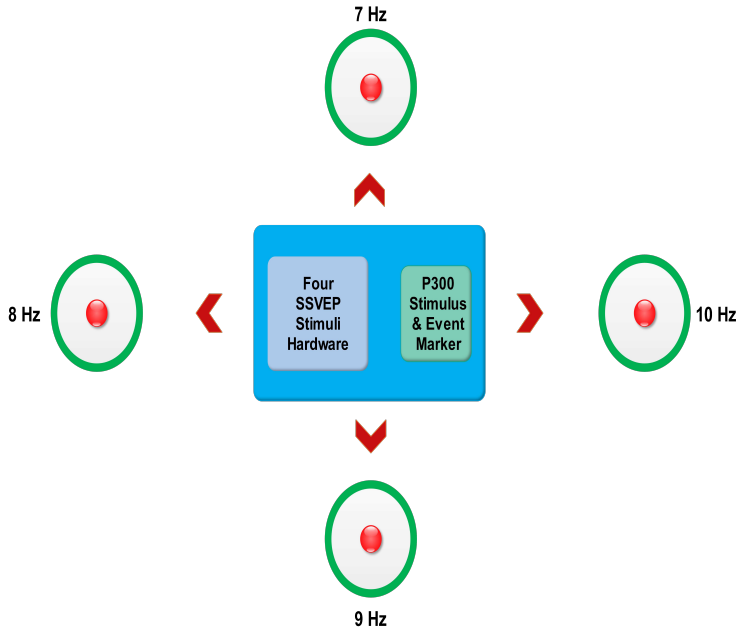

Figure 8.2: Hybrid stimulus design

Four LEDs, while flashing randomly, send marker values to the EMOTIV test bench software. The marker values for the red LEDs located in the radial rings 7, 8, 9, 10 Hz were marked as *111*, *222*, *333* and *444*, and these values were stored in the EDF data while recording. Figure 8.4 shows the Test-bench software screen capture, displaying the marker values. The serial communication was set to 115200 baud on both transmitter and receiver side. Each red LED flashed at random timings between 200 – 800 milliseconds using the random number generation function in the microcontroller with limits set between 200 – 800. The output frequencies were checked with a digital oscilloscope to ensure the precision of the visual stimulus.

8.3 Experimental Setup

To investigate the classification accuracies of the hybrid BCI using SSVEP and P300, five participants with perfect or corrected vision were chosen in the age group of 23 to 46 (three males and two females, mean age 35.6). The four radial stimuli along with four red LEDs were fixed on a black matte acrylic board at four locations as shown in Figure 8.5

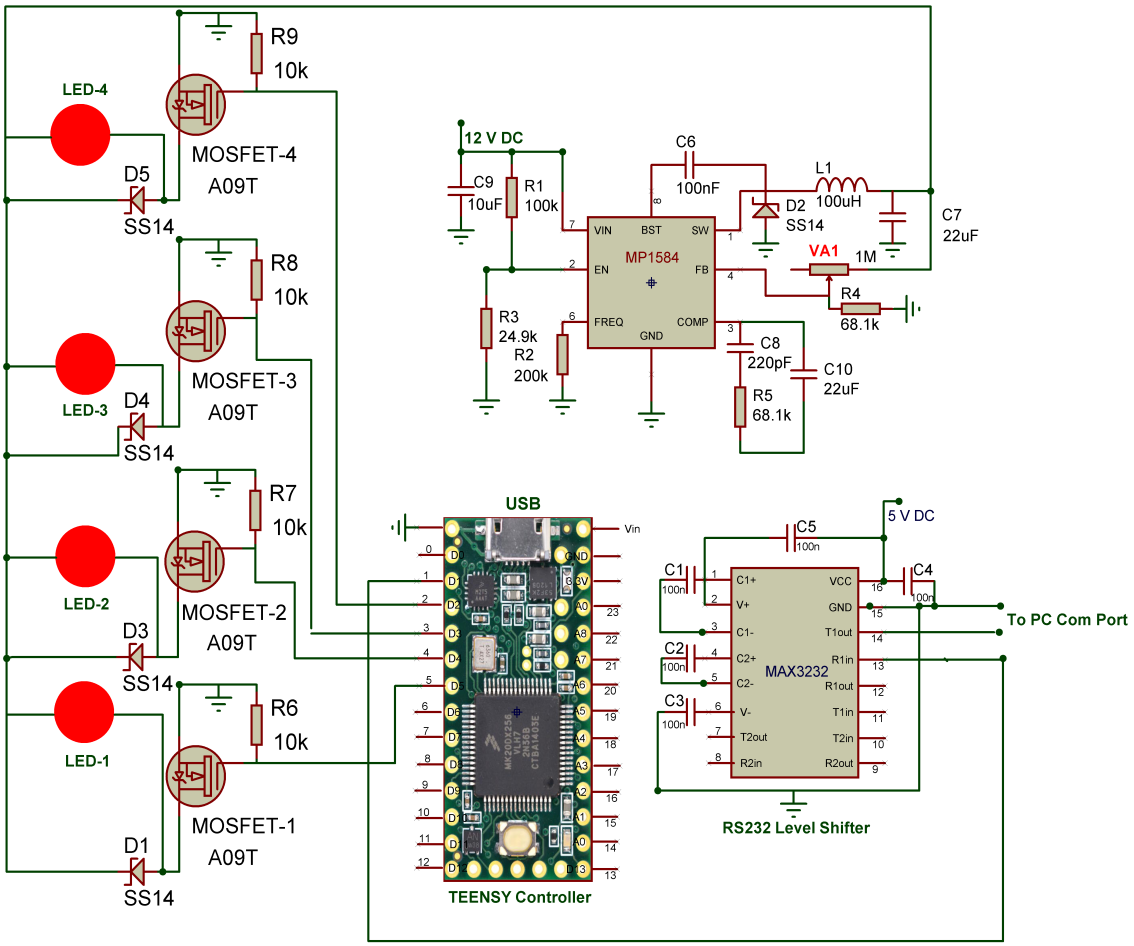

Figure 8.3: P300 stimulus with marker

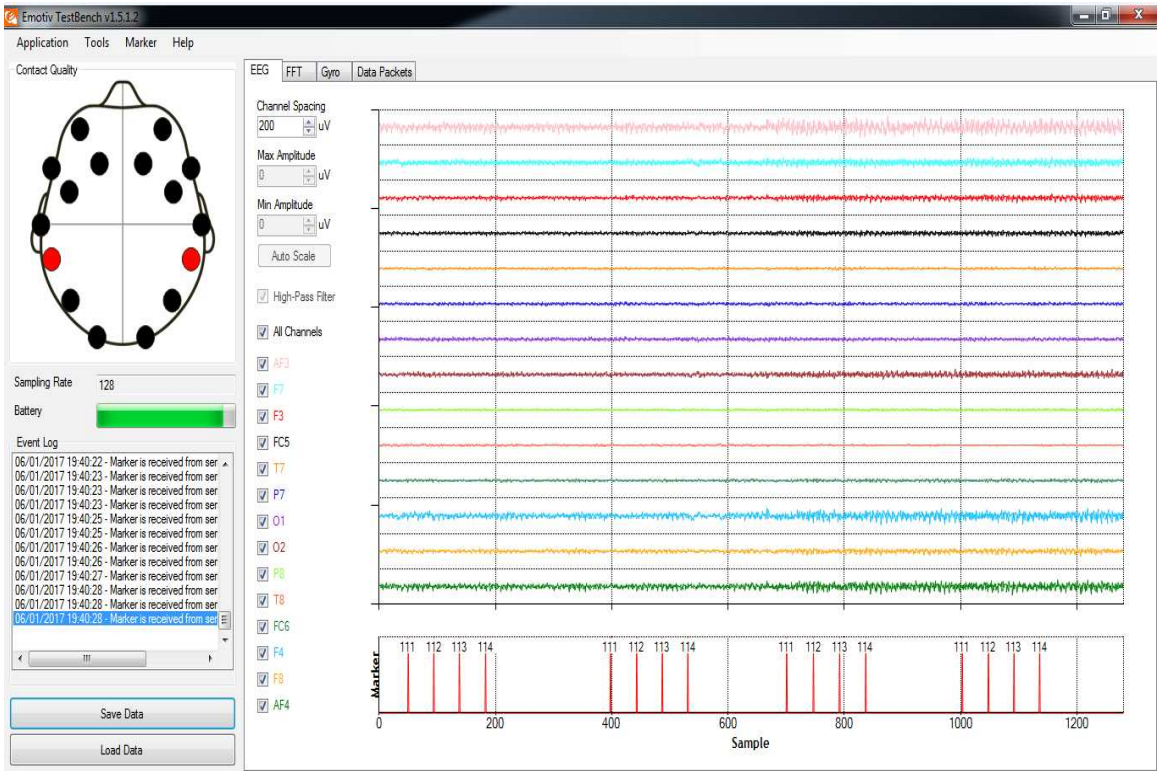

Figure 8.4: Test-bench software displaying the four marker values

and 8.6. The four locations has frequency values of 7, 8, 9 and 10 Hz in the anticlockwise direction starting from 7 Hz at the top. The P300 LEDs are place at the centre and the control hardware was mounted at the back of the acrylic board. In Figure 8.6, the random P300 flash is also visible in one of the radial rings while the visual stimulus was active. The acrylic board was fixed at eye level at 60 cm from each participant on an adjustable stand. For the EEG data collection, EMOTIV EPOC+ research edition was used, which has 14 electrodes. For this study, electrode O2 was used for SSVEP detection as SSVEP responses are higher in the occipital region and F4 for the P300 responses, since that is the closest electrode to the midline for EMOTIV (EMOTIV has static electrodes) where P300 responses are higher (Elsawy et al., 2017; Duvinage et al., 2013a). The EMOTIV headset was prepared with all electrodes fitted with saline soaked felts and positioned on participant's head. The connection quality of the electrodes were tested using the test bench software and the electrodes were adjusted accordingly.

The hybrid visual stimulus controllers were programmed for SSVEP with the desired frequencies for each radial LED, which continuously flashed without any interruptions

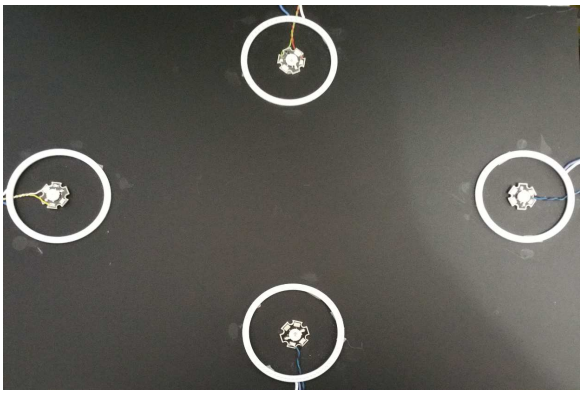

Figure 8.5: Hybrid LED stimuli set for investigating the classification accuracy

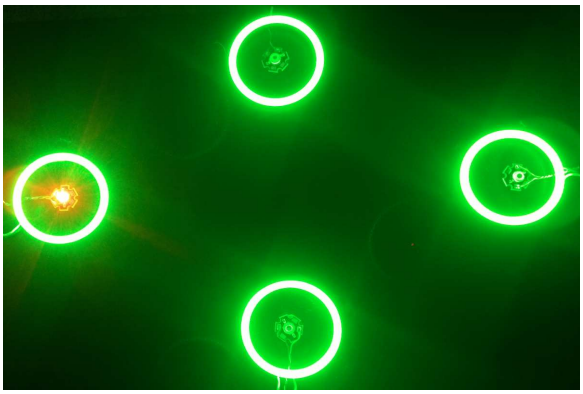

Figure 8.6: Hybrid LED stimuli showing the SSVEP and P300 stimulus

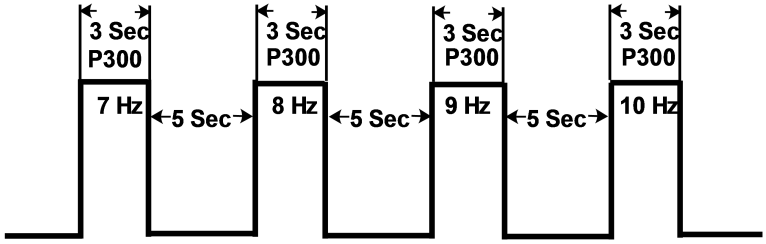

Figure 8.7: EEG recording timing for hybrid stimuli

with good frequency precision and with prolonged usage the frequency drift was observed to be less than ±0.02 Hz. The attention time for each radial stimulus was set to be three seconds for SSVEP and within the three seconds, at least one red LED flash occurred for the event marker to send the marker data to the recording software.

The EEG recording process started with the 7 Hz stimulus for three seconds followed by five second rest period when the participant looked away from the flashing stimulus. This was followed by frequencies of 8, 9 and 10 Hz with the same rest period to finish one complete session. Five sessions were recorded for each participant, which had EEG data for both SSVEP and P300 events. The stimulus timings are shown in Figure 8.7 for each frequency and rest period. Each three seconds on the timing chart is the focus time when the participants pay attention to each stimulus, and five seconds denotes the rest time between the changeovers from one stimulus to the next one in a sequential order. The recorded EEG data in EDF format was converted to MATLAB format using EEGLAB. Codes were then developed in MATLAB to process both the SSVEP and P300 event detections.

8.4 Signal Processing and Analysis

For SSVEP analysis, the data was extracted from the channel O2 for the required three second time period for each frequency and stored for further processing. The time period windows for the all the frequencies are shown in Table 8.1. In SSVEP data classification, the principle frequency along with first and second harmonics were analysed. The stored EEG data was filtered with a band-pass filter of 2 Hz bandwidth and centre frequency as

Table 8.1: Stimulus time windows for each frequency instances

7 Hz	8 Hz	9 Hz	10 Hz
3 - 6 sec	11 – 14 sec	19 -22 sec	27 – 30 sec

the stimulus frequency. This was performed for all principle frequencies and their harmonics. The variance of each filtered data was computed (as representing the energy), which included the principal frequency and the two harmonics, for classification analysis. It was decided to use the harmonics based on studies in which they had been shown to give better results (Guneysu and Akin, 2013; Bi et al., 2014).

For the P300 analysis, the data was extracted from channel F4 (closest to midline, that usually has the highest P300 response) along with the four event markers. The event markers were set as *111* for 7 Hz, *222* for 8 Hz, *333* for 9 Hz and *444* for 10 Hz. For the same time window as in SSVEP analysis as before when the participant focused on a stimulus, the algorithm checked for the event marker and found the peak value within 300 – 600 ms range from the event marker. P300 potential is generated approximately 300 ms after an event is triggered and hence a time window of 300 – 600 ms is used to detect the event marker (Ravden and Polich, 1999; Gray et al., 2004). This was performed for all four markers for four frequencies. The peak values for all the frequencies for the required time window were stored to analyse the classification accuracy. The evaluation of the portable hybrid stimulus was based on both SSVEP and P300 classification accuracy.

For classification, three approaches were used:

i Classification based on the computed energy with a principal frequency and two harmonics added together. The classification was taken as correct if the maximum of the four output energy values corresponds to the actual flash.

ii Using a threshold value by computing the mean of four output energy values and check if the maximum energy was greater than 1.6 x threshold. The value 1.6 was

Table 8.2: Classification Results

Participant	SSVEP classication accuracy without confidence measure (%)	Classification accuracy with SSVEP confidence measure (%)	Classication accuracy with confidence measure SSVEP + P300 (%)
P1	85	90	100
P2	75	90	100
P3	85	95	100
P4	85	90	100
P5	90	95	100

set based on preliminary trial and error and used as a confidence measure to decide on the correct classification i.e. the output was considered only if it exceeds the 1.6 x threshold; otherwise, the SSVEP data was dropped from consideration and would not affect the classification output.

iii If SSVEP confidence was low, instead of dropping this data as in (ii), an additional measure was utilised. P300 maximum peaks were computed for the four classes and the mean value was set as the threshold value and the maximum output value from four classes was checked if it was greater than 1.55 x threshold and if it is, then it was checked for correct or incorrect classification. Hence, this measure with P300 was used only for cases where there was no confidence from SSVEP output. If P300 output does not indicate confidence, then the data was dropped and not considered.

From Table 8.2, it can be observed that for all participants the classification accuracy for SSVEP used alone is above 75% and with confidence measure raises to above 90%. Combining both SSVEP and P300, all participants achieved success rates of 100% for all frequency ranges. However, it must be noted that due to the usage of the thresholds, outputs not indicating sufficient thresholds would have been dropped from the analysis resulting longer focus time for improved accuracy. Overall hybrid BCI approach would yield results that are more accurate while controlling BCI based applications.

8.5 Research Findings

The study explored the possibilities of combining two EEG paradigms to develop a hybrid BCI visual stimulus with reduced visual stimulus focus time and using only a single trial. The developed standalone hybrid stimulus successfully generated frequencies 7, 8, 9 and 10 Hz at 85% duty-cycle and 75% luminance level with narrow frequency division between the frequencies. P300 events were also generated simultaneously with four event markers and were successfully detected in the recorded EEG using MATLAB. From the analysis of data from the five participants, both SSVEP and BCI yielded better classification rates individually for the same time window for each frequency. P300 also gave good performance in a single trial. The combined classification results from SSVEP and P300 would improve the reliability in classification for controlling external application within a short time window of three seconds.

The participants responded that the hybrid stimuli did not induce any eyestrain, as the focus time was minimal and easy to move from one stimulus to other for classification requirements. Since the P300 stimulus was embedded in the radial rings, attention shift was also minimised producing maximal output in three second time window.

The stimulus video is available online at the URL below:
http://ssvep.co.uk/thesis/Four_stimuli_flicker.mp4 (Accessed on 20th January 2018)

8.6 Publication

Conference Proceeding

1. **Mouli, S.** & Palaniappan, R., 2017. Hybrid BCI utilising SSVEP and P300 event markers for reliable and improved classification using LED stimuli. In 2017 IEEE Symposium on Computer Applications & Industrial Electronics (ISCAIE), Langkawi, Malaysia, pp. 127 - 131.

Chapter 9

Online hybrid four class stimuli classification and control of wheelchair

9.1 Introduction

This chapter discusses the SSVEP online classification for four visual stimuli for controlling an external application. The visual stimulus is based on hybrid configuration discussed in chapter 8. The error correction is based on P300 event markers to improve the classification accuracy. The four radial stimuli in Figure 8.6 is arranged in such a way that it represents the four directions that could be used to navigate a wheelchair in four directions The stimulus frequencies 7, 8, 9 and 10 Hz were used for assigning the direction for the wheelchair movements. The SSVEP and P300 EEG data were streamed from the EMOTIV headset to the computer wirelessly and processed in near real-time using the previously developed confidence measure approach, to control the robot. The operations were successful with correct classification the majority of time in the first attempt within three seconds attention time, and sometimes by increasing the attention time to 1 or 2 seconds more. The demo was developed using a LEGO robot to imitate the movements for navigating a wheelchair.

9.2 SSVEP online classification

For the navigation control, four stimuli were used as described in chapter 8. The primary difference in EEG data analysis in this chapter is that the data was not stored for offline analysis. In this case, data was analysed in near real-time mode for the wheelchair navigation. For streaming the data from the EMOTIV headset to MATLAB, open source software called FieldTrip was used, which can stream data from the headset to MATLAB (Oostenveld et al. 2011). The EEG data was streamed continuously from the headset and stored in a temporary buffer before being processed in MATLAB. The required channel for the data stream has to be defined in the FieldTrip setting file 'emotive_config.txt'. Channel O2 and F4 were used for the data classification and for navigating the LEGO. The data was temporarily stored in a first-in first-out (FIFO) ring-buffer.

While a participant was focusing on the visual stimuli board, the data was processed in MATLAB for commands to be sent to the LEGO robot. The flowchart in Figure 9.1 shows the data processing algorithm for the hybrid stimulus. The acquired EEG data from channel O2 was filtered using four groups of band-pass filters for 7, 8, 9 and 10 Hz. Filtered data was stored in temporary variables and the maximum FFT values were computed and stored in an array. The index values of the arrays from 1 – 4 were classified using confidence measures based on SSVEP and P300 data and from this value, the command to move the robot in the required direction was assigned. LEGO NXT EV3 libraries were used for the LEGO operations in MATLAB. Two motors based on the required direction performed the motion control. Forward and backward motion used both motors working together whereas single motors performed left and right motions. Each activity took approximately 3 – 4 seconds of attention time for the command to be executed. For stopping the wheelchair the user can focus away from the stimulus that keeps the threshold level down using confidence measure algorithm for direction control, and that does not initiate any movements.

In some cases, the command *'right'* was overridden by the command *'left'* and this was rectified to some extent by changing the luminance level of the 8 Hz flicker to reduce the

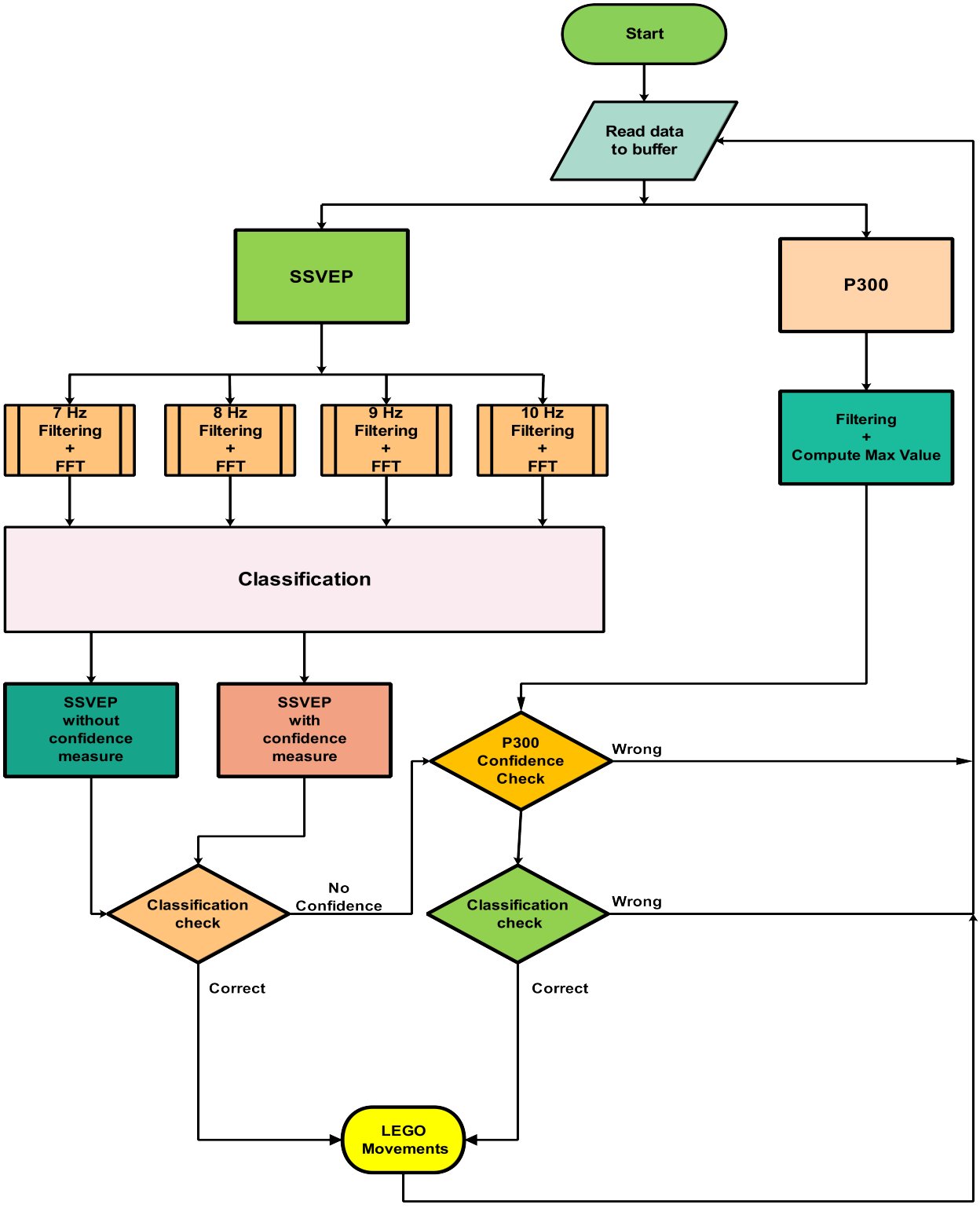

Figure 9.1: SSVEP online classification data flow

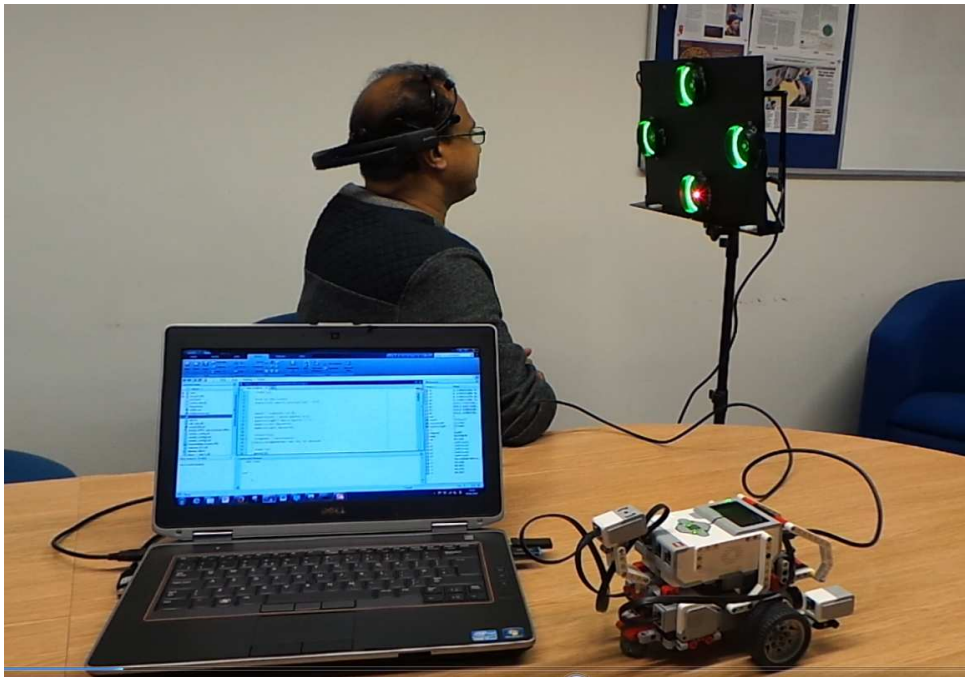

Figure 9.2: Stimulus presentation, data processing and LEGO operation

8 Hz response level in SSVEP. Figure 9.2 shows the complete stimulus setup with LEGO control using four visual stimuli in MATLAB.

9.3 Analysis of the practical implementation

SSVEP based command control was successfully implemented using the hybrid visual stimuli to control the movements of a wheelchair using LEGO robot. The visual stimulus with four low-frequency flickers was presented to the user for focusing one at a time to perform the motion commands for the LEGO robot. The commands were sent to the robot with a minimum attention time of 3 – 4 seconds on each visual stimulus. The movements of the robot were near real-time apart from minor delays in data processing and classification. The minor delays are approximately 3-4 sec for each motion and this is due to the data processing time required for the action. Occasional errors in classification, mainly between 8 Hz and 10 Hz for left and right directions, were corrected largely by changing the luminance level of 8 Hz to reduce the SSVEP response.

For the demonstration purpose, the controls were limited to four directions. The number of stimuli could be expanded to accommodate more function that could be implemented in a wheelchair like motorised seat height adjustment with additional pre-set stimuli, emergency support call that could dial a number when the user focuses on a set stimulus, posture adjustments and so on.

The implementation video is available online at the URL below.

http://ssvep.co.uk/thesis/Thesis_Lego_movements.mp4 (Accessed on 20th January 2018)

Chapter 10

Conclusion

This chapter discusses research findings and summaries of completed work. The contributions towards the SSVEP visual stimulus design are discussed first followed by possibilities to improve the SSVEP stimulus design with further work.

10.1 Contribution

This section highlights the main contribution of this thesis. Starting from chapter three, each chapter contributes to developing the hardware platform for improving the visual stimulus design to reduce visual fatigue and improve SSVEP EEG response. The main contributions of this thesis are listed below:

1. A new standalone hardware platform was developed using LEDs to generate precise visual flickers to evoke SSVEP to overcome the issues in generating flickers using traditional methods.

2. Identified that it is possible to reduce visual fatigue through LED based visual stimulus design with the possibility of generating frequencies with higher precision and portability than traditional systems.

3. The influence of visual flicker colour in evoking SSVEP was studied. Green was identified as the most responsive colour and also best for viewing comfort when

compared with red and blue.

4. Identified that visual stimulus orientation influences the elicitation level of SSVEP. In terms of visual stimulus orientation, horizontal stimulus orientation responses are higher than those from vertical stimulus orientation, when an array of LED based visual stimulus was presented to the user. Horizontal orientation also reduced the visual fatigue level and improved the comfort of the user.

5. Visual stimulus based on chip-on-board LEDs improves the comfort of the user and reduces the attention shift when using multiple stimuli.

6. Study of visual stimulus pattern identified that a radial stimulus gives better SSVEP response with lower visual fatigue.

7. Identified the influence of visual stimulus luminance in evoking SSVEP. With a visual stimulus luminance level of 100%, the SSVEP responses are lower than that with 75% luminance. Using 75% luminance rather than maximum brightness was also shown to reduce eyestrain for the user due to lower luminance level for SSVEP based applications.

8. Identified that SSVEP responses can be improved with visual flickers controlled by pulse width modulation. The ON and OFF period of the flashing LEDs can be customised with an increased LED ON period while maintaining the frequency precisely. This improved the SSVEP response and reduced the visual fatigue considerably for the user.

9. Developed hybrid visual stimulus hardware for using both SSVEP and P300 to improve the response and classification accuracy for BCI based applications. Developed P300 visual stimulus and event marker hardware to detect P300 events along with SSVEP.

10. To demonstrate the research findings in a practical way, LEGO robot control was performed to imitate a wheelchair navigation. With four stimuli, the robot moved

in four directions successfully with a minimum visual stimulus attention period of 3 seconds for each movement.

10.2 Discussion

This thesis has addressed issues found when evoking SSVEP with the visual stimulus presented traditionally on an LCD/CRT. In the traditional methods, the generated frequency of the visual stimulus is limited due to the fixed refresh rate of the screens, reducing the number of frequencies that could be generated. Users also experienced a higher level of visual fatigue due to on-screen stimulus presentation and also experienced interference when multiple stimuli are presented. The portable LED based visual stimulus system was shown to improve the comfort and reduce the eyestrain that the users experience with SSVEP based applications, without applying restrictions in frequency for generating flicker. Since the hardware is an embedded platform, It can be used be conveniently and quickly as soon as it is powered on.The developed hardware platform is fully customisable and also overcome the limitations of commercially available LED stimulation box.

EEG data were collected from many participants in this study for developing the hardware platform. The hardware went through many iterations to develop the platform for improving the SSVEP response, and to reduce the visual fatigue. A basic investigation was also performed for developing a dry electrode using pressure pins, though this was later dropped due to the non-availability of 3D printing facilities. Prototypes developed are shown in the Appendix A.

The research finding show that it is possible to develop a portable SSVEP based BCI platform with single EEG electrode (O2) that can classify the EEG data for four frequencies with low false alarm rates to control external applications. The developed platform is highly portable and battery operated and can operate continuously for 5- 6 hours when fully charged. The hardware is also reusable for other studies based on vision or psychology, as well as highly customisable through firmware reprogram ability.

10.3 Conclusion and Further Work

As reported in Chapter 8 regarding the hybrid stimulus, further research is needed to improve performance using joint classification of SSVEP and P300. Future work can also optimise the hardware platform in two ways: (1) by using higher level embedded platforms such as Raspberry Pi to generate the visual stimulus, and at the same time perform the analysis on-board to avoid the need for a standalone computer. This makes it a complete standalone platform for data acquisition and processing, (2) develop the Raspberry Pi or a similar powerful platform to include an intelligent visual stimulus that could automatically do a performance analysis of the visual stimulus for the user response, and adjust the duty-cycle and luminance levels of the visual stimulus for the maximum SSVEP response for that user.

Hybrid stimulus could also be explored by combining the SSVEP, P300 and audial stimulus to develop a multi-paradigm EEG BCI platform for controlling external application with greater accuracy with minimal stimulus time.

10.4 Publication arising from this research

1. Mouli, S. et al., (2013). Performance analysis of multi-frequency SSVEP-BCI using clear and frosted colour LED stimuli. In IEEE 13th International Conference on Bioinformatics and Bioengineering (BIBE), 2013. pp. 1–4. DOI: 10.1109/BIBE.2013.6701552.

2. Mouli, S.; Ramaswamy, P.; & Sillitoe, I.P., 2014. Arduino based configurable LED stimulus design for multi-frequency SSVEP-BCI. In PGBiomed/ISC 2014, the IEEE EMBS UKRI Postgraduate Conference on Biomedical Engineering. Warwick, pp. 1 - 4.

3. Mouli, S.; Palaniappan, R.; & Sillitoe, I.P., 2015. A configurable, inexpensive, portable, multi-channel, multi-frequency, multi-chromatic RGB LED system for SSVEP

stimulation. In T. A. Cassation, A.E. and Azar, ed. Brain-Computer Interfaces. Switzerland: Springer International Publishing, pp. 241 - 269.

4. Mouli, S.; Palaniappan, R.; & Sillitoe, I.P., 2015. Improving Steady State Visual Evoked Potentials Responses from LED Stimuli Through Orientation Analysis. Journal of Medical Imaging and Health Informatics, 5(5), pp.1070 - 1075.

5. Mouli, S. et al., 2015. Quantification of SSVEP responses using multi-chromatic LED stimuli: Analysis on colour, orientation and frequency. In 7th IEEE Computer Science and Electronic Engineering Conference (CEEC), 2015. pp. 93 - 98.

6. Mouli, S. & Palaniappan, R., (2016). Radial Photic Simulation for Maximal EEG Response for BCI Applications. In 9th International Conference on Human System Interaction (HSI), 2016. DOI: 10.1109/HSI.2016.7529658.

7. Mouli, S. & Palaniappan, R., 2016. Eliciting Higher SSVEP Response from LED Visual Stimulus with Varying Luminosity Levels. 2016 International Conference for Students on Applied Engineering (ICSAE), pp.201 - 206.

8. Mouli, S. & Palaniappan, R., 2017. Towards a reliable PWM based LED visual stimulus for improved SSVEP response with minimal visual fatigue. The Journal of Engineering (IET).

9. Mouli, S. & Palaniappan, R., 2017. Hybrid BCI utilising SSVEP and P300 event markers for reliable and improved classification using LED stimuli. In 2017 IEEE Symposium on Computer Applications & Industrial Electronics (ISCAIE), Langkawi, Malaysia, pp. 127 - 131.

References

1. Ahnate, L. and Scott, S. (2012). Reexamining Visual Orientation Anisotropies: A Bias Towards Simple Horizontal Stimuli on Temporal Order Judgments. In *34th Annual Conference of the Cognitive Science Society*, Austin, TX: Cognitive Science Society, pp. 1912–1917.

2. Al-Fahoum, A. S. and Al-Fraihat, A. A. (2014). Methods of eeg signal features extraction using linear analysis in frequency and time-frequency domains. *ISRN neuroscience*, 2014.

3. Alcaide-Aguirre, R. E. and Huggins, J. E. (2014). Novel hold–release functionality in a P300 brain–computer interface. *Journal of Neural Engineering*, 11(6), p. 66010.

4. Aloise, F. et al. (2011). P300-based brain–computer interface for environmental control: an asynchronous approach. *Journal of Neural Engineering*, 8(2), p. 025025.

5. Aminaka, D., Makino, S. and Rutkowski, T. M. (2014). Chromatic SSVEP BCI paradigm targeting the higher frequency EEG responses. In *Asia-Pacific Signal and Information Processing Association, 2014 Annual Summit and Conference (APSIPA)*, pp. 1–7.

6. Antranik (2016). Functional areas of the cerebral cortex. www.antranik.org/functional-areas-of-the-cerebral-cortex, Online; accessed on 15-January-2018.

7. Asensio-Cubero, J., Gan, J. Q. and Palaniappan, R. (2016). Multiresolution analysis

over graphs for a motor imagery based online BCI game. *Computers in Biology and Medicine*, 68, pp. 21–26.

8. Aydin, S. (2008). Model order sensitivity of burg method for eeg diagnosis. In *2008 IEEE 16th Signal Processing, Communication and Applications Conference*, pp. 1–2.

9. Aznar-Casanova, J. A. et al. (2017). Visual fatigue while watching 3D stimuli from different positions. *Journal of Optometry*, 10(3), pp. 149–160.

10. Benitez, D. S., Toscano, S. and Silva, A. (2016). On the use of the Emotiv EPOC neuroheadset as a low cost alternative for EEG signal acquisition.

11. Berger, H. (1929). Über das elektrenkephalogramm des menschen. *European Archives of Psychiatry and Clinical Neuroscience*, 87(1), pp. 527–570.

12. Berger, T. W. et al. (2008). *Brain-Computer Interfaces: An international assessment of research and development trends*. Springer Science & Business Media.

13. Bi, L. et al. (2014). A speed and direction-based cursor control system with P300 and SSVEP. *Biomedical Signal Processing and Control*, 14, pp. 126–133.

14. Birbaumer, N. et al. (1990). Slow potentials of the cerebral cortex and behavior. *Physiological Reviews*, 70(1), pp. 1 LP – 41.

15. Birbaumer, N. et al. (1999). A spelling device for the paralysed. *Nature*, 398(6725), pp. 297–298.

16. Birbaumer, N. et al. (2000). The thought translation device (TTD) for completely paralyzed patients.

17. Birbaumer, N. et al. (2003). The thought-translation device (TTD): neurobehavioral mechanisms and clinical outcome. *IEEE Transactions on Neural Systems and Rehabilitation Engineering*,, 11(2), pp. 120–123.

18. Blanuša, J. and Zdravković, S. (2015). Horizontal-vertical illusion in mental imagery: quantitative evidence. *Frontiers in Human Neuroscience*, 9, p. 33.

19. Brazier, M. A. B. (1964). The Electrical Activity of the Nervous System. *Science*, 146(3650), pp. 1423 –1428.

20. Bright, P. (2012). *Neuroimaging – Cognitive and Clinical Neuroscience*. Croatia: InTech.

21. Bronzino, J. D. (2006). *Biomedical Engineering Fundamentals*. Florida: Taylor & Francis Group, 3rd edn.

22. Buzsáki, G. (2006). *Rhythms of the Brain*. New York: Oxford Univ Press.

23. Caixeta, L., Ghini, B. G. and Peres, J. F. P. (2011). Neuroimaging in Dementia and Other Amnestic Disorders. In J. F. P. Peres, ed., *Neuroimaging for Clinicians – Combining Research and Practice*, Croatia: InTech, chap. 1, pp. 3 –14.

24. Cecotti, H. and Rivet, B. (2011). Effect of the visual signal structure on Steady-State Visual Evoked Potentials detection. In *International Conference on Acoustics, Speech and Signal Processing (ICASSP), 2011 IEEE*, pp. 657–660.

25. Chang, M. H. et al. (2014). An amplitude-modulated visual stimulation for reducing eye fatigue in SSVEP-based brain–computer interfaces. *Clinical Neurophysiology*, 125(7), pp. 1380–1391.

26. Chang, M. H. et al. (2016a). Eliciting dual-frequency SSVEP using a hybrid SSVEP-P300 BCI. *Journal of Neuroscience Methods*, 258, pp. 104–113.

27. Chang, M. H. et al. (2016b). Eliciting dual-frequency SSVEP using a hybrid SSVEP-P300 BCI. *Journal of Neuroscience Methods*, 258, pp. 104–113.

28. Chang-Hee, H., Han-Jeong, H. and Chang-Hwan, I. (2013). Modified pattern-reversal visual checkerboard stimuli with dual alternating frequencies for multi-class ssvep-based brain-computer interfaces. In *International Winter Workshop on Brain-Computer Interface (BCI), 2013*, pp. 86–88.

29. Chen, M.-T. and Lin, C.-C. (2004). Comparison of tft-lcd and crt on visual recognition and subjective preference. *International Journal of Industrial Ergonomics*, 34(3), pp. 167 – 174.

30. Chen, X. et al. (2014). Hybrid frequency and phase coding for a high-speed SSVEP-based BCI speller. In *36th Annual International Conference of the IEEE Engineering in Medicine and Biology Society 2014*, pp. 3993–3996.

31. Cheng, L. et al. (2014). A sandwich structure of multi-chip COB LED with double flat glass boards coated with phosphors film by screen printing technique. In *15th International Conference on Electronic Packaging Technology (ICEPT), 2014*, pp. 1486–1490.

32. Cheng, M. et al. (2001). Multiple color stimulus induced steady state visual evoked potentials. In *Engineering in Medicine and Biology Society, 2001. Proceedings of the 23rd Annual International Conference of the IEEE*, vol. 2, pp. 1012–1014 vol.2.

33. Cheryl L. Dickter and Kieffaber, P. D. (2014). *EEG Methods for the Psychological Sciences*. London: SAGE Publications Inc.

34. Chi, Y. M. et al. (2012). Dry and Noncontact EEG Sensors for Mobile Brain–Computer Interfaces. *IEEE Transactions on Neural Systems and Rehabilitation Engineering,*, 20(2), pp. 228–235.

35. Christian Andreas, K. and Scott, M. (2013). BCILAB: a platform for brain–computer interface development. *Journal of Neural Engineering*, 10(5), p. 56014.

36. Chua, F. B. et al. (2004). Effects of a single green flash versus a white flash of light on saccadic oculomotor metrics. In *Bioengineering Conference, 2004. Proceedings of the IEEE 30th Annual Northeast*, pp. 9–10.

37. Cincotti, F. et al. (2008). Non-invasive brain–computer interface system: Towards its application as assistive technology. *Brain Research Bulletin*, 75(6), pp. 796–803.

38. Collins, J. B. (1959). Visual Fatigue and Its Measurement. *The Annals of Occupational Hygiene*, 1(3), pp. 228–236.

39. Combaz, A. and Hulle, M. M. (2015). Simultaneous detection of P300 and steady-state visually evoked potentials for hybrid brain-computer interface. *PLoS One*, 10.

40. Cui, X. et al. (2011). A quantitative comparison of NIRS and fMRI across multiple cognitive tasks. *NeuroImage*, 54(4), pp. 2808–2821.

41. da Silva Pinto, M. A. et al. (2011). A low-cost, portable, micro-controlled device for multi-channel LED visual stimulation. *Journal of Neuroscience Methods*, 197(1), pp. 82–91.

42. Daly, J. J. and Huggins, J. E. (2015). Brain-Computer Interface: Current and Emerging Rehabilitation Applications. *Archives of Physical Medicine and Rehabilitation*, 96(3), pp. S1–S7.

43. Dan, Z. et al. (2009). An independent brain-computer interface based on covert shifts of non-spatial visual attention. In *Annual International Conference of the IEEE Engineering in Medicine and Biology Society, EMBC 2009.*, pp. 539–542.

44. Decety, J. (1996). The neurophysiological basis of motor imagery. *Behavioural Brain Research*, 77(1–2), pp. 45–52.

45. Delorme, A. and Makeig, S. (2004). EEGLAB: an open source toolbox for analysis of single-trial EEG dynamics including independent component analysis. *Journal of Neuroscience Methods*, 134(1), pp. 9–21.

46. Delorme, A. et al. (2011). Eeglab, sift, nft, bcilab, and erica: new tools for advanced eeg processing. *Computational Intelligence and Neuroscience*, 2011, p. 10.

47. Demontis, G. C. et al. (2005). A simple and inexpensive light source for research in visual neuroscience. *Journal of Neuroscience Methods*, 146(1), pp. 13–21.

48. Devrim, M. et al. (1999). Slow cortical potential shifts modulate the sensory threshold in human visual system. *Neuroscience Letters*, 270(1), pp. 17–20.

49. Diez, P. F. et al. (2013). Commanding a robotic wheelchair with a high-frequency steady-state visual evoked potential based brain–computer interface. *Medical Engineering & Physics*, 35(8), pp. 1155–1164.

50. Dong-Ok, W. et al. (2014). A BCI speller based on SSVEP using high frequency stimuli design. In *IEEE International Conference on Systems, Man and Cybernetics (SMC), 2014*, pp. 1068–1071.

51. Dong-Ok, W. et al. (2016). Effect of higher frequency on the classification of steady-state visual evoked potentials. *Journal of Neural Engineering*, 13(1), p. 16014.

52. Duez, L. et al. (2016). Added diagnostic value of magnetoencephalography (MEG) in patients suspected for epilepsy, where previous, extensive EEG workup was unrevealing. *Clinical Neurophysiology*, 127(10), pp. 3301–3305.

53. Duschek, S. and Schandry, R. (2003). Functional transcranial Doppler sonography as a tool in psychophysiological research. *Psychophysiology*, 40(3), pp. 436–454.

54. Duvinage, M. et al. (2013a). Performance of the emotiv epoc headset for p300-based applications. *Biomedical Engineering Online*, 12(1), p. 56.

55. Duvinage, M. et al. (2013b). Performance of the emotiv epoc headset for p300-based applications. *Biomedical Engineering Online*, 12(1), p. 56.

56. Eaton, J. (2015). *Brain-Computer Music Interfacing: Designing Practical Systems For Creative Applications*. Phd thesis, Plymouth University.

57. Edlinger, G., Krausz, G. and Guger, C. (2012). A dry electrode concept for SMR, P300 and SSVEP based BCIs. In *International Conference on Complex Medical Engineering (CME), 2012 ICME*, pp. 186–190.

58. Elbuni, A. et al. (2009). ECG Parameter Extraction Algorithm using (DWTAE) Algorithm. In *International Conference on Computer Technology and Development, 2009. ICCTD '09.*, vol. 2, pp. 57–62.

59. Elsawy, A. S. et al. (2017). MindEdit: A P300-based text editor for mobile devices. *Computers in Biology and Medicine*, 80, pp. 97–106.

60. Ergenoglu, T. et al. (1998). Slow cortical potential shifts modulate P300 amplitude and topography in humans. *Neuroscience Letters*, 251(1), pp. 61–64.

61. Erwei, Y. et al. (2015). A Dynamically Optimized SSVEP Brain-Computer Interface (BCI) Speller. *IEEE Transactions on Biomedical Engineering*, 62(6), pp. 1447–1456.

62. Farwell, L. A. and Donchin, E. (1988). Talking off the top of your head: toward a mental prosthesis utilizing event-related brain potentials. *Electroencephalography and Clinical Neurophysiology*, 70(6), pp. 510–523.

63. Fazel-Rezai, R. (2013). *Brain-Computer Interface Systems – Recent Progress and Future Prospects*. Croatia: InTech.

64. Files, B. T. and Marathe, A. R. (2016). A regression method for estimating performance in a rapid serial visual presentation target detection task. *Journal of Neuroscience Methods*, 258, pp. 114–123.

65. Fouad, M. M. et al. (2015). Brain Computer Interface: A Review. In T. Hassanien, A.E. and Azar, ed., *Intelligent Systems Reference Library 74*, Switzerland: Springer International Publishing, chap. 1, pp. 3 –30.

66. Friganović, K., Medved, M. and Cifrek, M. (2016). Brain-computer interface based on steady-state visual evoked potentials.

67. Geng, L. et al. (2011). On brain-computer interface technology based on dual- layer SSVEP. In 2011, ed., *30th Chinese Control Conference (CCC), 2011*, pp. 3206–3209.

68. Gong, C. (2009). Human-Computer Interaction: Process and Principles of Human-Computer Interface Design. In *International Conference on Computer and Automation Engineering, 2009. ICCAE*, pp. 230–233.

69. Gore, J. C. (2003). Principles and practice of functional MRI of the human brain. *Journal of Clinical Investigation*, 112(1), pp. 4–9.

70. Gray, H. M. et al. (2004). P300 as an index of attention to self-relevant stimuli. *Journal of Experimental Social Psychology*, 40(2), pp. 216–224.

71. Guger, C., Edlinger, G. and Krausz, G. (2011). Hardware/software components and applications of BCIs. In P. R. Fazel, ed., *Recent Advances in Brain-Computer Interface Systems*, InTech, chap. Hardware/S, pp. 1–23.

72. Guneysu, A. and Akin, H. L. (2013). An SSVEP based BCI to control a humanoid robot by using portable EEG device. In *35th Annual International Conference of the IEEE Engineering in Medicine and Biology Society (EMBC), 2013*, pp. 6905–6908.

73. Hai-bin, Z. et al. (2009). Brain-computer interface design based on slow cortical potentials using matlab/simulink. In *International Conference on Mechatronics and Automation, 2009. ICMA 2009.*, pp. 1044–1048.

74. Halder, S. et al. (2011). Neural mechanisms of brain–computer interface control. *NeuroImage*, 55(4), pp. 1779–1790.

75. Hassanien, A. E. and Azar, A. T. (2015). *Brain-Computer Interfaces-Current Trends and Applications*. Switzerland: Springer.

76. Henk-Van Der Twell (1990). The Eye of Man, the Brain of the Physicist: A System's Approach to Vision. In E. R. John, ed., *Machinery of the Mind*, New York: Birkhäuser Boston, chap. 8, pp. 86–88.

77. Herrmann, C. S. (2001). Human EEG responses to 1-100 Hz flicker: resonance phenomena in visual cortex and their potential correlation to cognitive phenomena. *Experimental Brain Research*, 137(3-4), pp. 346–353.

78. Hill, N. J. and Wolpaw, J. R. (2016). Brain–Computer Interface BT - Reference Module in Biomedical Sciences. In *Reference Module in Biomedical Sciences*, Elsevier, chap. Brain–Comp, pp. 210–312.

79. Hillyard, S. A. and Anllo-Vento, L. (1998). Event-related brain potentials in the study of visual selective attention. *Proceedings of the National Academy of Sciences*, 95(3), pp. 781–787.

80. Hinterberger, T. et al. (2004). Brain-computer communication and slow cortical potentials.

81. Howell, J., Symmons, M. and Doorn, G. V. (2013). Using traditional horizontal-vertical illusion figures and single lines to directly compare haptics and vision.

82. Hu, M. and Wu, Y. (2014). Full-color LED display research based on chip on board(COB) package. In *15th International Conference on Electronic Packaging Technology (ICEPT), 2014*, pp. 97–100.

83. Huang, G. et al. (2012). Effect of duty cycle in different frequency domains on SSVEP based BCI: A preliminary study. In *Annual International Conference of the IEEE Engineering in Medicine and Biology Society (EMBC), 2012*, pp. 5923–5926.

84. Hwang, H. J. et al. (2012). Development of an SSVEP-based BCI spelling system adopting a QWERTY-style LED keyboard. *J Neurosci Methods*, 208(1), pp. 59–65.

85. Hwang, H. J. et al. (2013a). A new dual-frequency stimulation method to increase the number of visual stimuli for multi-class SSVEP-based brain-computer interface (BCI). *Brain Research*, 1515, pp. 66–77.

86. Hwang, H.-J. et al. (2013b). EEG-Based Brain-Computer Interfaces: A Thorough Literature Survey. *International Journal of Human–Computer Interaction*, 29(12), pp. 814–826.

87. Hwang, H.-J. et al. (2013c). Implementation of a mental spelling system based on steady-state visual evoked potential (SSVEP). In *International Winter Workshop on Brain-Computer Interface (BCI), 2013*, pp. 81–83.

88. Iacoviello, D. et al. (2015). A real-time classification algorithm for EEG-based BCI driven by self-induced emotions. *Computer Methods and Programs in Biomedicine*, 122(3), pp. 293–303.

89. Islam, M. R., Hirose, K. and Molla, M. K. (2013). Artifact suppression and analysis of brain activities with electroencephalography signals. *Neural Regeneration Research*, 8(16), p. 1500.

90. John, J. W. and Palaniappan, R. (2011). Analogue mouse pointer control via an online steady state visual evoked potential (SSVEP) brain–computer interface. *Journal of Neural Engineering*, 8(2), p. 25026.

91. Kalunga, E. K. et al. (2016). Online SSVEP-based BCI using Riemannian geometry. *Neurocomputing*, 191, pp. 55–68.

92. Kappenman, E. S. and Luck, S. J. (2011). *The Oxford Handbook of Event-Related Potential Components*. Oxford University Press.

93. Kaufmann, T., Herweg, A. and Kubler, A. (2014). Toward brain-computer interface based wheelchair control utilizing tactually-evoked event-related potentials. *Journal of Neuroengineering and Rehabilitation*, 11(1).

94. Kelly, S. P. et al. (2005). Visual spatial attention tracking using high-density SSVEP data for independent brain-computer communication. *IEEE Transactions on Neural Systems and Rehabilitation Engineering,*, 13(2), pp. 172–178.

95. Khalid, M. B. et al. (2009). Towards a Brain Computer Interface using wavelet transform with averaged and time segmented adapted wavelets.

96. Khalid, M. I. et al. (2015). MEG data classification for healthy and epileptic subjects using linear discriminant analysis.

97. Kilintari, M. et al. (2016). Brain activation profiles during kinesthetic and visual imagery: An fMRI study. *Brain Research*, 1646, pp. 249–261.

98. Kim, G. J. (2015). *Human–Computer Interaction : Fundamentals and Practice*. New York: Taylor & Francis Group, LLC.

99. Kirk, U. et al. (2016). Mindfulness training increases cooperative decision making in economic exchanges: Evidence from fMRI. *NeuroImage*, 138, pp. 274–283.

100. Kobayashi, N. and Nakagawa, M. (2015). BCI-based control of electric wheelchair. In *2015 IEEE 4th Global Conference on Consumer Electronics (GCCE)*, pp. 429–430.

101. Krusienski, D. J. et al. (2008). Toward enhanced P300 speller performance. *Journal of Neuroscience Methods*, 167(1), pp. 15–21.

102. Kuś, R. et al. (2013). On the quantification of SSVEP frequency responses in human EEG in realistic BCI conditions. *PLoS ONE*, 8(10), p. e77536.

103. Lee, T.-S. et al. (2013). Efficacy and usability of a brain-computer interface system in improving cognition in the elderly. *Alzheimer's & Dementia: The Journal of the Alzheimer's Association*, 9(4).

104. Leuthardt, E. C. et al. (2004). A brain–computer interface using electrocorticographic signals in humans. *Journal of Neural Engineering*, 1(2), p. 63.

105. Li, Y. Q. et al. (2013). A hybrid BCI system combing P300 and SSVEP and its application to wheelchair control. *IEEE Trans Biomed Eng*, 60.

106. Lin, C.-C. and Huang, K.-C. (2013). Effects of ambient illumination conditions and background color on visual performance with TFT-LCD screens. *Displays*, 34(4), pp. 276–282.

107. Liu, Y. et al. (2012). Implementation of SSVEP based BCI with Emotiv EPOC. In *International Conference on Virtual Environments Human-Computer Interfaces and Measurement Systems (VECIMS), 2012 IEEE*, IEEE, pp. 34–37.

108. Lopes, A. C., Pires, G. and Nunes, U. (2013). Assisted navigation for a brain-actuated intelligent wheelchair. *Robotics and Autonomous Systems*, 61(3), pp. 245–258.

109. Lopez-Gordo, M. A., Pelayo, F. and Prieto, A. (2010). A high performance SSVEP-BCI without gazing. In *The 2010 International Joint Conference on Neural Networks (IJCNN),*, pp. 1–5.

110. Lopez-Gordo, M. A. et al. (2011). Customized stimulation enhances performance of independent binary SSVEP-BCIs. *Clinical Neurophysiology*, 122(1), pp. 128–133.

111. Lotze, M. and Halsband, U. (2006). Motor imagery. *Journal of Physiology*, 99(4–6), pp. 386–395.

112. Luauté, J. and Laffont, I. (2015). BCIs and physical medicine and rehabilitation: The future is now. *Annals of Physical and Rehabilitation Medicine*, 58(1), pp. 1–2.

113. Luauté, J., Morlet, D. and Mattout, J. (2015). BCI in patients with disorders of consciousness: Clinical perspectives. *Annals of Physical and Rehabilitation Medicine*, 58(1), pp. 29–34.

114. Luck, S. J. (2014). *An Introduction to the Event-Related Potential Technique*. MIT Press, 2nd edn.

115. Luzheng, B. et al. (2013). A SSVEP brain-computer interface with the hybrid stimuli of SSVEP and P300. In *International Conference on Complex Medical Engineering (CME), 2013 ICME*, pp. 211–214.

116. Lyskov, E. et al. (1998). Steady-state visual evoked potentials to computer monitor flicker. *International Journal of Psychophysiology*, 28(3), pp. 285–290.

117. Makri, D., Farmaki, C. and Sakkalis, V. (2015). Visual fatigue effects on Steady State Visual Evoked Potential-based Brain Computer Interfaces. In *7th International IEEE/EMBS Conference on Neural Engineering (NER) 2015*, pp. 70–73.

118. Martinez, P., Bakardjian, H. and Cichocki, A. (2007). Fully online multicommand brain-computer interface with visual neurofeedback using SSVEP paradigm. *Intell Neuroscience*, 2007, p. 13.

119. Martinez-Leon, J.-A., Cano-Izquierdo, J.-M. and Ibarrola, J. (2016). Are low cost Brain Computer Interface headsets ready for motor imagery applications? *Expert Systems with Applications*, 49, pp. 136–144.

120. Martišius, I. and Damaševičius, R. (2016). A Prototype SSVEP Based Real Time BCI Gaming System. *Computational Intelligence and Neuroscience*, 2016, p. 3861425.

121. Matthew, J. B. et al. (2013). Probabilistic co-adaptive brain–computer interfacing. *Journal of Neural Engineering*, 10(6), p. 66008.

122. McCane, L. M. et al. (2015). P300-based brain-computer interface (BCI) event-related potentials (ERPs): People with amyotrophic lateral sclerosis (ALS) vs. age-matched controls. *Clinical Neurophysiology*, 126(11), pp. 2124–2131.

123. Menozzi, M., Näpflin, U. and Krueger, H. (1999). CRT versus LCD: A pilot study on visual performance and suitability of two display technologies for use in office work. *Displays*, 20(1), pp. 3–10.

124. Menozzi, M. et al. (2001). CRT versus LCD: effects of refresh rate, display technology and background luminance in visual performance. *Displays*, 22(3), pp. 79–85.

125. Middendorf, M. et al. (2000). Brain-computer interfaces based on the steady-state visual-evoked response. *IEEE Trans Neural Syst Rehabil Eng*, 8.

126. Mikołajewska, E. and Mikołajewski, D. (2014). Non-invasive EEG-based brain-computer interfaces in patients with disorders of consciousness. *Military Medical Research*, 1, p. 14.

127. Min, B.-K., Marzelli, M. J. and Yoo, S.-S. (2010). Neuroimaging-based approaches in the brain–computer interface. *Trends in Biotechnology*, 28(11), pp. 552–560.

128. Min, B.-K. et al. (2013). Bright illumination reduces parietal eeg alpha activity during a sustained attention task. *Brain research*, 1538, pp. 83–92.

129. Mouli, S. et al. (2013). Performance analysis of multi-frequency SSVEP-BCI using clear and frosted colour LED stimuli. In *13th International Conference on Bioinformatics and Bioengineering (BIBE), 2013 IEEE*, pp. 1–4.

130. Mulder, T. (2007). Motor imagery and action observation: cognitive tools for rehabilitation. *Journal of Neural Transmission*, 114(10), pp. 1265–1278.

131. Muller-Putz, G. R. and Pfurtscheller, G. (2008). Control of an Electrical Prosthesis With an SSVEP-Based BCI. *IEEE Transactions on Biomedical Engineering*, 55(1), pp. 361–364.

132. Müller-Putz, G. R. et al. (2011). Tools for brain-computer interaction: a general concept for a hybrid bci. *Frontiers in Neuroinformatics*, 5.

133. Mun, S. et al. (2012). SSVEP and ERP measurement of cognitive fatigue caused by stereoscopic 3D. *Neuroscience Letters*, 525(2), pp. 89–94.

134. Munzert, J. and Zentgraf, K. (2009). Motor imagery and its implications for understanding the motor system. In J. G. J. Markus Raab and R. H. Hauke, eds., *Progress in Brain Research*, vol. Volume 174, Elsevier, pp. 219–229.

135. Nagarajan, S. S., Ranasinghe, K. G. and Vossel, K. A. (2016). Chapter 15 - Brain Imaging With Magnetoencephalography During Rest and During Speech and Language Processing A2 - Lehner, Thomas. In B. L. Miller and M. W. State, eds., *Genomics, Circuits, and Pathways in Clinical Neuropsychiatry*, San Diego: Academic Press, pp. 233–245.

136. Ng, D. W.-K., Soh, Y.-W. and Goh, S.-Y. (2014). Development of an Autonomous BCI Wheelchair. In *IEEE Symposium on Computational Intelligence in Brain Computer Interfaces (CIBCI), 2014*, pp. 1–4.

137. Nicolas-Alonso, L. F. and Gomez-Gil, J. (2012). Brain Computer Interfaces, a Review. *Sensors*, 12(2), pp. 1211–1279.

138. Nishifuji, S. and Kuroda, T. (2012). Impact of mental focus on steady-state visually evoked potential under eyes closed condition for binary brain computer interface. In *Annual International Conference of the IEEE Engineering in Medicine and Biology Society (EMBC), 2012*, pp. 1765–1768.

139. Obrig, H. (2014). NIRS in clinical neurology — a 'promising' tool? *NeuroImage*, 85, Part 1, pp. 535–546.

140. Oralhan, Z. and Tokmakçi, M. (2016). The Effect of Duty Cycle and Brightness Variation of Visual Stimuli on SSVEP in Brain Computer Interface Systems. *IETE Journal of Research*, 62(6), pp. 795–803.

141. Pal, P. R., Khobragade, P. and Panda, R. (2011). Expert system design for classification of brain waves and epileptic-seizure detection. In *Students' Technology Symposium (TechSym), 2011 IEEE*, Kharagpur, India: IEEE Xplore, pp. 187–192.

142. Panicker, R. C., Puthusserypady, S. and Sun, Y. (2011). An asynchronous P300 BCI with SSVEP-based control state detection. *IEEE Trans Biomed Eng*, 58.

143. Pastor, M. A. et al. (2003). Human Cerebral Activation during Steady-State Visual-Evoked Responses. *Journal of Neuroscience*, 23(37), pp. 11621–11627.

144. Pichiorri, F. et al. (2015). Brain–computer Interface Boosts Motor Imagery Practice During Stroke Recovery. *Annals of Neurology*, 77(5), pp. 851–865.

145. Pires, G., Nunes, U. and Castelo-Branco, M. (2012). Evaluation of Brain-computer Interfaces in Accessing Computer and other Devices by People with Severe Motor Impairments. *Proceedings of the 4th International Conference on Software Development for Enhancing Accessibility and Fighting Info-exclusion (DSAI 2012)*, 14, pp. 283–292.

146. Po-Lei, L. et al. (2011). An SSVEP-Based BCI Using High Duty-Cycle Visual Flicker. *IEEE Transactions on Biomedical Engineering,*, 58(12), pp. 3350–3359.

147. Prueckl, R. and Guger, C. (2010). Controlling a robot with a brain-computer interface based on steady state visual evoked potentials. In *The 2010 International Joint Conference on Neural Networks (IJCNN)*, pp. 1–5.

148. Puanhvuan, D. and Wongsawat, Y. (2011). Illuminant effect on LCD and LED stimulators for P300-based brain-controlled wheelchair. In *International Conference on Biomedical Engineering, (BMEiCON) 2011*, pp. 254–257.

149. Punsawad, Y. and Wongsawat, Y. (2012). Motion visual stimulus for SSVEP-based BCI system. In *Annual International Conference of Engineering in Medicine and Biology Society (EMBC), 2012*, pp. 3837–3840.

150. Purves, D., George J, A. and David, F. (2004). *NEUROSCIENCE*. Sunderland,USA: Sinauer Associates, 4th edn.

151. Ravden, D. and Polich, J. (1999). On p300 measurement stability: habituation, intra-trial block variation, and ultradian rhythms. *Biological Psychology*, 51(1), pp. 59–76.

152. Read, J. C. A. and Cumming, B. G. (2004). Understanding the Cortical Specialization for Horizontal Disparity. *Neural Computation*, 16(10), pp. 1983–2020.

153. Resalat, S. N. et al. (2011). Appropriate twinkling frequency and inter-sources distance selection in SSVEP-based HCI systems. In *International Conference on Signal and Image Processing Applications (ICSIPA), 2011 IEEE*, pp. 12–15.

154. Resalat, S. N. et al. (2012). High-speed SSVEP-based BCI: Study of various frequency pairs and inter-sources distances. In *International Conference on Biomedical and Health Informatics (BHI), 2012 IEEE-EMBS*, Hong Kong, China: IEEE, pp. 220–223.

155. Rice, J. K. et al. (2013). Subject position affects EEG magnitudes. *NeuroImage*, 64(0), pp. 476–484.

156. Rogers, B. et al. (2012). A low cost color visual stimulator for fMRI. *Journal of Neuroscience Methods*, 204(2), pp. 379–382.

157. Saha, K. M. S. and Lingaraju, G. (2015). EEG Based Brain Computer Interface for Speech Communication: Principles and Applications. In A. T. Azar, ed., *Brain-Computer Interfaces-Currnt Trends and Applicationse*, Switzerland: Springer-Verlag, chap. 10, p. 273.

158. Sanchez, J. C. and Principe, J. C. (2007). *Brain–Machine Interface Engineering*. USA: Morgan & Claypool.

159. Shiavi, R. (2007). *Introduction to Applied Statistical Signal Analysis : Guide to Biomedical and Electrical Engineering Applications*. UK: Elsevier Inc, 3rd edn.

160. Shieh, K.-K. (2000). Effects of reflection and polarity on LCD viewing distance. *International Journal of Industrial Ergonomics*, 25(3), pp. 275–282.

161. Shih, J. J., Krusienski, D. J. and Wolpaw, J. R. (2012). Brain-Computer Interfaces in Medicine. *Mayo Clinic Proceedings*, 87(3), pp. 268–279.

162. Siegenthaler, E. et al. (2012). Reading on LCD vs e-Ink displays: effects on fatigue and visual strain. *Ophthalmic and Physiological Optics*, 32(5), pp. 367–374.

163. Simon, A. J. et al. (2017). A brain computer interface to detect Alzheimer's disease. *Alzheimer's & Dementia: The Journal of the Alzheimer's Association*, 7(4), pp. S145–S146.

164. Singh, H. and Daly, I. (2015). Translational algorithms: The heart of a brain computer interface. In A. E. Hassanien and A. T. Azar, eds., *Brain-Computer Interfaces: Current Trends and Applications*, Cham: Springer International Publishing, pp. 97–121.

165. Singla, R., Khosla, A. and Jha, R. (2014). Influence of stimuli colour in SSVEP-based BCI wheelchair control using support vector machines. *Journal of Medical Engineering & Technology*, 38(3), pp. 125–134.

166. Sitaram, R. et al. (2007). fMRI Brain-Computer Interface: A Tool for Neuroscientific Research and Treatment. *Computational Intelligence and Neuroscience*, 2007, p. 25487.

167. Spuler, M. (2015). A Brain-Computer Interface (BCI) system to use arbitrary Windows applications by directly controlling mouse and keyboard. In *37th Annual International Conference of the IEEE Engineering in Medicine and Biology Society (EMBC) 2015*, pp. 1087–1090.

168. Stern, J. M. and Jerome Engel, J. (2015). *Atlas of EEG Patterns*. London: Wolters Kluwer.

169. Subasi, A. (2005). Automatic recognition of alertness level from EEG by using neural network and wavelet coefficients. *Expert Systems with Applications*, 28(4), pp. 701–711.

170. Sur, S. and Sinha, V. K. (2009). Event-related potential: An overview. *Industrial Psychiatry Journal*, 18(1), pp. 70–73.

171. Takalo, R., Hytti, H. and Ihalainen, H. (2005). Tutorial on Univariate Autoregressive Spectral Analysis. *Journal of Clinical Monitoring and Computing*, 19(6), pp. 401–410.

172. Taylor, C. (2001). Visual and haptic perception of the horizontal-vertical illusion. *Percepual and MotorSkill*, 92(0031-5125).

173. Teikari, P. et al. (2012). An inexpensive Arduino-based LED stimulator system for vision research. *Journal of Neuroscience Methods*, 211(2), pp. 227–236.

174. Teng, C. et al. (2012). Flashing color on the performance of SSVEP-based brain-computer interfaces. In *Annual International Conference of the IEEE Engineering in Medicine and Biology Society (EMBC), 2012*, pp. 1819–1822.

175. Teplan, M. (2002). Fundamentals of EEG measurement. *Measurement science review*, 12, pp. 1–11.

176. Trauer, S. M. et al. (2012). Capture of lexical but not visual resources by task-irrelevant emotional words: A combined ERP and steady-state visual evoked potential study. *NeuroImage*, 60(1), pp. 130–138.

177. Vakrilov, N., Andonova, A. and Kafadarova, N. (2015). Study of high power COB LED modules with respect to topology of chips. In *38th International Spring Seminar on Electronics Technology (ISSE), 2015*, pp. 108–113.

178. Van Dokkum, L. E. H., Ward, T. and Laffont, I. (2015). Brain computer interfaces for neurorehabilitation – its current status as a rehabilitation strategy post-stroke. *Annals of Physical and Rehabilitation Medicine*, 58(1), pp. 3–8.

179. Vidal, J. J. (1973). Toward Direct Brain-Computer Communication. *Annual Review of Biophysics and Bioengineering*, 2(1), pp. 157–180.

180. Volosyak, I., Cecotti, H. and Gräser, A. (2009). Impact of frequency selection on LCD screens for SSVEP based brain-computer interfaces. In *Bio-Inspired Systems: Computational and Ambient Intelligence*, Springer, pp. 706–713.

181. Volosyak, I. et al. (2011). BCI Demographics II: How Many (and What Kinds of) People Can Use a High-Frequency SSVEP BCI? *Transactions on Neural Systems and Rehabilitation Engineering, IEEE*, 19(3), pp. 232–239.

182. Walter, S. et al. (2012). Effects of overt and covert attention on the steady-state visual evoked potential. *Neuroscience Letters*, 519(1), pp. 37–41.

183. Wang, F. et al. (2015a). A Novel Audiovisual Brain-Computer Interface and Its Application in Awareness Detection. *Scientific Reports*, 5, p. 9962.

184. Wang, M. et al. (2015b). A new hybrid BCI paradigm based on P300 and SSVEP. *Journal of Neuroscience Methods*, 244, pp. 16–25.

185. Wang, M. et al. (2015c). A new hybrid BCI paradigm based on P300 and SSVEP. *Journal of Neuroscience Methods*, 244, pp. 16–25.

186. Wang, Y., Wang, Y. T. and Jung, T. P. (2010). Visual stimulus design for high-rate SSVEP BCI. *Electronics Letters*, 46(15), pp. 1057–1058.

187. Wang, Y. et al. (2009). Practical designs of brain–computer interfaces based on the modulation of EEG rhythms. In *Brain-Computer Interfaces*, Springer, pp. 137–154.

188. Weston, H. C. (1953). Visual Fatigue: With Special Reference to Lighting. *Transactions of the Illuminating Engineering Society*, 18(2_IEStrans), pp. 39–66.

189. Wolpaw, J. R. et al. (2002). Brain–computer interfaces for communication and control. *Clinical Neurophysiology*, 113(6), pp. 767–791.

190. Won, D. O. et al. (2014). A BCI speller based on SSVEP using high frequency stimuli design. In *International Conference on Systems, Man, and Cybernetics (SMC) 2014 IEEE*, San Diego, CA, USA: IEEE, pp. 1068–1071.

191. Woodman, G. F. (2010). A Brief Introduction to the Use of Event-Related Potentials (ERPs) in Studies of Perception and Attention. *Attention, Perception & Psychophysics*, 72(8), p. 10.3758/APP.72.8.2031.

192. Wriessnegger, S. C. et al. (2016). Cooperation in mind: Motor imagery of joint and single actions is represented in different brain areas. *Brain and Cognition*, 109, pp. 19–25.

193. Wu, C.-H. et al. (2011). Frequency recognition in an SSVEP-based brain computer interface using empirical mode decomposition and refined generalized zero-crossing. *Journal of Neuroscience Methods*, 196(1), pp. 170–181.

194. Wu, Z. (2016). Physical connections between different SSVEP neural networks. *Scientific Reports*, 6, p. 22801.

195. Wu, Z. et al. (2008). Stimulator selection in SSVEP-based BCI. *Bioengineering*, 30(8), pp. 1079–1088.

196. Yijun, W. et al. (2006). A practical VEP-based brain-computer interface. *Neural Systems and Rehabilitation Engineering, IEEE Transactions on*, 14(2), pp. 234–240.

197. Yin, E. et al. (2015). A hybrid brain-computer interface based on the fusion of P300 and SSVEP scores. *IEEE Trans Neural Syst Rehabil Eng*, 23.

198. Yoto, A. et al. (2007). Effects of object color stimuli on human brain activities in perception and attention referred to eeg alpha band response. *Journal of Physiological Anthropology*, 26(3), pp. 373–379.

199. Yu, J.-H. and Sim, K.-B. (2016). Classification of color imagination using Emotiv EPOC and event-related potential in electroencephalogram. *Optik - International Journal for Light and Electron Optics*, 127(20), pp. 9711–9718.

200. Yueh-Ru, Y. (2010). Implementation of a colorful RGB-LED light source with an 8-bit microcontroller. In *5th IEEE Conference on Industrial Electronics and Applications (ICIEA), 2010*, pp. 1951–1956.

201. Zhang, Y. et al. (2013). L1-regularized multiway canonical correlation analysis for SSVEP-based BCI. *IEEE Trans Neural Syst Rehabil Eng*, 21.

202. Zhu, D. et al. (2010). A Survey of Stimulation Methods Used in SSVEP-Based BCIs. *Computational Intelligence and Neuroscience*, 2010.

203. ŽVAN, B. (2012). Functional transcranial doppler sonography. *Periodicum biologorum*, 114(3), pp. 313–319.

Appendix A

Prototype

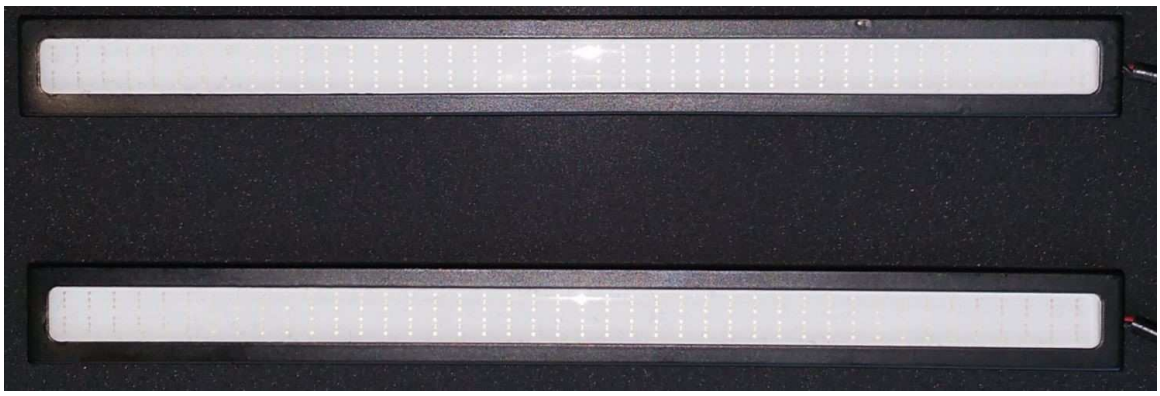

Figure A.1: Dual line COB LED Stimulus

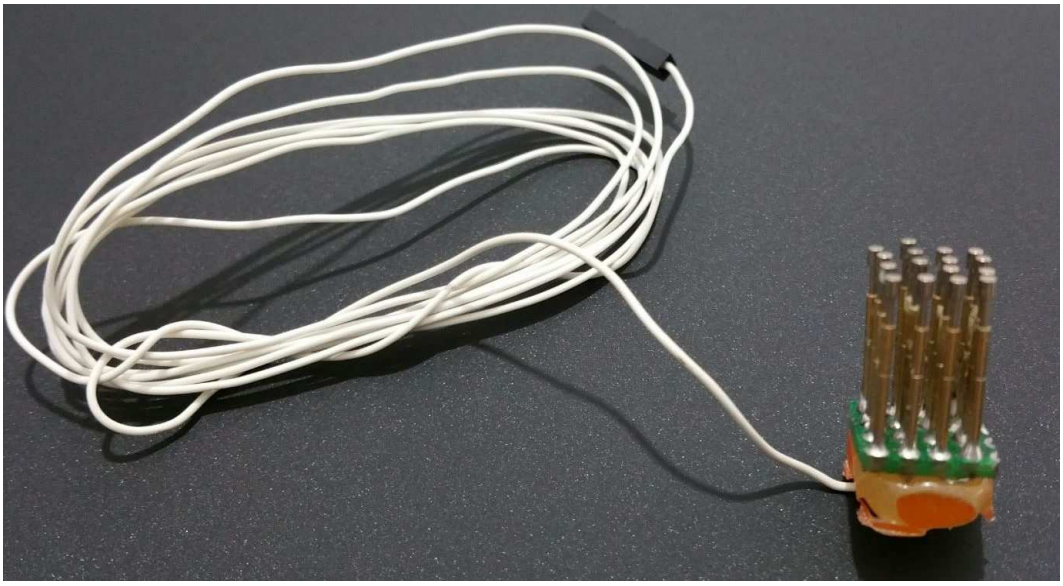

Figure A.2: Dry electrode based on height adjustable pins for improved scalp contact

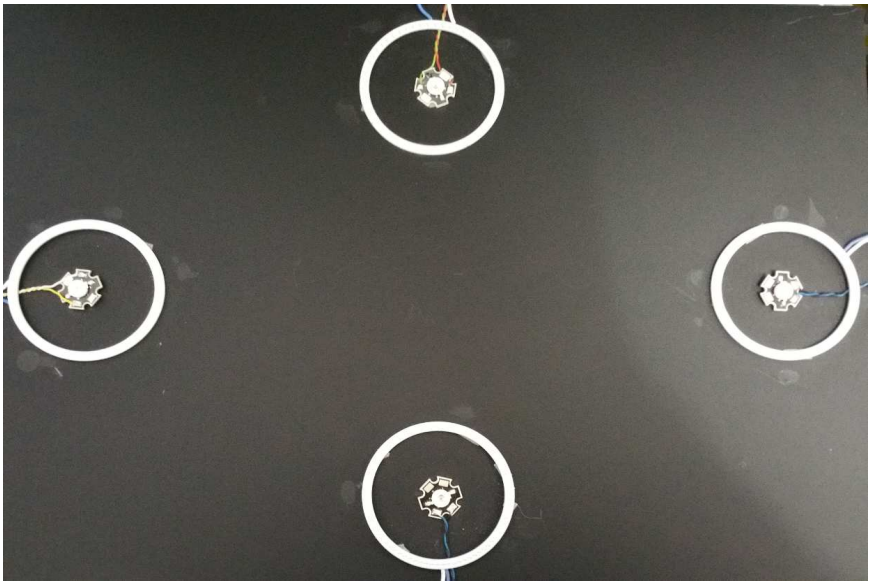

Figure A.3: Visual stimulus controller with four SSVEP stimuli and four P300 stimuli

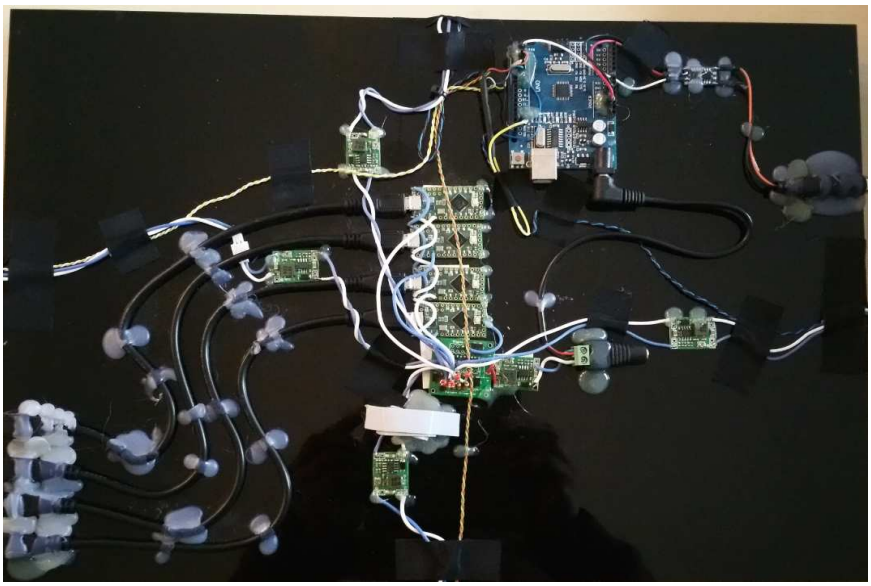

Figure A.4: Visual stimulus hardware with microcontrollers and interconnections

Appendix B

Visual Stimulus Waveforms

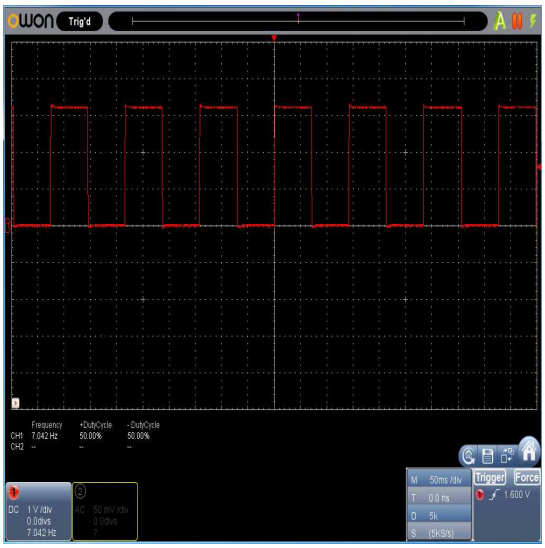

(a) Signal at 50% DC

Period = 142.0 ms	Frequency = 7.042 Hz
RiseTime = <250.0 us	FallTime = <250.0 us
+PulseWidth = 71.00 ms	- PulseWidth = 71.00 ms
+DutyCycle = 50.00%	- DutyCycle = 50.00%
Vpp = 3.400 V	Vmax = 3.320 V
Vmin = -80.00 mV	Vamp = 3.240 V
Vtop = 3.240 V	Vbase = 0.000 mV
Overshoot = 2.47%	Preshoot = 2.47%
Vavg = 1.624 V	Vrms = 2.288 V

(b) Waveform details

Figure B.1: Information snapshot of duty-cycle at 50% for 7 Hz

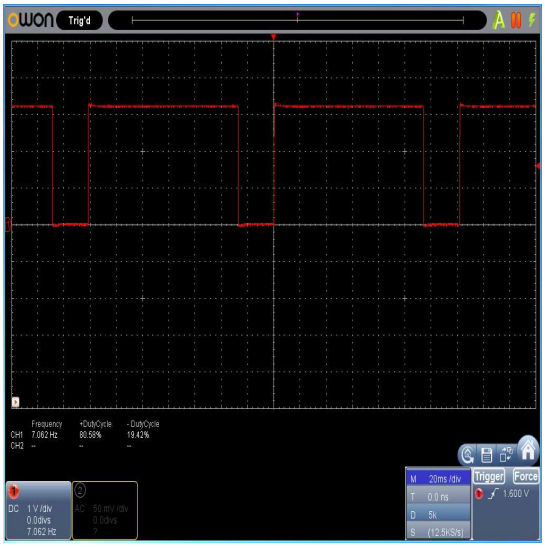

(a) Signal at 80% DC

Period = 141.6 ms	Frequency = 7.062 Hz
RiseTime = <100.0 us	FallTime = <100.0 us
+PulseWidth = 114.1 ms	- PulseWidth = 27.50 ms
+DutyCycle = 80.58%	- DutyCycle = 19.42%
Vpp = 3.360 V	Vmax = 3.320 V
Vmin = -40.00 mV	Vamp = 3.240 V
Vtop = 3.240 V	Vbase = 0.000 mV
Overshoot = 2.47%	Preshoot = 1.23%
Vavg = 2.568 V	Vrms = 2.881 V

(b) Waveform details

Figure B.2: Information snapshot of duty-cycle at 80% for 7 Hz

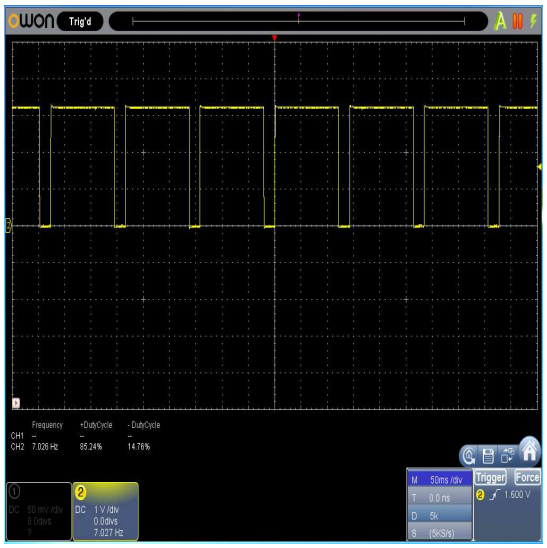

(a) Signal at 85% DC

Period = 142.2 ms	Frequency = 7.034 Hz
RiseTime = <250.0 us	FallTime = <250.0 us
+PulseWidth = 121.3 ms	- PulseWidth = 21.00 ms
+DutyCycle = 85.24%	- DutyCycle = 14.76%
Vpp = 3.400 V	Vmax = 3.320 V
Vmin = -80.00 mV	Vamp = 3.280 V
Vtop = 3.240 V	Vbase = -40.00 mV
Overshoot = 2.44%	Preshoot = 1.22%
Vavg = 2.749 V	Vrms = 2.982 V

(b) Waveform details

Figure B.3: Information snapshot of duty-cycle at 85% for 7 Hz

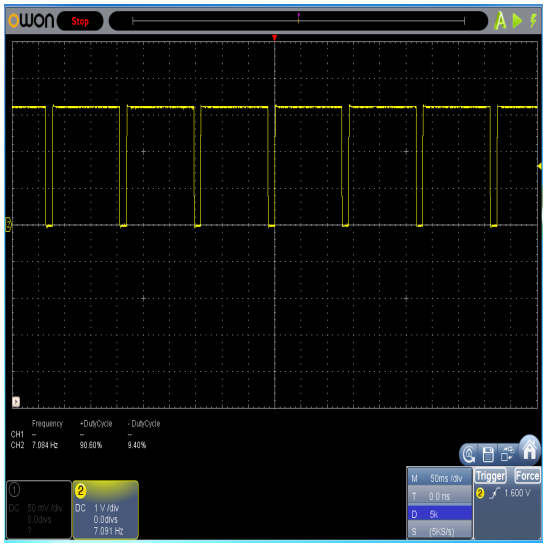

(a) Signal at 90% DC

Period = 141.2 ms	Frequency = 7.084 Hz
RiseTime = <250.0 us	FallTime = <250.0 us
+PulseWidth = 127.8 ms	- PulseWidth = 13.25 ms
+DutyCycle = 90.60%	- DutyCycle = 9.40%
Vpp = 3.360 V	Vmax = 3.280 V
Vmin = -80.00 mV	Vamp = 3.280 V
Vtop = 3.240 V	Vbase = -40.00 mV
Overshoot = 1.22%	Preshoot = 1.22%
Vavg = 2.931 V	Vrms = 3.077 V

(b) Waveform details

Figure B.4: Information snapshot of duty-cycle at 90% for 7 Hz

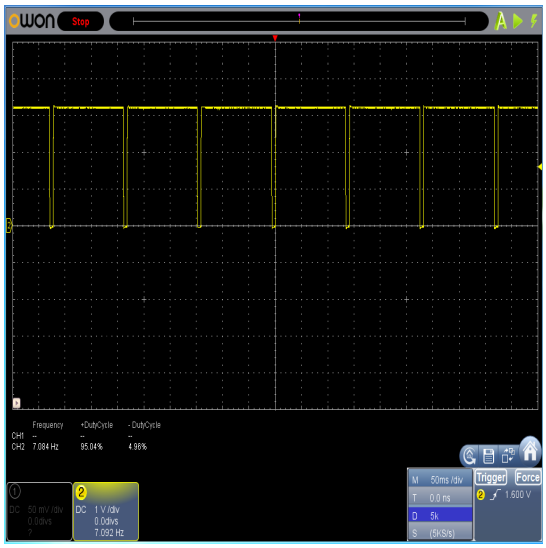

(a) Signal at 95% DC

Period = 141.2 ms	Frequency = 7.084 Hz
RiseTime = <250.0 us	FallTime = <250.0 us
+PulseWidth = 134.0 ms	- PulseWidth = 7.000 ms
+DutyCycle = 95.04%	- DutyCycle = 4.96%
Vpp = 3.360 V	Vmax = 3.280 V
Vmin = -80.00 mV	Vamp = 3.280 V
Vtop = 3.240 V	Vbase = -40.00 mV
Overshoot = 1.22%	Preshoot = 1.22%
Vavg = 3.067 V	Vrms = 3.147 V

(b) Waveform details

Figure B.5: Information snapshot of duty-cycle at 95% for 7 Hz

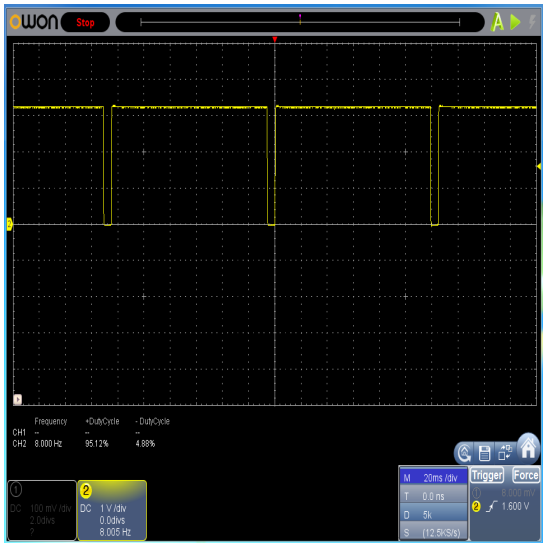

(a) Signal at 95% DC

Period = 125.0 ms	Frequency = 8.000 Hz
RiseTime = <300.0 us	FallTime = <200.0 us
+PulseWidth = 119.0 ms	- PulseWidth = 6.100 ms
+DutyCycle = 95.12%	- DutyCycle = 4.88%
Vpp = 3.320 V	Vmax = 3.280 V
Vmin = -40.00 mV	Vamp = 3.280 V
Vtop = 3.240 V	Vbase = -40.00 mV
Overshoot = 1.22%	Preshoot = 0%
Vavg = 3.087 V	Vrms = 3.160 V

(b) Waveform details

Figure B.6: Information snapshot of duty-cycle at 95% for 8 Hz

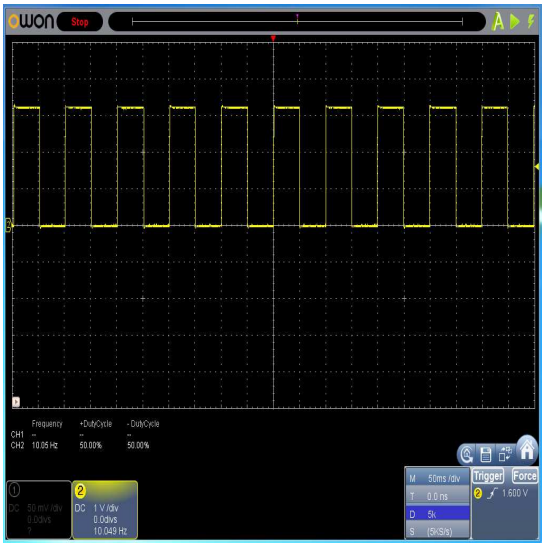

(a) Signal at 50% DC

Period = 99.50 ms	Frequency = 10.05 Hz
RiseTime = <250.0 us	FallTime = <250.0 us
+PulseWidth = 49.75 ms	- PulseWidth = 49.75 ms
+DutyCycle = 50.00%	- DutyCycle = 50.00%
Vpp = 3.400 V	Vmax = 3.320 V
Vmin = -80.00 mV	Vamp = 3.280 V
Vtop = 3.240 V	Vbase = -40.00 mV
Overshoot = 2.44%	Preshoot = 1.22%
Vavg = 1.601 V	Vrms = 2.281 V

(b) Waveform details

Figure B.7: Information snapshot of duty-cycle at 50% for 10 Hz

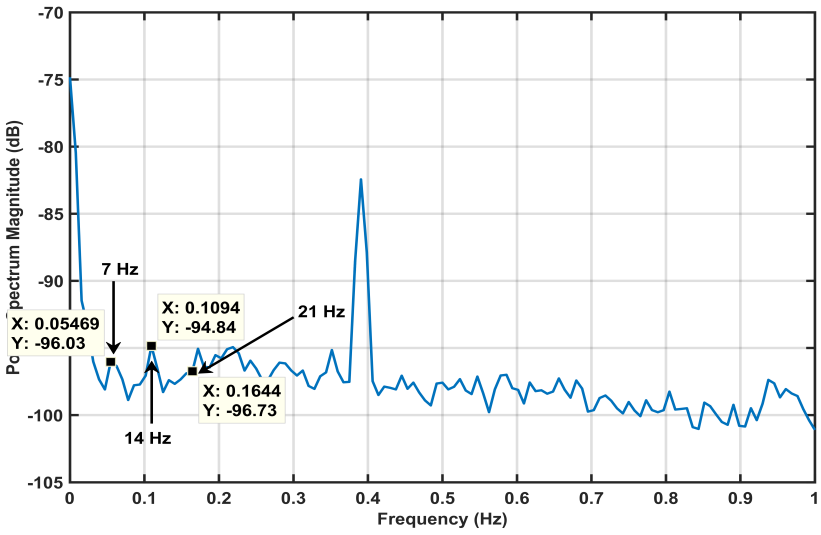

Figure B.8: SSVEP Responses for 7 Hz with harmonics at 14 Hz and 21 HZ

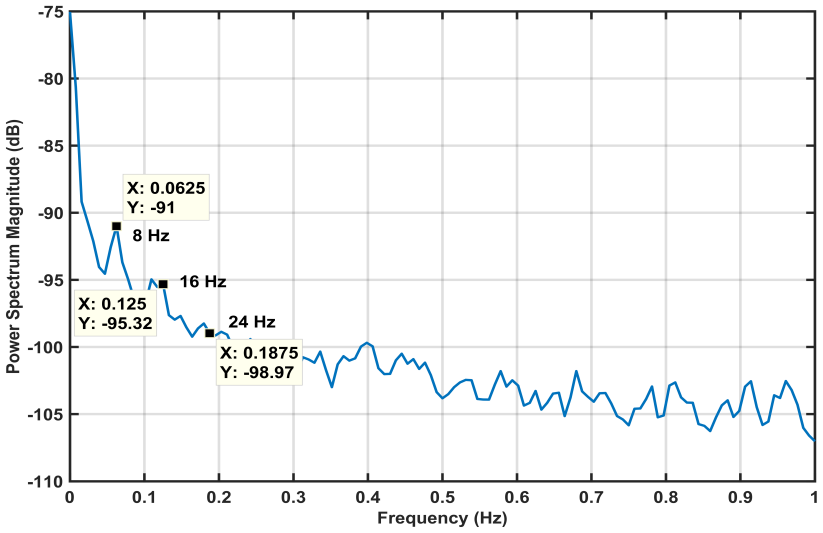

Figure B.9: SSVEP Responses for 8 Hz with harmonics at 16 Hz and 24 HZ

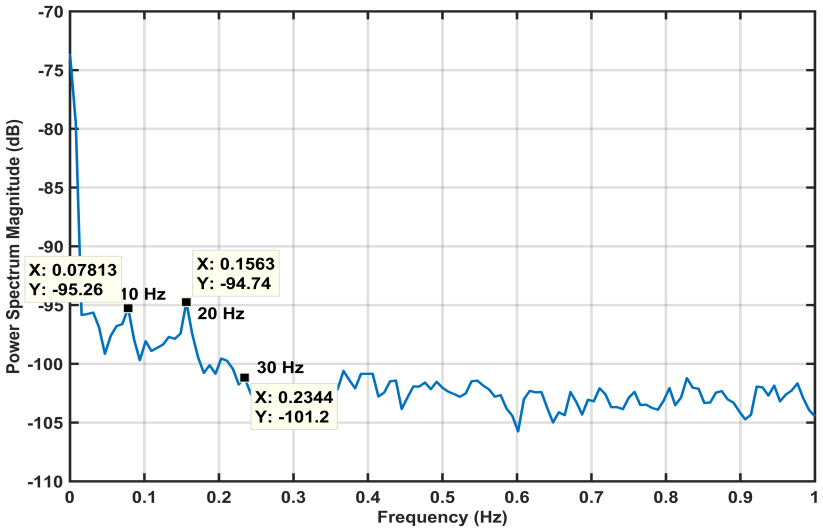

Figure B.10: SSVEP Responses for 10 Hz with harmonics at 20 Hz and 30 HZ

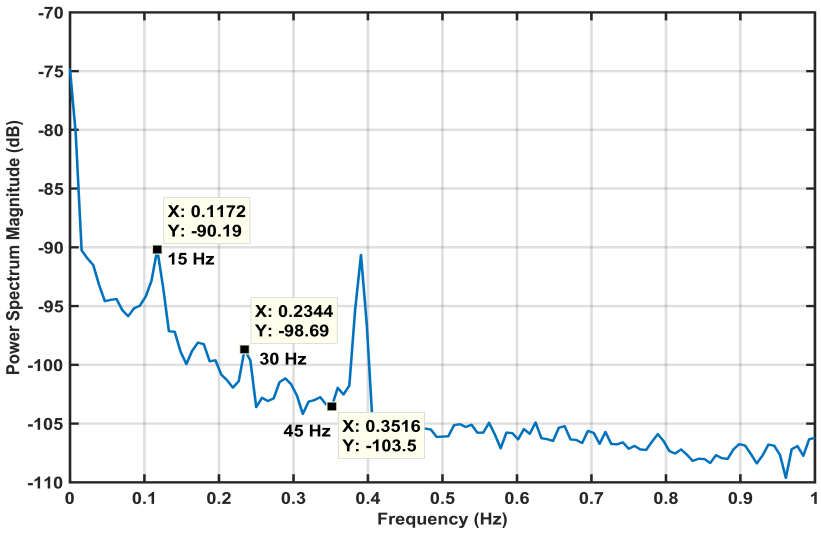

Figure B.11: SSVEP Responses for 15 Hz with harmonics at 30 Hz and 45 HZ

Appendix C

Participant Questionnaire

Before the start of an experiment, the participant was briefed on all the details of the experiment and short demo of how the systems work was shown. The participant was comfortably seated and questions from part 1 of the questionnaire in Appendix C was asked. The participant was also requested to follow the instructions in Appendix C while focusing on the visual stimulus. After completing the recording sessions, the participant was requested to answer the questions in part 2 of Appendix C. The experimental procedure is included in Appendix D.

Instructions for Participants

Participants are requested to follow the instructions below during the experiment

- No chewing gum.
- Be sure you are sitting comfortably without any tension in the neck.
- Be relaxed and calm.
- Minimise movements, especially blinking, movement of eyes and also avoid excessive swallowing.
- Concentrated on visual task and be relaxed.

Table C.1: SSVEP Visual Stimulus Analysis Questionnaire (pre experiment)

SSVEP Visual Stimulus Analysis Questionnaire		
Part - 1 (Before the experiments)		
Questions	**Response**	
	Yes	No
Do you have any pain, behind or around the eyes?		
Do you have any Fatigue / eyes feel tired of reading or computer?		
Headaches when reading or performing visual tasks?		
Sensitivity to light?		
Restricted field of vision / reduced peripheral vision?		
Blurry vision at near?		
Is the distance comfortable from the visual stimulus (60 cm)?		

Table C.2: SSVEP Visual Stimulus Analysis Questionnaire (post experiment)

SSVEP Visual Stimulus Analysis Questionnaire			
Part - 2 (After the experiments)			
Questions	**Response**		
	Yes	**No**	
Do you have any pain,behind or around the eyes?			
Do you have any headache / watery eyes while performing the task?			
Colour comfort (Please circle)	Red	Green	Blue
LED Type (Please circle)	Clear	Frosted	
Orientation Type (Please circle)	Horizontal	Vertical	Radial

Table C.3: Radial Stimulus Comfort Survey

Stimulus Comfort Survey (Pease tick)										
Stimulus Type	**Comfort rating (Highest - 10)**									
	1	**2**	**3**	**4**	**5**	**6**	**7**	**8**	**9**	**10**
70 mm Radial										
90 mm Radial										
110 mm Radial										
Concentric Circles										
Horizontal										

Appendix D

Experimental Procedure

Headset Alignment

The first part of the study used g.tech MOBILAB+ EEG data acquisition system. The hardware consists of one main unit and signal acquisition unit. The electrodes are gel based and used with an EEG cap. The electrodes are fitted on the cap at locations Oz, Fpz and A2.

Connectivity

1. Each electrode needs to be connected to the data acquisition box starting from channel Ao.
2. Connect the main unit to the computer using the USB to serial converter and the port number need to be noted as it is required in MATLAB.
3. Perform a test run to ensure EEG data is streamed to MATLAB continuously.

Data Recording

1. Fill the electrodes on the cap and fill with electrodes with conductive gel.
2. Align the EEG cap on participants head according to 10/20 international standard.
3. Make sure the cap is securely fitted and the electrode is closer to the scalp.

4. If the experiments take longer time, apply conductive gel periodically to ensure the electrodes are wet.

Visual Stimulus Positioning

1. Position the visual stimulus at eye level of the participant.
2. Ensure the stimulus distance is exactly 60 cm from the participant's eyes.

The second part of the study uses EMOTIV EEG headset. EMOTIV is based on saline felt electrodes which are at fixed locations.

Communication and Data Recording

1. The headset communication is via Bluetooth which needs to be paired with the computer.
2. The connection quality of the electrodes are shown in green colour in Testbench software and that ensures better signal quality.
3. The data recording is performed using EMOTIV Testbench software from the electrode at position O2.
4. Perform a test run in Testbench to ensure data is streamed from the headset without any interruptions or packet loss
5. The recorded data needs to be converted from EDF format to be MATLAB format for analysis.
6. Perform a test run to ensure EEG data is streamed to MATLAB continuously.

Visual Stimulus Positioning

1. Position the visual stimulus at eye level of the participant.
2. Ensure the stimulus distance is exactly 60 cm from the participant's eyes.

Data collection tips

- While using g.tech MOBILAB+, always connect the EEG hardware with a serial cable to the computer as the Bluetooth system within the g.tech frequently loses connectivity losing data packets.
- Gel-based electrodes can get dried during longer recording sessions leading to poor data quality, gel top-up, approximately every 30 min would be required to maintain the signal quality.
- For EMOTIV headset, the wireless connectivity is stable and the saline felts should be wetted every 45 min for longer EEG recording periods.
- The participants should be asked not to forcefully focus on the stimulus, as it degrades the quality of the signal. The participants should relax and focus on the stimulus for better results.

Appendix E

Additional Tables

SSVEP analysis from ten participants is shown in the Tables below (Table E1 - E10) from Chapter 7. Each table shows the mean and standard deviation for each frequency and duty-cycle. It can be observed that 85% duty-cycle gave the highest SSVEP response for all the visual stimulus frequencies.

Table E.1: Kruskal-Wallis mean rank, average of maximal FFT (and standard deviation)- S1

Participant	**Duty Cycle**										
	Freq (Hz)	**50%**		**80%**		**85%**		**90%**		**95%**	
		Mean rank	**Average ± SD**	**Mean rank**	**Average ±SD**	**Mean rank**	**Average ± SD**	**Mean rank**	**Average ± SD**	**Mean rank**	**Average ± SD**
S1	7 Hz	387.1	537.6 ± 4.7	387.3	538.1 ± 3.5	**649.2**	562.8 ± 8.6	377.4	535.1 ± 5.1	76.5	417.4 ± 8.7
	8 Hz	366.8	581.5 ± 8.5	594.2	591.9 ± 6.3	**597.1**	651.1 ± 0.8	236.3	531.6 ± 6.9	83.1	490.2 ± 9.4
	9 Hz	466.5	531.6 ± 2.6	545.5	535.9 ± 9.4	**558.6**	536.5 ± 0.3	188.9	490.1 ± 8.4	117.8	484.4 ± 7.5
	10 Hz	404.5	503.8 ± 7.1	474.4	507.1 ± 2.2	**646.9**	533.2 ± 2.2	218.9	482.5 ± 9.3	132.6	487.8 ± 5.6

Table E.2: Kruskal-Wallis mean rank, average of maximal FFT (and standard deviation)-S2

Participant	**Duty Cycle**										
	Freq (Hz)	**50%**		**80%**		**85%**		**90%**		**95%**	
		Mean rank	**Average ± SD**	**Mean rank**	**Average ±SD**	**Mean rank**	**Average ± SD**	**Mean rank**	**Average ± SD**	**Mean rank**	**Average ± SD**
S2	7 Hz	330.3	532.1 ± 4.7	554.1	557.7 ± 8.6	**598.2**	561.9 ± 7.6	310.1	536.2 ± 3.1	85.0	486.2 ±3.9
	8 Hz	416.5	581.4 ± 9.1	489.8	591.3 ± 8.8	**659.9**	632.1 ± 9.9	209.5	538.1 ±7.2	101.6	519.2 ±1.4
	9 Hz	411.6	525.9 ± 8.1	577.2	535.6 ± 0.1	**581.1**	534.0 ± 5.9	193.1	494.3 ± 9.9	114.3	489.0 ± 8.6
	10 Hz	514.2	535.8 ± 4.3	516.5	531.5 ± 7.5	**534.4**	538.9 ± 4.8	235.7	514.0 ±8.6	76.5	443.8 ±6.3

Table E.3: Kruskal-Wallis mean rank, average of maximal FFT (and standard deviation)-S3

Participant	**Duty Cycle**										
	Freq (Hz)	**50%**		**80%**		**85%**		**90%**		**95%**	
		Mean rank	**Average ± SD**	**Mean rank**	**Average ±SD**	**Mean rank**	**Average ± SD**	**Mean rank**	**Average ± SD**	**Mean rank**	**Average ± SD**
S3	7 Hz	405.6	528.3 ± 4.6	485.5	529.2 ± 9.9	**665.2**	558.7 ± 8.1	244.5	509.4 ± 9.4	76.5	443.5 ±2.4
	8 Hz	376.1	537.6 ± 2.4	533.6	576.2 ±7.6	**636.7**	593.7 ± 8.7	155.1	489.9 ±7.1	155.9	489.7 ±6.5
	9 Hz	431.7	527.4 ± 1.1	560.6	531.1 ± 5.1	**574.3**	536.1 ± 0.7	191.7	492.2 ± 0.2	119.0	488.8 ±8.6
	10 Hz	340.7	503.4 ± 7.3	492.1	514.9 ± 5.8	**670.9**	535.7 ± 5.3	196.1	493.2 ±7.5	177.6	489.6 ±1.4

Table E.4: Kruskal-Wallis mean rank, average of maximal FFT (and standard deviation)-S4

Participant	**Duty Cycle**										
	Freq (Hz)	**50%**		**80%**		**85%**		**90%**		**95%**	
		Mean rank	**Average ± SD**	**Mean rank**	**Average ±SD**	**Mean rank**	**Average ± SD**	**Mean rank**	**Average ± SD**	**Mean rank**	**Average ± SD**
S4	7 Hz	463.5	535.1 ± 4.4	475.7	533.6 ± 3.8	**621.5**	547.8 ± 7.9	193.2	496.1 ± 3.7	123.3	484.9 ±8.1
	8 Hz	446.4	536.3 ± 8.3	437.1	534.3 ±1.7	**672.9**	574.7 ± 8.3	184.2	510.1 ±5.2	136.7	505.7 ±1.8
	9 Hz	441.1	582.1 ± 0.5	555.1	535.1 ± 5.9	**567.1**	537.8 ± 7.1	196.7	491.6 ± 0.1	117.2	482.4 ±1.2
	10 Hz	371.2	507.7 ± 0.2	516.1	520.1 ± 7.9	**665.6**	536.4 ± 6.1	195.6	492.7 ±7.3	123.8	487.8 ±5.6

Table E.5: Kruskal-Wallis mean rank, average of maximal FFT (and standard deviation)-S5

Participant	Freq (Hz)	Duty Cycle 50%		80%		85%		90%		95%	
		Mean rank	Average ± SD	Mean rank	Average ±SD	Mean rank	Average ± SD	Mean rank	Average ± SD	Mean rank	Average ± SD
S5	7 Hz	337.10	528.9 ±7.1	436.3	535.7 ±2.1	**656.1**	554.8 ± 6.5	328.4	526.7 ± 1.1	79.2	487.9 ±9.1
	8 Hz	416.63	537.9 ±4.9	416.7	538.4 ±0.8	**670.9**	591.9 ± 8.9	293.8	525.1 ±6.1	79.3	491.6 ±0.4
	9 Hz	433.79	526.7 ±9.3	561.4	535.5 ± 8.3	**572.2**	536.4 ± 0.3	180.4	494.6 ±8.7	129.6	490.9 ±0.9
	10 Hz	401.51	510.2 ±4.2	530.6	520.0 ± 7.9	**636.1**	536.2 ± 4.7	155.8	442.2 ±6.3	150.4	443.4 ±6.5

Table E.6: Kruskal-Wallis mean rank, average of maximal FFT (and standard deviation)-S6

Participant	Freq (Hz)	Duty Cycle 50%		80%		85%		90%		95%	
		Mean rank	Average ± SD	Mean rank	Average ±SD	Mean rank	Average ± SD	Mean rank	Average ± SD	Mean rank	Average ± SD
S6	7 Hz	346.1	535.7 ±2.1	455.6	536.3 ±8.2	**667.9**	559.9 ± 6.3	329.9	534.1 ± 3.9	77.9	536.2 ±9.9
	8 Hz	484.1	526.7 ±6.1	459.3	525.6 ±7.8	**561.8**	535.1 ± 9.2	211.9	501.2 ±7.5	160.3	495.1 ±5.8
	9 Hz	379.1	505.8 ±9.4	505.9	510.9 ±5.7	**669.9**	533.1 ±5.2	240.4	482.4 ±9.5	82.2	465.6 ±8.2
	10 Hz	411.3	514.1 ±7.6	491.8	520.3 ± 5.9	**667.1**	536.1 ± 6.1	182.8	492.1 ±8.5	124.3	487.9 ±7.4

Table E.7: Kruskal-Wallis mean rank, average of maximal FFT (and standard deviation)-S7

Participant	Freq (Hz)	Duty Cycle 50%		80%		85%		90%		95%	
		Mean rank	Average ± SD	Mean rank	Average ±SD	Mean rank	Average ± SD	Mean rank	Average ± SD	Mean rank	Average ± SD
S7	7 Hz	379.9	535.6 ±5.7	391.1	535.8 ±7.1	**650.8**	561.3 ± 8.2	368.7	534.2 ±9.2	86.9	504.1 ±9.3
	8 Hz	353.7	509.9 ±7.5	519.3	526.6 ±6.3	**636.4**	537.1 ± 0.9	495.6	498.8 ±9.3	156.1	489.8 ±1.3
	9 Hz	355.7	494.2 ±0.8	526.2	537.1 ±6.1	**674.5**	580.2 ±3.2	194.1	477.7 ±0.4	126.9	472.1 ±1.8
	10 Hz	345.9	509.1 ±3.6	507.1	520.1 ± 7.9	**658.7**	535.5 ± 7.9	282.6	504.1 ±7.6	83.1	473.4 ±2.6

Table E.8: Kruskal-Wallis mean rank, average of maximal FFT (and standard deviation)-S8

Participant	Duty Cycle										
	Freq (Hz)	50%		80%		85%		90%		95%	
		Mean rank	Average ± SD	Mean rank	Average ±SD	Mean rank	Average ± SD	Mean rank	Average ± SD	Mean rank	Average ± SD
S8	7 Hz	404.6	535.2 ±1.2	435.5	539.4 ±7.6	**638.9**	559.2 ±6.2	303.3	526.9 ±3.2	95.1	495.8 ±9.5
	8 Hz	248.9	561.2 ±6.7	495.9	592.8 ±6.2	**645.1**	616.8 ±9.6	397.8	546.3 ±7.2	89.7	524.6 ±1.4
	9 Hz	414.1	511.8 ±9.1	490.4	516.3 ±5.7	**670.3**	532.1 ±4.9	175.5	452.3 ±7.9	127.2	448.3 ±7.9
	10 Hz	368.8	508.1 ±3.2	594.8	535.5 ±7.6	**601.5**	535.7 ±5.3	236.2	492.7 ±7.3	76.1	463.1 ±6.8

Table E.9: Kruskal-Wallis mean rank, average of maximal FFT (and standard deviation)-S9

Participant	Duty Cycle										
	Freq (Hz)	50%		80%		85%		90%		95%	
		Mean rank	Average ± SD	Mean rank	Average ±SD	Mean rank	Average ± SD	Mean rank	Average ± SD	Mean rank	Average ± SD
S9	7 Hz	369.1	530.4 ±6.8	424.3	538.1 ±4.8	**648.8**	558.2 ±8.1	332.9	529.8 ±4.3	102.3	508.4 ±3.7
	8 Hz	380.1	538.3 ±8.8	531.4	592.8 ±6.2	**659.7**	611.3 ±9.5	175.7	452.7 ±8.5	130.4	482.5 ±7.5
	9 Hz	411.1	488.4 ±9.2	490.7	495.1 ±1.7	**674.4**	532.0 ±5.2	215.3	410.3 ±8.2	84.7	396.1 ±7.1
	10 Hz	372.6	501.2 ±6.9	592.7	534.6 ±7.8	**607.4**	531.2 ±6.2	182.4	454.3 ±9.8	122.3	447.3 ±6.6

Table E.10: Kruskal-Wallis mean rank, average of maximal FFT (and standard deviation)-S10

Participant	Duty-Cycle										
	Freq (Hz)	50%		80%		85%		90%		95%	
		Mean rank	Average ± SD	Mean rank	Average ±SD	Mean rank	Average ± SD	Mean rank	Average ± SD	Mean rank	Average ± SD
S10	7 Hz	388.5	534.4 ±9.8	426.1	534.8 ±1.2	**659.1**	559.8 ±7.8	316.2	525.1 ±6.5	87.4	498.2 ±1.2
	8 Hz	421.8	582.5 ±8.5	482.1	594.8 ±7.7	**667.3**	651.1 ±1.8	229.6	528.1 ±5.1	76.6	489.2 ±9.1
	9 Hz	242.9	486.4 ±1.5	531.3	524.3 ±5.8	**658.7**	531.1 ±5.6	368.1	500.8 ±12.2	76.3	439.4 ±7.7
	10 Hz	418.1	484.7 ±6.8	459.6	490.6 ±1.4	**671.7**	531.2534.6 ±6.3	249.1	469.5 ±6.9	78.9	430.1 ±8.7